High Performance Computing Usage

Annual Report

2025



Supercomputer Education and Research Centre
Indian Institute of Science
Bangalore – 560012

Table of Contents

1 SERC High Performance Computing (HPC) Facilities 1

1.1 Clusters 2

1.2 Visualization and Data Analysis Infrastructure 3

1.3 Storage Infrastructure 4

2 Usage in 2025 4

3 IISc's Scientific Applications on SERC HPC Usage 9

3.1 Department of Aerospace Engineering (AE) 10

3.2 Centre for Atmospheric and Oceanic Sciences 25

3.3 Centre for Earth Science 32

3.4 Chemical Engineering 33

3.5 Computation and Data Sciences (CDS) 40

3.6 Department of Inorganic Physical Chemistry 49

3.7 Department of Material Research Centre 50

3.8 Mechanical Engineering 52

3.9 Molecular Biophysics Unit 56

3.10 Department of Physics 60

4 Awards and Recognitions based on Research with SERC HPC Resources 63

5 Access to External Users 64

6 Publications in 2025 Using SERC HPC Resources 64

1 SERC High Performance Computing (HPC) Facilities

The Supercomputer Education and Research Centre (SERC) at IISc has been at the forefront of providing high performance computing (HPC) facilities to the academic and research community of Indian Institute of Science (IISc) and beyond for conducting HPC and AI-based and data-intensive scientific research. For over four decades, SERC has provided advanced computational infrastructure, scientific software environments, and expert system administration support to enable cutting-edge research across science and engineering disciplines.

SERC operates a 24×7 computing ecosystem comprising petascale supercomputing systems, AI-focused GPU platforms, advanced visualization resources, and high-performance storage infrastructure. The Centre currently hosts PARAM Pravega, one of India's most powerful academic supercomputers, NVIDIA DGX-H100 systems for AI and machine learning workloads, dedicated visualization resources, and approximately 4 PB of high-performance storage. These facilities support a wide range of computational activities, including large-scale simulations, first-principles modelling, computational science workflows, data analytics, and AI/ML applications.

In 2025, SERC supported research activities across **24 departments**, **89 research groups**, and **330 active users** at IISc. The Centre enabled research in diverse areas including aerospace engineering, computational fluid dynamics, climate and atmospheric sciences, earth and geophysical sciences, computational chemistry, materials modelling and discovery, nanoscience, molecular biophysics, plasma physics, high-speed propulsion, computational and data sciences, quantum materials, and artificial intelligence.

The growing demand for advanced computational resources was reflected in the extensive usage of SERC facilities during the year. Researchers collectively consumed over **194 million CPU core-hours** and **700k GPU-hours**, executing around **93,000 computational jobs** across HPC platforms. The increasing adoption of GPU-accelerated computing and AI-driven research highlights the expanding role of advanced computing in addressing complex scientific and engineering challenges.

In addition to supporting IISc researchers, SERC continued to serve the broader research community by enabling computational research for external institutions and collaborative projects across the country. The Centre supported 2 external research groups from 2 institutions, reinforcing its role as a national computational resource.

Research carried out using SERC's computational infrastructure resulted in **67 publications** in leading journals and conferences during the reporting period. These efforts have contributed to significant advances in computational science, engineering, and AI-enabled research, while also facilitating the development of scientific software and computational methodologies across multiple domains.[1]

The scientific impact of research enabled by SERC is reflected in several prestigious recognitions received during the year, including the **Dr. A.P.J. Abdul Kalam HPC Award 2025**, **the Director's**

[1] *Selected portions of the report text were drafted with the assistance of AI-based writing tools and subsequently reviewed, edited, and validated by the authors. All statistics, analyses, visualizations, and technical content are derived from actual SERC operational and usage data.*

Discretionary Award for Compute Allocation on Frontier awarded by Oak Ridge National Laboratory (ORNL), USA, and **the Kawazoe Award from the Asian Consortium on Computational Materials Science (ACCMS), Japan**. These achievements underscore the growing international visibility and excellence of computational research supported by SERC.

SERC continues to expand and strengthen its HPC, AI, visualization, and storage infrastructure to meet the rapidly growing computational demands of modern scientific discovery, engineering innovation, and data-driven research.

1.1 Clusters

1.1.1 PARAM Pravega

Commissioned in 2022 under the National Supercomputing Mission (NSM), PARAM Pravega is one of India's most powerful supercomputers in an academic Institute in India. The system delivers a peak computational performance of **3.3 PFLOPS** and is built on a hybrid CPU-GPU architecture optimized for large-scale scientific computing, data analytics, and AI-enabled workflows.

PARAM Pravega comprises **428 regular compute nodes with 20,544 Intel Xeon Cascade Lake CPU cores**, **156 high-memory nodes with 7,488 CPU cores**, and **40 GPU nodes equipped with NVIDIA V100 GPUs**. The system provides **approximately 4 PB of high-performance storage** and is interconnected through a high-speed Mellanox HDR InfiniBand network based on a fat-tree topology, enabling efficient execution of tightly coupled parallel workloads.

During the reporting period, the systems achieved an average utilization of **92-98%** for GPUs and **90-94%** for CPUs, accounting for approximately **571k GPU-card hours** and **184 million CPU corehours** of computation. A total of **58,453 jobs** were executed, comprising **8,895 GPU jobs** and **49,558 CPU jobs**. The largest completed simulation utilized 19,200 CPU cores, consuming 460,944 core-hours, demonstrating the capability of the system to support extremely large-scale parallel applications.

Analysis of system utilization on PARAM Pravega indicates a continued shift towards larger and more computationally intensive workloads. While the total number of submitted CPU jobs decreased by 18.36% compared to the previous year, **average computation size per job increased by 16.4%**, reflecting improved parallel efficiency and growing demand for high-resolution simulations. PARAM Pravega supported research across aerospace engineering, climate science, computational chemistry, earth sciences, materials modelling, molecular biophysics, plasma physics, computational data sciences, and many other disciplines.

The system also serves as a national resource, supporting researchers from multiple institutions across India and enabling collaborations in computational science, engineering, and AI research.

1.1.2 DGX-H100 Systems

SERC hosts NVIDIA DGX-H100 systems to support advanced Artificial Intelligence (AI), Machine Learning (ML), and data-intensive research. Built on the NVIDIA Hopper architecture, these systems provide exceptional performance for training and inference of large-scale deep learning models and scientific AI applications.

The DGX-H100 infrastructure supports research in natural language processing, computer vision, computational biology, materials discovery, scientific machine learning, foundation models, and

generative AI. Researchers benefit from high-bandwidth GPU interconnects, optimized AI software environments, and scalable multi-GPU performance for demanding workloads.

During the reporting period, DGX-H100 systems achieved an **average utilization of 81.52%**, accounting for approximately **55,961 GPU card-hours** of computation across **5,544 executed jobs**. Comparing with its legacy counterpart, the Volta-based DGX-1, highlights the strong research demand for the new architecture.

AI and machine learning activities on the DGX-H100 platform were carried out by **26 active project groups** comprising **55 unique users**, representing nearly **17% of all active HPC users** across the centre. The high utilization of DGX-H100 resources reflects the rapidly growing computational demands of deep learning, large-scale model training, and scientific AI applications leveraging Hopper-class Tensor Cores and optimized Transformer Engines.

1.1.3 RNC cluster

The RNC cluster serves small-scale HPC workloads. Anchored by **1,824 CPU cores** and **2 dedicated NVIDIA V100 GPU nodes**, the RNC cluster supports multi-disciplinary workloads, spanning quantum chemistry, fluid dynamics, and molecular dynamics. During the 2025 reporting period, the RNC CPU queue recorded a **steady utilization of 79%**, delivering approximately **10.47 million core-hours** of computation across **25,136 CPU jobs**. Meanwhile, the RNC GPU queue operated at a critical utilization load of **50.84%**, consuming **29,560 card-hours**, representing a **10.8% increase in GPU usage** compared to 2024. Providing a fast turnaround time with an **average queue wait of only 3.5 hours**, the RNC cluster supported an active community of **102 unique researchers**, proving to be an indispensable resource for local, high-frequency computational tasks.

1.1.4 DGX 1

Complementing the Hopper architecture, the legacy NVIDIA DGX-1 cluster, powered by **NVIDIA Volta V100 GPUs**, continues to serve as a highly resilient and reliable platform for SERC's AI and machine learning community. Though representing an older generation of accelerated hardware, the DGX-1 system remains a vital asset, providing stable compute capacity for model prototyping, hyperparameter tuning, and standard deep learning training runs. In 2025, the cluster experienced a dramatic surge in adoption, achieving an **average utilization of 76.9%** and accounting for **44,003 GPU card-hours** of computation, a staggering **163.5% increase** over the previous year. A total of **1,800 GPU-enabled jobs** were successfully executed on the platform by **20 unique researchers**, proving that this robust infrastructure continues to play a critical role in alleviating wait times on newer platforms and supporting diverse computational research across the campus.

1.2 Visualization and Data Analysis Infrastructure

SERC maintains dedicated visualization and analysis servers that enable researchers to interactively explore and interpret the large datasets generated by simulations and AI workflows. These systems provide high-memory environments, advanced graphics capabilities, and remote visualization tools that support post-processing, data analytics, rendering, and scientific visualization.

The visualization infrastructure plays a critical role in transforming large-scale computational results into scientific insights across domains such as fluid dynamics, climate modelling,

materials science, computational biology, and earth sciences. Researchers use these facilities for interactive analysis, image generation, volumetric rendering, and interpretation of multi-dimensional datasets produced by HPC applications.

1.3 Storage Infrastructure

SERC's HPC ecosystem is supported by a scalable storage infrastructure providing approximately 4 PB of high-performance storage for scientific computing workloads. The storage platform is designed to support high throughput parallel I/O requirements while ensuring reliable data access across compute, AI, and visualization environments.

The storage subsystem enables seamless movement of data between compute clusters, GPU platforms, and visualization resources, facilitating efficient execution of end-to-end scientific workflows. As research increasingly relies on large-scale simulations, AI training datasets, and data-intensive analyses, the storage infrastructure continues to play a critical role in supporting the Institute's computational research ecosystem.

2 Usage in 2025

The High-Performance Computing (HPC) facilities at the Supercomputing Education and Research Centre (SERC) have witnessed extensive usage during the year 2025. Researchers from diverse departments at the Indian Institute of Science (IISc), as well as collaborating national and international institutions, have leveraged PARAM Pravega, NVIDIA DGX-H100, DGX-1, and hybrid Roddam Narasimha Cluster (RNC) systems for computationally intensive projects.

Over this reporting period (2025), SERC's HPC infrastructure was utilized with the following footprint:

- **Active User Base**: More than **300 active users** from approximately **89 faculty groups** across IISc and partner research centres.
- **Academic Reach**: Serving researchers spanning **24 departments** across the Institute.
- **Throughput & Scale**: Execution of around **93,000 jobs** across.
- **Computational Capacity Consumed**: Over **194 million CPU core-hours** and **700k GPU card-hours** of processing.
- **Academic Output**: Research enabled by SERC HPC resources has contributed to numerous peer-reviewed publications and at least **35 PhD dissertations**.

The clusters together supported an **average of 7,735+ jobs each month**, with overall **system-wide CPU utilization averaging 74.5%** (77.9% adjusted for operational downtime) and **GPU card utilization averaging 76.9%** (79.6% adjusted for operational downtime). Collectively, these efforts underscore the critical role of SERC's HPC ecosystem in advancing cutting-edge scientific research and technological innovation.

Following are the various domain areas of research carried out on Param Pravega.

- Aerodynamics & Computational Fluid Dynamics (CFD)
- Turbulence Modelling, Flow Physics & Aeroacoustics
- Compressible, High-Speed & Hypersonic Flows (Scramjets, SWBLI)
- Aeroelasticity, Flight Dynamics & Propulsion Systems
- Fluid-Structure Interaction, Cavitation & Multiphase Flows

- Bio-Inspired Propulsion & Underwater Acoustics
- Climate Modelling & Earth System Science
- Indian Monsoon Dynamics, Tropical Meteorology & ENSO
- Air-Sea Interactions & Ocean-Atmosphere Coupling
- Solar Geoengineering, Aerosol-Climate Interactions & Climate Intervention
- Paleoclimate, Climate Variability & Risk Assessment
- Mantle Convection, Geodynamics & Planetary Interiors
- Computational Materials Science & Engineering
- Two-Dimensional Materials, Nanomaterials & Membranes
- Catalysis, Reaction Engineering & Separation Processes
- Electronic Structure & Density Functional Theory (DFT)
- Molecular Dynamics (MD) & Multiscale Simulations
- Computational Chemistry, Quantum Materials & Materials Discovery
- Computational Biophysics, Structural Biology & Neuroscience

The following section presents consolidated statistics across all HPC clusters, offering insights into overall usage patterns through metrics such as total users, submitted jobs, CPU hours, GPU hours, and related resource consumption.

	DGX-1	**DGX H100**	**RNC**	**Param Pravega**	**Total**
Number of Faculty Groups	13	26	35	60	89
Number of Users	20	55	102	240	330
Number of Departments	8	13	17	20	20

**Totals reflect unique counts of users, research groups, or departments, not aggregated sums.*

Cluster	**CPU Core Hours**	**GPU Node Hours**	**CPU Utilization %**	**GPU Utilization %**
DGX-1	0	44,003	0.00%	76.9%
DGX H100	0	55,962	0.00%	81.52%
RNC	10,472,355	29,559	79%	50.84%
Param Pravega	174,293,985	571,292	90-94%	92-98%

**The utilization percentages shown above represent this cluster's share of resource consumption, excluding idle periods or downtime.*

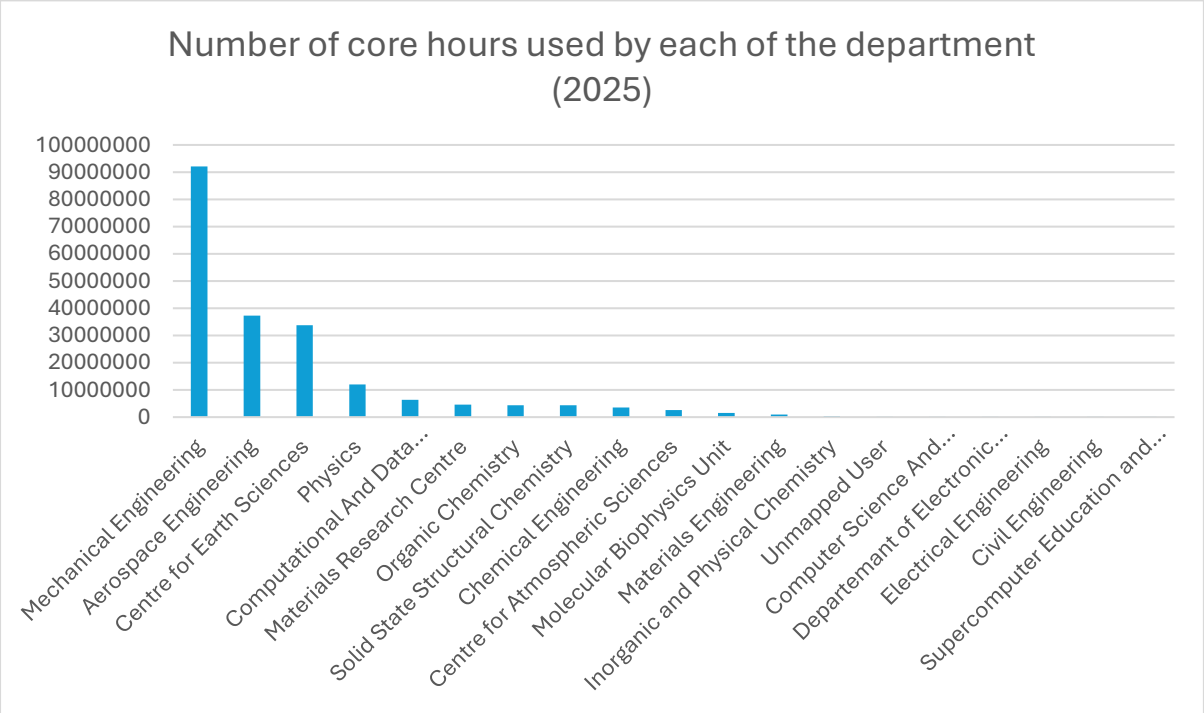
Metric	Year 2024	Year 2025	YoY Change (%)
Active Users	316 users	330 users	**+4.43%**

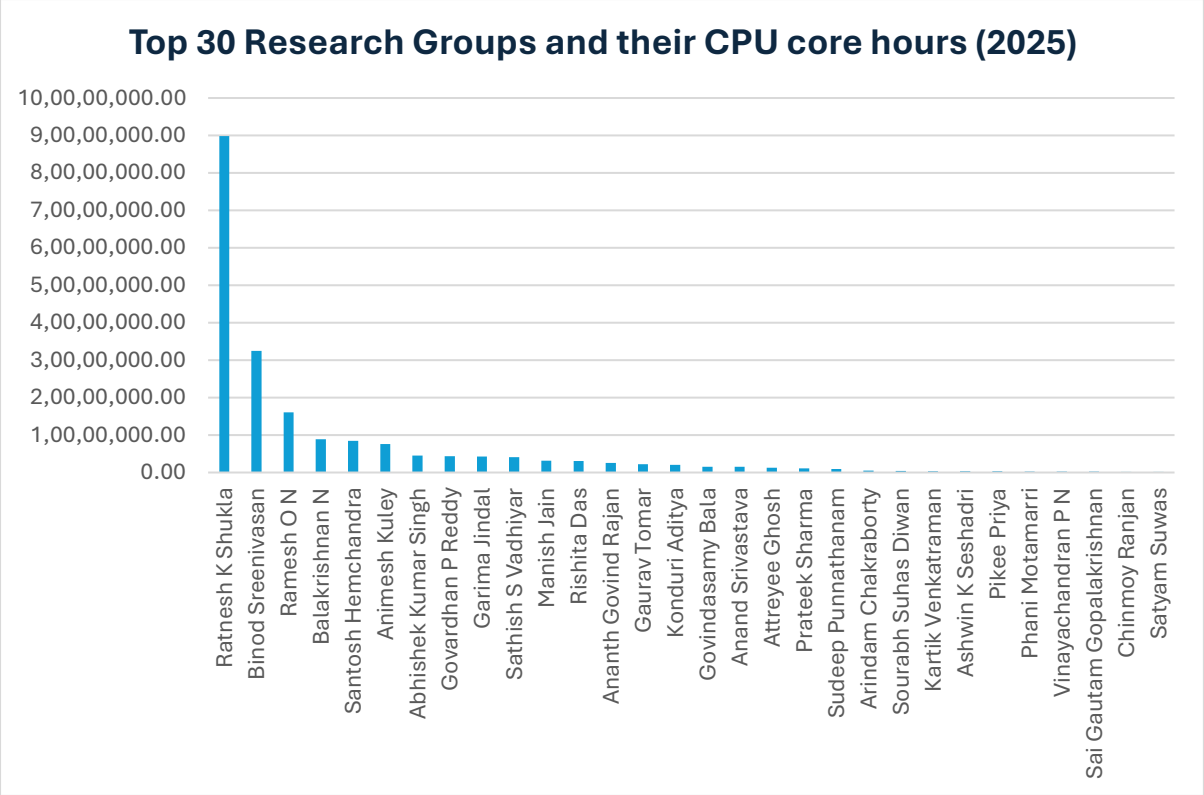
Total Jobs Executed	108,105 jobs	93,247 jobs	**-13.74%**
Total CPU Jobs	91,144	74,694	**-18.05%**
Unique CPU Users	284	264	**-7.04%**
CPU Core-Hours Consumed	206.52M	194.77M	**-5.69%**
Total GPU Jobs	17,309	18,126	**+4.72%**
GPU Card-Hours Consumed	540.18K	700.82K	**+29.74%**
Unique GPU Users	113	161	**+42.48%**

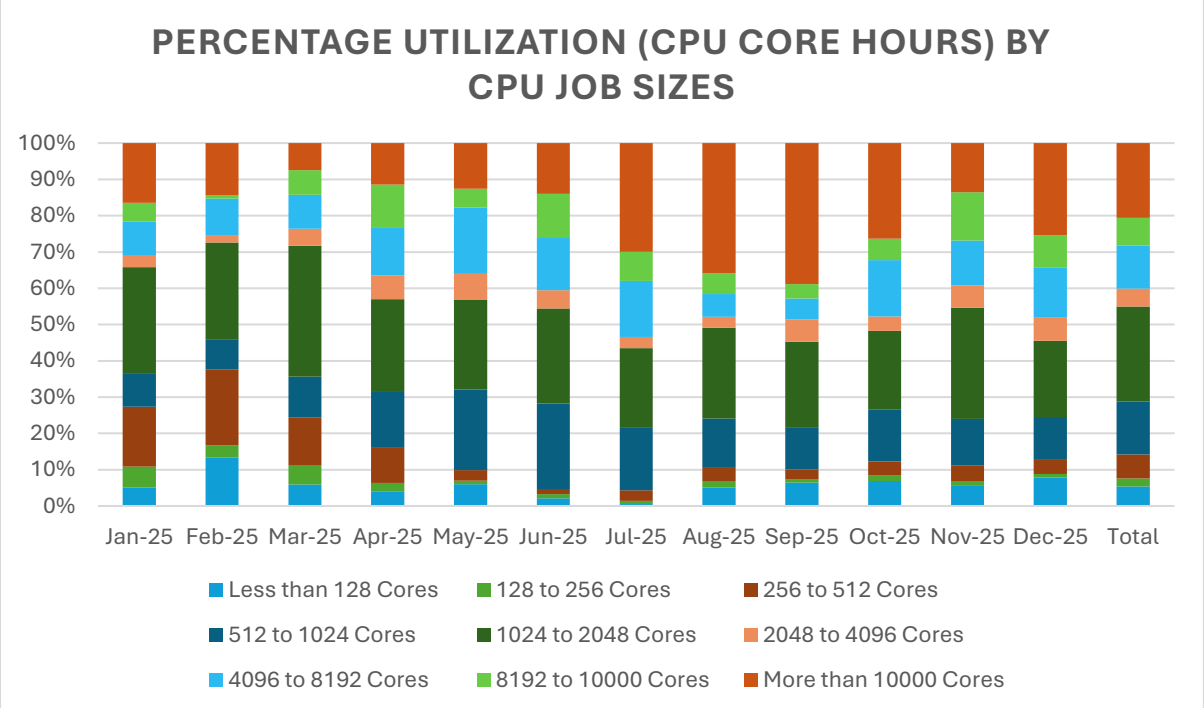
[1] Operational Downtime Adjustment: Unadjusted CPU core-hours reflect calendar totals. Adjusting for 2025 maintenance periods (excluding the downtime reveals a +3.43% increase in actual CPU consumption rate during operational months).

[2] Parallel Efficiency Shift: The discrepancy between a minor decline in CPU core-hours (-5.69%) and a steep drop in job submissions (-18.05%) indicates that the average size of executed CPU simulations grew by 15.08% (from 2,266 to 2,608 core-hours per job), showing a shift to more efficient multi-node parallel processing.

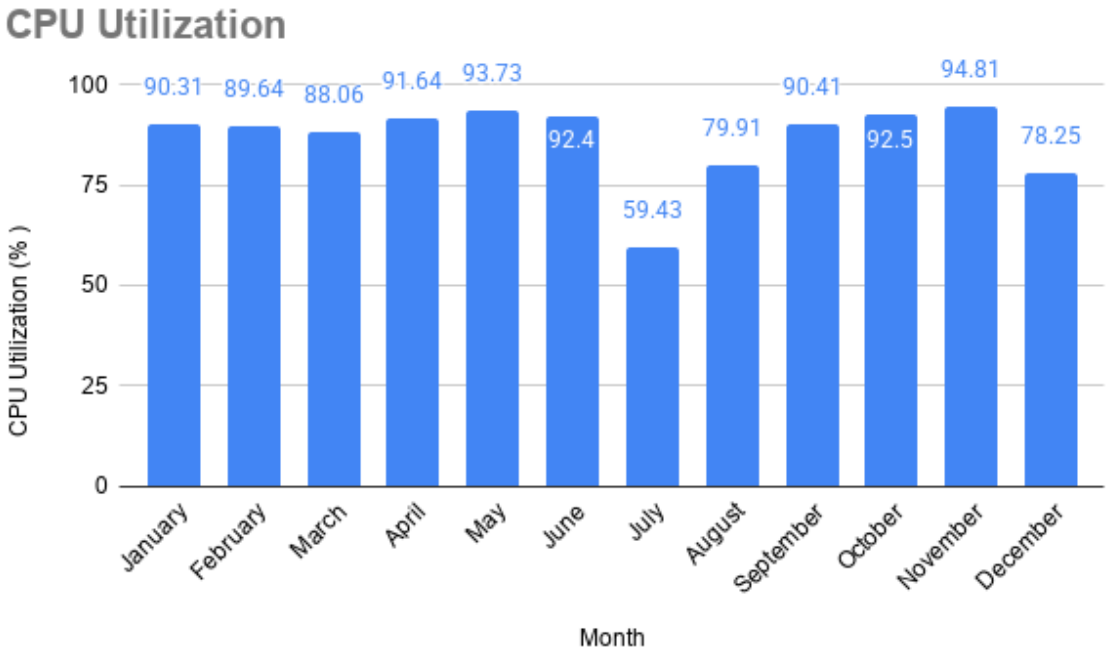
[3] Workload Migration: A portion of CPU user decline is attributed to researchers transitioning their scientific pipelines to GPU-accelerated environments (such as the Hopper-based DGX-H100) to support accelerated deep learning and AI-driven models.



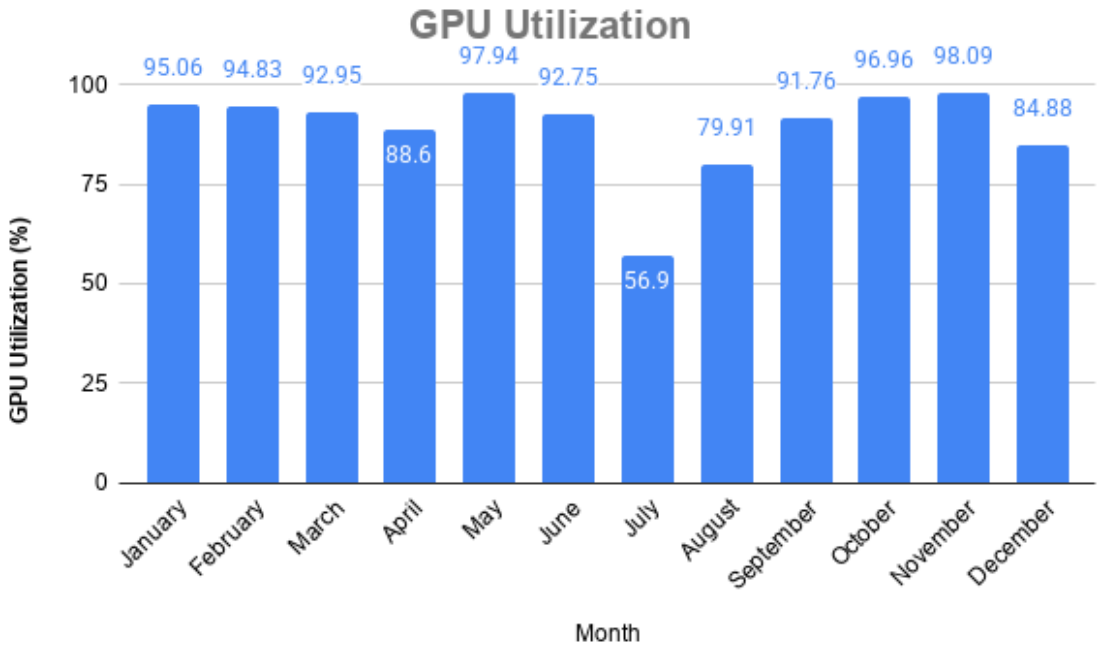




**The above graph shows Param Pravega's CPU core-hour utilization in 2025, broken down by job sizes (number of cores) in each month.*



The above graph shows Param Pravega's monthly CPU utilization in 2025



The above graph shows Param Pravega's monthly GPU utilization in 2025

3 IISc's Scientific Applications on SERC HPC Usage

In 2025, the HPC facilities at SERC were extensively utilized by researchers across IISc for a wide range of scientific and engineering applications. The availability of PARAM Pravega, NVIDIA DGX-H100 systems, DGX-1, Roddam Narasimha Cluster (RNC) systems, visualization platforms, and large-scale storage enabled projects requiring massive computational power and data handling capabilities.

The applications broadly covered:

- **Aerodynamics & Propulsion Systems:** Computational Fluid Dynamics (CFD), turbulence modeling (LES and DNS), aeroacoustics and flow-induced noise, compressible high-speed flows, Shock-Wave Boundary Layer Interactions (SWBLI), hypersonic/scramjet aerodynamics, aeroelasticity, cavitation, underwater acoustics, and bio-inspired propulsion.
- **Climate Science & Earth System Modeling:** Long-term simulations of climate variability, monsoon predictability, carbon cycle feedbacks, solar geoengineering, aerosol-climate interactions, paleoclimate, ocean-atmosphere coupled processes, geodynamics, and mantle convection.
- **Materials Science & Chemistry:** First-principles materials modeling, catalyst design, Density Functional Theory (DFT) calculations, molecular dynamics, spintronics, nanomaterials/membranes, high-entropy alloys, and digital twin modeling.
- **Computational Biology & Life Sciences:** Biomolecular simulations, genomics, protein folding, protein-membrane interactions, computational neuroscience, and drug discovery applications using GPU-accelerated codes.
- **Physics & Astrophysics:** Plasma turbulence, fusion energy research, magnetically confined plasmas, galaxy formation, black hole accretion models, geodynamos, and exascale computing algorithms.
- **Artificial Intelligence & Machine Learning:** Training of large language models, deep learning for computer vision and NLP, generative AI, scientific machine learning, and data-intensive analytics on DGX-H100 and DGX-1 systems.

These diverse applications underscore the central role of SERC's HPC ecosystem in enabling IISc's research community to address grand scientific challenges, produce high-impact publications, and contribute to national and global scientific progress.

The following sections give details of the usage of HPC for various computational science problems.

3.1 Department of Aerospace Engineering (AE)

3.1.1 Prof. N. Balakrishnan's Lab

3.1.1.1 Problem areas:

The primary focus area of research in the lab during the year 2025 was Aeroacoustics. The objective of these computations was to understand the acoustic field associated with cavity flows. These are typically high-fidelity DES/DDES simulations requiring large computational resource. In terms of understanding the physics of cavity acoustics, effect of thickness of the boundary layer at the leading edge of the cavity and effect of outer flow Mach number have been considered. In addition, the effect of presence of stores on the cavity acoustics is also studied, with an objective of understanding the uncertainty in aerodynamic loads experienced by the stores because of the unsteady flow prevailing in the cavity. This input is critical to store separation studies.

In addition, algorithms pertaining to planform optimization and time adaptivity for unsteady flow simulations have also been considered. Large scale unsteady simulations to understand store separation dynamics, rotary wing aerodynamics and hypersonic scramjet flows have also been performed.

3.1.1.2 SERC's Resources:

Typically, each of the cavity acoustics studies discussed above requires about .75 to 1 Million CPU core hours. In order to meet all the objectives of the studies, computations have been performed on various supercomputing platforms in the country, in addition to the SERC facilities. Other computations mentioned typically need over 200K core hours

3.1.1.3 Parallelization strategies:

For all the computations discussed above, the HiFUN solver (sandi.co.in) is made use of. The code is MPI parallel for CPU computing and OpenACC parallel for hybrid CPU-GPU computing.

3.1.1.4 Performance/Scalability:

The code HiFUN is highly scalable with an ability to scale over several thousand processor cores and multi-node GPU systems. Details of scalability may be had from the following links:

https://www.researchgate.net/publication/388142871_PERFORMANCE_OF_CODE_HIFUN_IN_SPICES_09

https://doi.org/10.13140/RG.2.2.15096.78082

https://www.nvidia.com/en-us/on-demand/session/gtcspring21-s31758/

3.1.1.5 Research Outcome:

a. Publications:

1. Abhiyan Paudel, Sharanjeet Kaur, Nikhil Vijay Shende and N Balakrishnan, Aerodynamic shape optimization of a rectangular wing for long endurance Unmanned Aerial Vehicle, ECCOMAS AeroBest 202, 22–24 April 2025, Lisboa, Portugal.
2. Argha Saha, O N Ramesh, N Balakrishnan, Effect of Mach Number on Cavity Acoustics, 26th Annual AeSI CFD Symposium 2025, 11th-13th August 2025, Bangalore.

3. Saranraj A, Saha Argha, Akshay Nagdeve, Mohideen Ansar, Ramesh O N, Balakrishnan N, Uncertainty Quantification of Aerodynamic Loads on a Store Using Detached Eddy Simulation (DES), 26th Annual AeSI CFD Symposium 2025, 11th-13th August 2025, Bangalore.
4. Mohammed Shaheen Suhail, Munikrishna, Balakrishnan N, Residual Driven Adaptive Time Stepping for Unsteady Flows, 26th Annual AeSI CFD Symposium 2025, 11th-13th August 2025, Bangalore.
5. Mohideen Ansar A, Akshay Nagadeve, Manoj Kumar K, Rajni Kanth B and N Balakrishnan, CFD Analysis of SPICES 4 Hypersonic Intake Configuration using HiFUN, 26th Annual AeSI CFD Symposium 2025, 11th-13th August 2025, Bangalore.

b. Contribution to the nation/Industry/societal Projects:

Cavity acoustics is very critical in the design of internal weapons bay of stealth combat aircrafts. Apart from the dynamic structural design of the weapons bay, it is important for ensuring safe separation of stores. In fact, the work carried out has provided important design input for one of the combat aircraft programs of the country.

c. Awards and recognition:

The following paper was awarded the best paper award in AeSI CFD symposium, 2025:

- Argha Saha, O N Ramesh, N Balakrishnan, Effect of Mach Number on Cavity Acoustics, 26th Annual AeSI CFD Symposium 2025, 11th-13th August 2025, Bangalore.

d. Students graduated during the 2025

1. Mohammed Shaheen Suhail, Residual-Driven Adaptive Time Stepping Strategy for Unsteady Flow Computations, MTech Thesis, Department of Aerospace Engineering, June 2025.
2. Saranraj Anbalagan, High fidelity numerical investigation of unsteady cavity flows and Aerodynamic load characterization on internal stores using Detached Eddy Simulation, MTech Thesis, Department of Aerospace Engineering, June 2025.

3.1.2 Prof. Pikee Priya's Lab

3.1.2.1 Problem areas:

Our research focuses on computational materials design of multi-component alloys using first-principles Density Functional Theory (DFT) simulations. During 2025, SERC HPC resources were extensively used to investigate the mechanical and thermodynamic properties of complex alloys across wide composition spaces.

The major problems addressed include:

- Calculation of **bulk modulus, elastic constants, and equation of state** of multi-component alloys for mechanical stability assessment.
- Computation of **surface energies** of different crystallographic planes to understand phase stability and surface segregation tendencies.
- Large-scale **DFT simulations of disordered alloys** using Special Quasirandom Structures (SQS) to model realistic chemical disorders.
- Systematic exploration of **composition–property relationships** across binary and ternary alloy systems.

- Prediction of energetically favorable alloy configurations for advanced structural and high-temperature applications.
- Automated high-throughput DFT workflows for screening candidate materials in large compositional spaces.
- Comparative analysis of alloy stability using formation energies and electronic structure calculations.

These studies help accelerate **materials discovery and design** for advanced engineering applications.

3.1.2.2 SERC's resources:

- SERC high-performance computing clusters were used for large-scale DFT simulations.
- Typical simulations employed **128–512 CPU cores** per job depending on system size.
- Thousands of parallel batch jobs were executed for high-throughput composition screening.
- Large-memory nodes were used for complex supercell calculations of disordered alloys.
- Storage resources were used extensively for wavefunction files and post-processing datasets.

3.1.2.3 Parallelization Strategies:

- **MPI-based parallelization** across k-points and electronic bands.
- Parallel execution of multiple independent DFT jobs for high-throughput workflows.
- Domain decomposition techniques for large supercell calculations.
- Efficient job scheduling using batch queuing systems for optimal resource utilization.
- Hybrid parallelism combining distributed memory MPI and shared memory OpenMP.

3.1.2.4 Performance and Scalability:

- Excellent strong scaling observed up to several hundred CPU cores for large supercell calculations.
- Significant reduction in computation time (≈70–85%) compared to small local clusters.
- High-throughput workflows enable simultaneous exploration of multiple alloy compositions.
- Large-memory nodes allowed simulations that were otherwise infeasible on conventional systems.
- Efficient parallelization reduced wall-time for complex surface calculations from weeks to days.

3.1.2.5 Research Outcome:

Results Obtained Through DFT

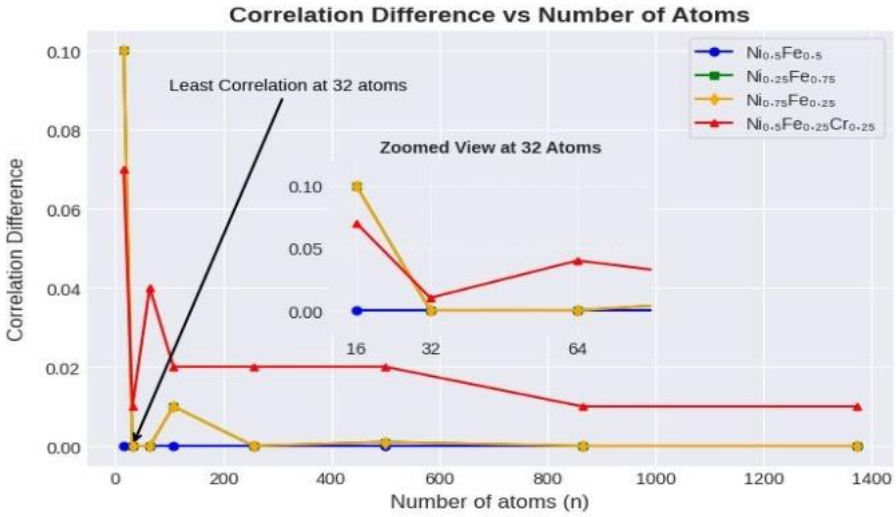


Figure 1 Correlation Difference between finites disordered supercell with the perfect disordered supercell, varying with Number of atoms. Here we achieved that the 32 atoms has least correlation.

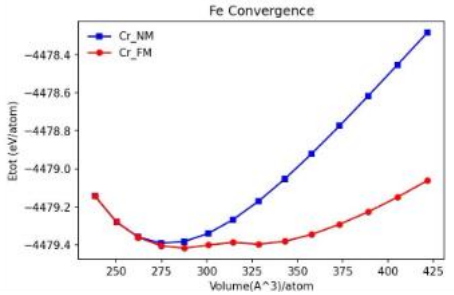


Figure 2 Energy vs Atomic Volume curve of Cr have NM -Non magnetic, FM-Ferromagnetic and AFM – antiferro magnetic

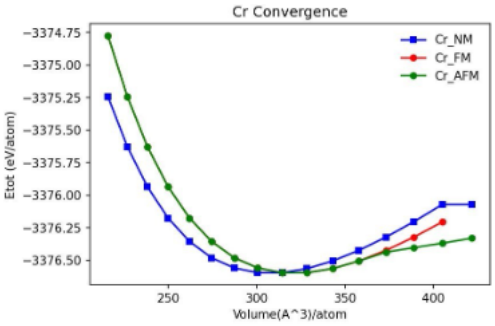


Figure 3 Ground state Energy vs Atomic Volume curve of Fe having NM – Non magnetic and FM-Ferromagnetic nature.

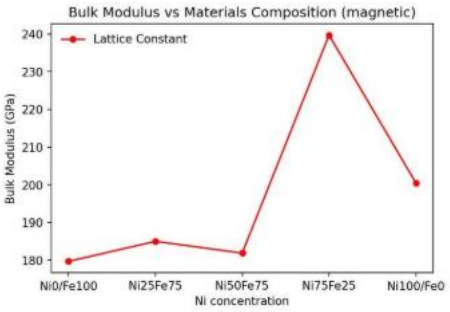


Figure 4 Bulk modulus varying with composition space

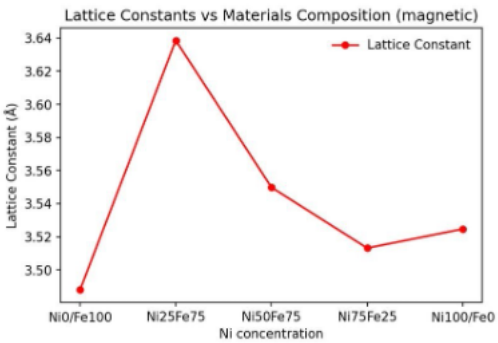


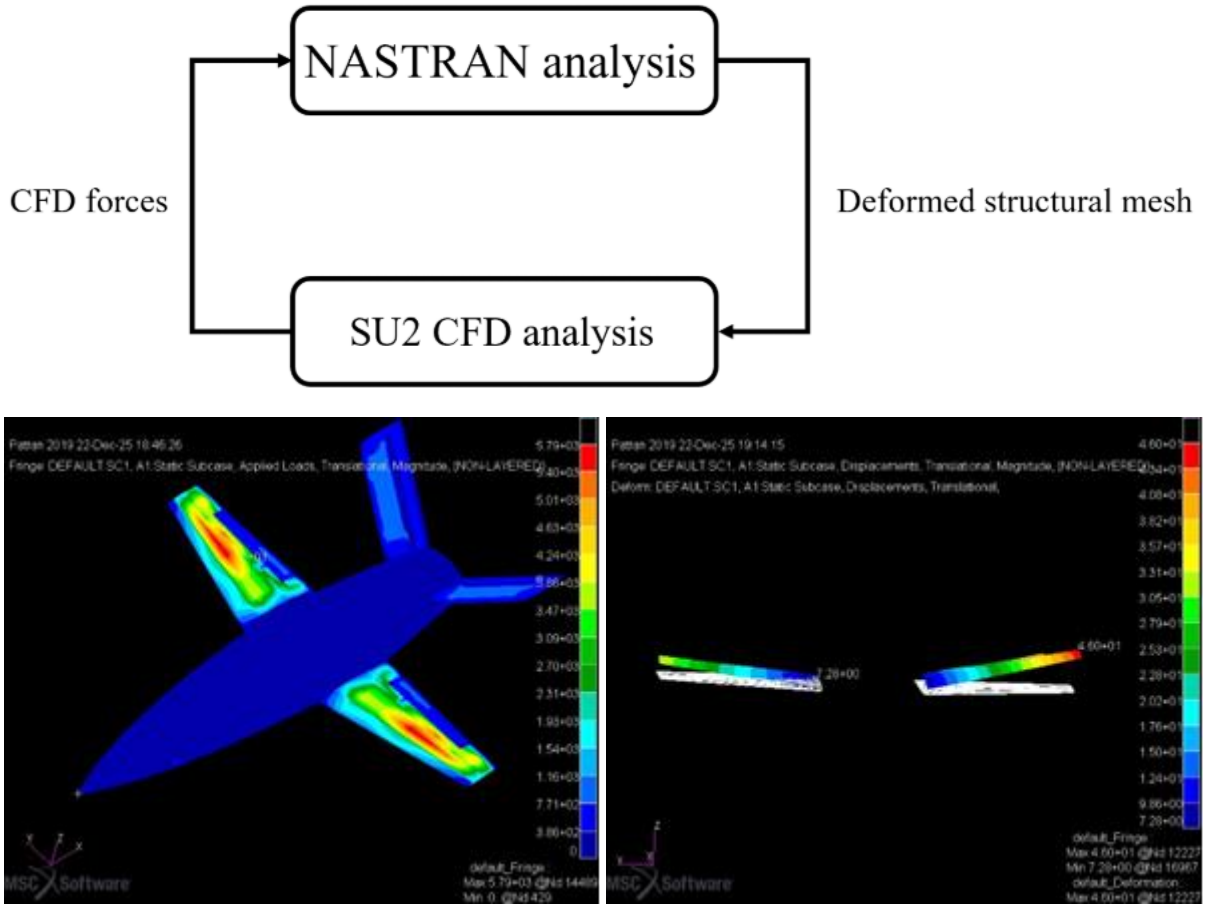
Figure 5 Lattice Parameter varying with composition space

3.1.3 Prof. Kartik Venkatraman's Lab

3.1.3.1 Problem areas:

Aeroelastic equilibrium maneuver trim analysis with CFD corrections

Estimation of loads is important part for structural design of aircraft. Accurate estimation will help in reducing the margin of safety during structural design of aircraft. Aero-elasticity is the subject that concerns with the interaction of aerodynamic, inertia and elastic forces. Each of its interaction leads to vibration, flight mechanics, static and dynamic aero-elasticity. Static aero-elasticity considers the non-oscillatory effects of aerodynamic forces acting on the flexible aircraft structure whereas dynamic aero-elasticity considers oscillatory effects on aero-elastic phenomenon. The aim of this research is to estimate the loads that is generated on flexible aircraft due *to* equilibrium manoeuvres which comes under static aeroelasticity. Initially, static aeroelastic analysis of a complete aircraft, for given Mach number and a range of dynamic pressure, under equilibrium maneuver using a potential flow based doublet panel method. Thereafter, trim analysis for select Mach numbers and Reynolds numbers and a range of dynamic pressure, for these equilibrium maneuvers are corrected with high fidelity CFD (RANS) corrections. All RANS simulations were carried out on PARAM PRAVEGA with around 300-500 cores.



Tail buffeting of a trapezoidal planform in a transonic flow

In modern high-performance combat aircraft, the sizing and placement of the vertical and horizontal tail is critical, especially in twin-tail configurations. The vertical tail is subjected to the

effects of unsteady aerodynamic flow and gives rise to buffeting and flutter. At moderate angle of attack the strong energized vortex generated on the suction side surface breaks down into smaller eddies. These turbulent vortical structures then impinge upon the aft horizontal and vertical aerodynamic surfaces, such as the horizontal and vertical tail. Transonic flow over the vertical and horizontal tail, including the influence of the elastodynamics of the wing, nose, forward sweep intake, and fuselage, is investigated using an Unsteady Reynolds-Averaged Navier–Stokes (URANS) solver tightly coupled with a finite element solver for both steady and unsteady flows over over a flat plate model of a trapezoidal wing aircraft planform with vertical and horizontal tail at a moderate angle-of-attack. This study clearly shows that flexible aircraft structure elastodynamics to have significant effect on the unsteady flow over the aircraft when compared to that of a rigid aircraft.

3.1.3.2 SERC's Resources:

All simulations were done on Param Pravega using approximately 500-700 cores.

3.1.3.3 Research Outcome:

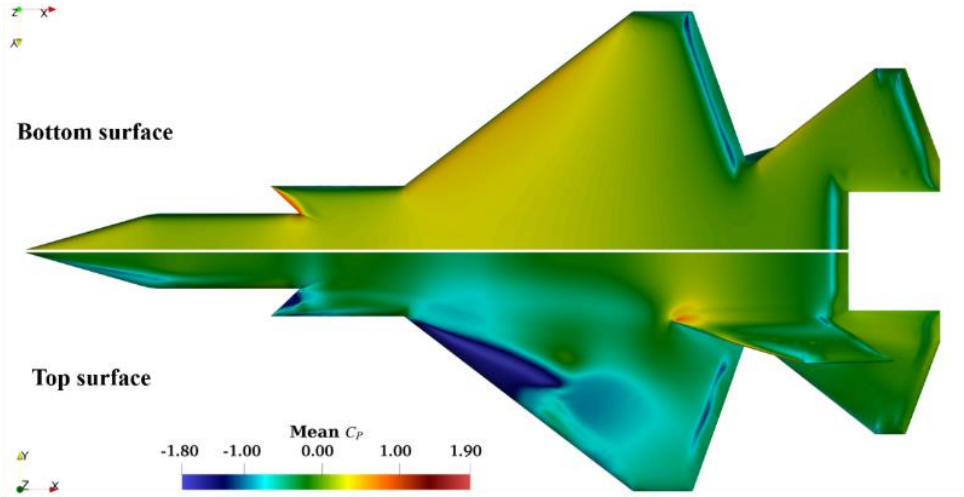
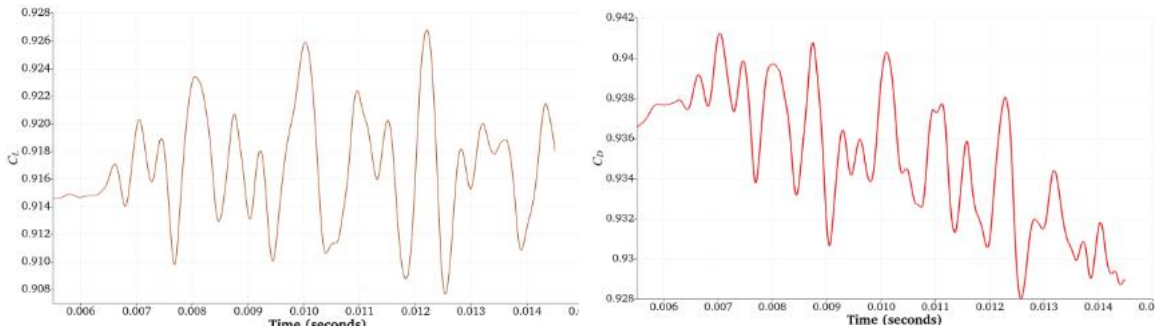


Figure 1 Full flexible aircraft mean CP top and bottom surface



Temporal lift and drag variation on the flexible aircraft

a. Publication

1. M I Vellaisamy Dinu, Adithya Udupa, Sudha U P V, and Kartik Venkatraman. 2025. Horizontal and vertical tail buffeting of a trapezoidal planform in a transonic flow. Aeronautical Society of India 26th Annual CFD Symposium 2025. August 11th - 13th.

3.1.4 Prof. O. N. Ramesh' Lab

3.1.4.1 Problem areas:

This research focuses on the numerical investigation of compressible cavity flow and the resulting acoustic oscillations in a transitional-open cavity configuration. Such flows are particularly relevant in aerospace applications such as aircraft weapon bays, where strong selfsustained pressure oscillations can occur when the cavity door is opened during flight. These oscillations can produce sound pressure levels exceeding 160 dB, posing risks to structural integrity and onboard electronics.

The present work (during the year 2025) investigates the influence of free-stream Mach number on the acoustic characteristics of cavity flows. Detached Eddy Simulation (DES) is employed using the HiFUN solver to capture the unsteady flow structures and pressure fluctuations inside the cavity.

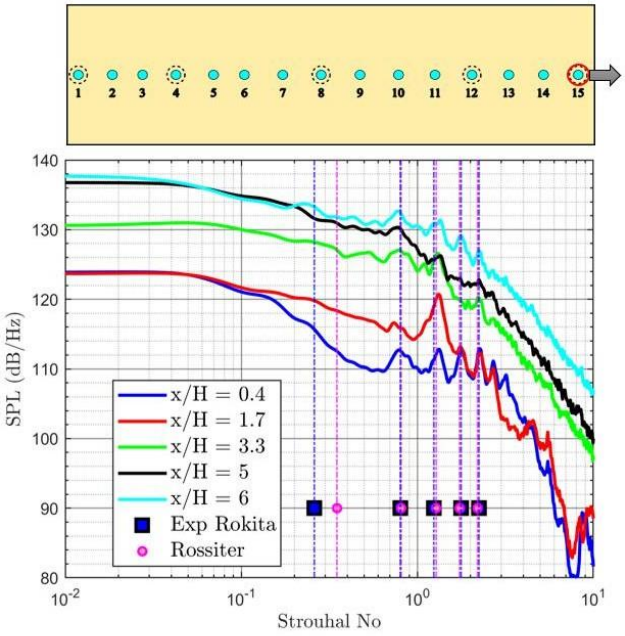


Fig : SPL Plot at the 5 locations of cavity top

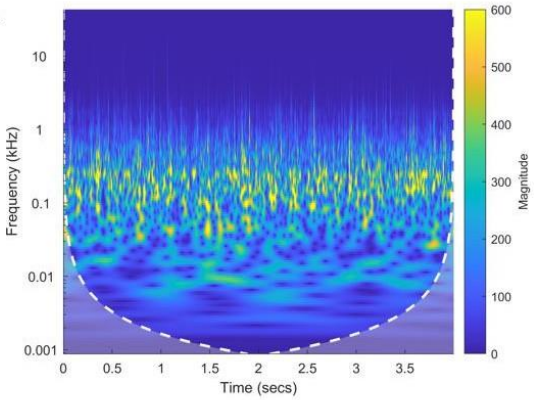


Fig : Time frequency plot at M 0.4 at cavity top (downstream)

3.1.4.2 SERC's resources:

All numerical simulations were performed using the HiFUN compressible flow solver. The computational mesh consisted of approximately 24 million control volumes, with a high concentration of grid refinement within the cavity and shear layer region to accurately capture the dominant flow structures. Generally, 170 or 340 Nodes have been used in Medium and Large Jobs. Each 24 Hr simulation in Medium could give me a physical time step of 70,000 and to conclude on each Mach Number of choice we had to run such 6 runs. As per the queue, for one medium job, we had to wait for 24-28 days.

3.1.4.3 Parallelisation and Performance:

The HiFUN solver was executed in a parallel high-performance computing environment.

The computational workload was distributed across multiple processors using domain decomposition techniques. Each 24 Hr simulation in Medium could give us a physical time step of 70,000 and to conclude on each Mach Number of choice we had to run such 6 runs. As per the queue, for one medium job, we had to wait for 24-28 days. The strategy was such that each core

could handle 3000 cell volumes in finite volume structure. Beyond that the data transfer speed would become more prominent.

3.1.4.4 Research Outcome:

a. Publications:

1. Argha Saha, O. N. Ramesh, and N. Balakrishnan, “Effect of Mach Number on Cavity Acoustics,” 26th Annual AeSI CFD Symposium, Bangalore, India, August 2025. – This paper won 3rd prize in the conference.

3.1.4.5 Problem areas:

Wall-bounded Turbulence Research:

This work is towards solving longstanding, unresolved problems in wall-bounded turbulent flows. Problems such as the scaling laws governing Very Large Scale Motions (VLSMs) and the "bursting" phenomenon—key components of turbulence production have been investigated. Understanding these is critical for applications like turbulence management and drag reduction. Direct Numerical Simulations (DNS) are performed for turbulent channel flow (TCF) using SERC’s Param Pravega HPC facility to completely capture and resolve all scales of the flow, making such simulations computationally highly intensive. This is used to support the experimental data to establish the universality of the developed scalings.

3.1.4.6 SERC's resources:

This work uses SERC’s Param Pravega supercomputers with jobs that involve up to small72 cores at a frequency of 2 jobs/month. The frequency of usage is much higher when using smaller cores due to faster turn around times.

3.1.4.7 Parallelization strategies:

The open source code Incompact3d is employed in performing the DNS. A parallelisation strategy evolving from a 1D dual domain decomposition to a more advanced 2D "pencil" decomposition is employed. Both methods use MPI and global transpose operations to handle implicit high-order schemes.

3.1.4.8 Performance and scalability:

Excellent strong and weak scaling is achieved. The initial 1D decomposition scales well to 1024 cores, while the 2D "pencil" strategy scales acceptably up to O(10^5) cores.

3.1.4.9 Research Outcome:

a. Publications:

1. Raghuram, S., & Ramesh, O. N. (2025). Bursting phenomenon in turbulent wall-bounded flows. Physics of Fluids, 37(2).
2. “Large Scale Motion in a Turbulent Channel Flow” to be submitted to Physical Review Letters shortly.

b. PhD, Masters and UG students graduated during 2022-24, whose work was based on the use of SERC HPC resources.

- PhD Students: Dr. S. Raghuram (2023)

c. Images and videos:

Wall-bounded Turbulence Research:

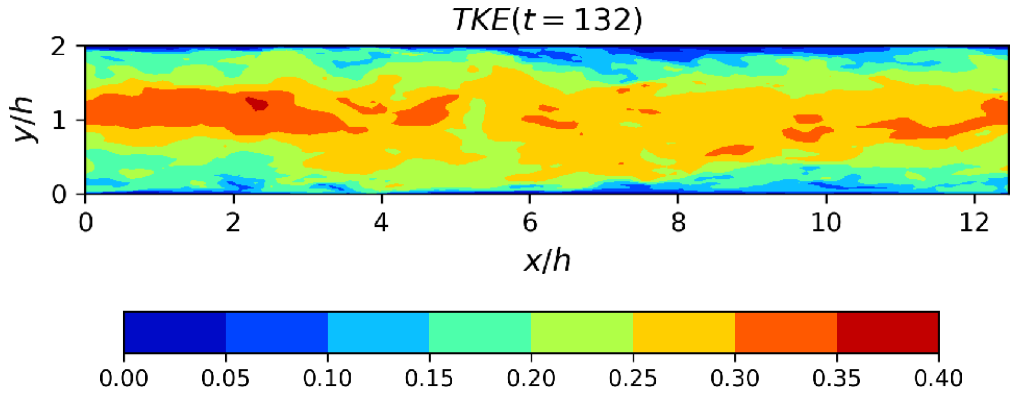


Figure shows turbulent kinetic energy (TKE) contours in a fully developed turbulent channel flow (streamwise (x) - wall-normal (y) plane) using direct numerical simulations (DNS). TKE is low close to the wall due to the no-slip condition, increases away from the wall due to shear-driven vortex stretching, leading to well-formed coherent structures.

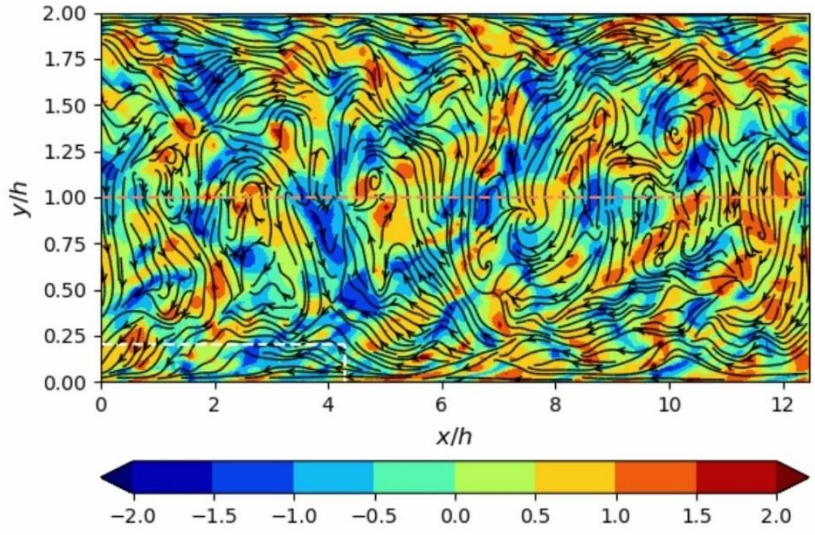


Figure shows correlation contours of streamwise and wall-normal components of velocity. The contours show well-formed inclined structures that extend till and pushing beyond the centerline of the channel, happening alternatively on either sides This is supported by the streamlines juxtaposed on the contours, refereced to the centerline velocity, showing large circulating activity close to the centerline.
Complete animation available here: https://youtu.be/AshyFDribn8

3.1.4.10 Problem area:

This research investigates shock–boundary layer interaction (SBLI) in transonic flows, a phenomenon responsible for wave drag and flow separation in aerodynamic configurations. The study considers turbulent transonic flowover an axisymmetric body with an ellipticalnose, cylindrical midsection, and circular-arc hump. As the boundary layer accelerates over the hump, the flow locally becomes supersonic and forms a shock wave. The resulting adverse pressure gradient induces boundary layer separation, creating an unsteady separation bubble followed by

downstream reattachment. Computational Fluid Dynamics (CFD) simulations were performed to predict shock location, separation bubble dynamics, and low-frequency unsteadiness associated with SBLI. The work also includes low-speed simulations of the same geometry to study separation behaviour and assess turbulence modeling aspects by comparing with experimental measurements. The computational results were validated against wind-tunnel pressure measurements and provide insight into turbulence-model performance for engineering prediction of SBLI phenomena.

3.1.4.11 SERC's Resources:

Computations were performed using the HiFUNCFD solver on the Param Pravega supercomputing facility at SERC, IISc. Unsteady RANS simulations with the Spalart–Allmaras turbulence model were conducted on grids of approximately 42 million cells. Each simulation utilized 170 compute nodes (48 cores per node, 8160 CPU cores) and required about 192 hours of wall-clock time. Additional low-speed laminar simulations were performed using 40 compute nodes (1920 CPU cores) with about 10 hours of wall-clock time per run.

3.1.4.12 Parallelization strategies

The HiFUN solver was executed in a hybrid MPI + OpenMP parallel framework. The computational grid was distributed among MPI ranks using domain decomposition, enabling efficient parallel computation across nodes. Within each node, OpenMP threading was used to exploit shared-memory parallelism and improve CPU utilization. This hybrid strategy helped reduce communication overhead and improve scalability for large CFD simulations.

3.1.4.13 Performance and Scalability:

The solver demonstrated near-linear scalability up to approximately 7000 CPU cores for computational grids of order O(50 million) cells, achieving around 80% parallel efficiency. Access to the Param Pravega HPC facility significantly reduced turnaround time, enabling simulations that previously required several weeks on smaller clusters to be completed within a few days. This computational capability made it feasible to perform long-time unsteady simulations required to capture low-frequency shock motion and separation dynamics.

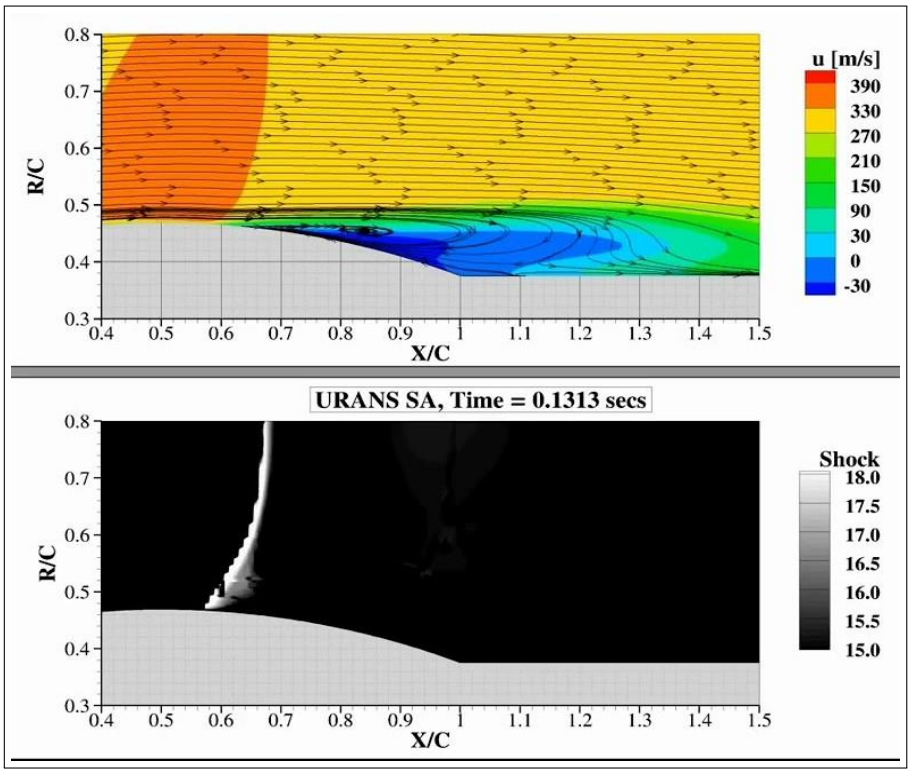


Figure 1 Figure showing instantaneous picture of shock motion and separation-bubble evolution from Unsteady RANS Simulation with Turbulence Model: SA at Transonic Speed. (For Animation, click on the figure

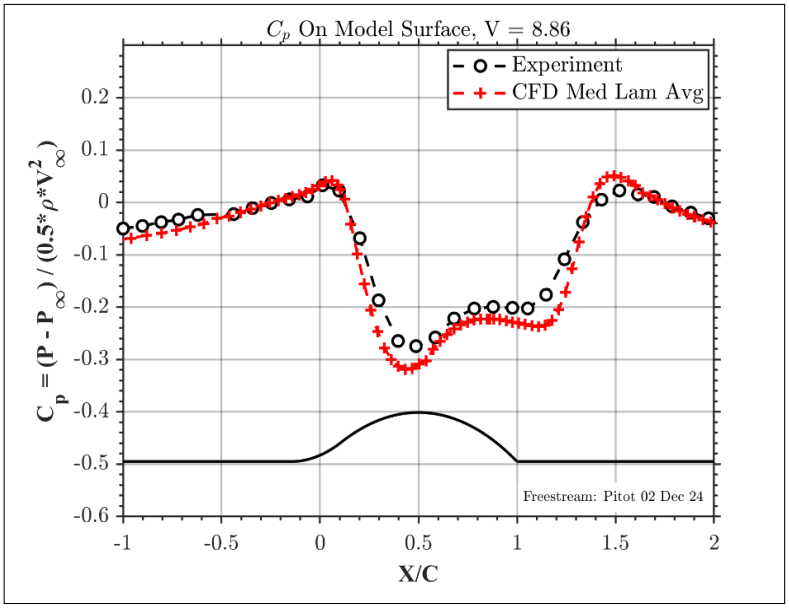


Figure 2 Pressure coefficient (Cp) distributions on Model Wall from Laminar Simulation at low speed. (For Animation, click on the figure)

The simulations contribute to a better understanding of shock–boundary layer interaction in transonic flows, which is important for aerospace vehicle design and aerodynamic performance optimization. Improved predictive capability for SBLI helps in reducing drag, improving stability, and enhancing overall aerodynamic efficiency in aircraft and high-speed aerodynamic systems.

3.1.5 Prof. Rishita Das's Lab

3.1.5.1 Problem areas:

Over the past year, we have leveraged Param Pravega supercomputer to conduct large-eddy simulations (LES) and direct numerical simulations (DNS) of turbulent flows. Specifically, computations and analysis of the following flows were conducted in Param Pravega supercomputer:

- **Shock-wave/turbulent boundary layer interaction (SWTBLI):** LES of supersonic turbulent boundary layers subjected to impinging oblique shocks, targeting to understand the complex coupled dynamics of the shock and wall-bounded turbulence. Information theoretic methods were used to study the low-frequency large-scale motion of the shock and identify the causal mechanisms leading to this unsteadiness.
- **Hypersonic scramjet intake flow:** LES simulations are currently ongoing for hypersonic flow through ISRO scramjet intake geometry, aimed at characterizing flow instabilities and transition mechanisms relevant to propulsion applications.
- **Incompressible turbulent channel flow:** DNS simulations of wall-bounded turbulence with emphasis on identifying and analysing near-wall coherent structures responsible for drag production.
- **Isotropic turbulence and intermittency:** DNS of incompressible isotropic turbulence for the rigorous statistical quantification of intermittency across inertial and dissipation scales.

SERC resources have supported both the execution of these simulations and the large-scale postprocessing and data analysis pipelines. Additionally, NVIDIA DGX-1 and DGX-H100 GPU clusters have been utilized to train scientific ML models for synthetic turbulent inflow generation, super-resolution of turbulent flow fields, and extreme events prediction in turbulent flows.

3.1.5.2 SERC's resources:

Typically, LES/DNS simulations are conducted using 40-50 nodes (1920-2400 cores) over long durations. Machine learning models for turbulence are trained using 1-2 H100 GPU cards at a time.

3.1.5.3 Parallelization strategies:

MPI-parallel codes.

3.1.5.4 Research Outcome:

a. Publication:

1. Muruganandam, A.P., Hemchandra, S. and Das, R., 2026. Oblique Shock Wave/Turbulent Boundary Layer Interaction: Information-Theoretic Approach. In *AIAA SCITECH 2026 Forum* (p. 2341).

b. Contributions to the national/Industry/societal projects due to the executions, and the resulting impact and benefits.

ISRO-IISc STC project on unsteadiness of shock-wave turbulent boundary layer interaction and study of hypersonic flow through scramjet intake. Our simulations are helping understand the flow separation and unsteady characteristics of shock waves in a scramjet engine intake.

c. PhD, Masters and UG students graduated during 2025, whose work was based on the use of SERC HPC resources.

Two MTech students graduated.

3.1.6 Prof Sourabh S. Diwan's Lab

3.1.6.1 Problem areas:

DNS of Speech generated flows

Respiratory diseases like COVID-19 spread through droplets expelled during coughing, sneezing, breathing, and speaking. Speech generates turbulent jets carrying muco-salivary droplets, with the amount expelled strongly depending on speech loudness. Modelling realistic speech flows is challenging due to their complexity and variability. To address this, direct numerical simulations (DNS) of speech flows have been performed using the MEGHA-5 code at the IISc Supercomputing Facility. Two cases were studied: Case I with 10 speech cycles from person 1 and zero flow from person 2 (a silent listener), and Case II with 10 staggered speech cycles from both persons, simulating turn-taking conversation. To more accurately reflect natural human interactions, we also introduced variations in the loudness levels of the two speakers. By changing the domain size (speaker separation) in conjunction with these varying loudness levels, we were able to quantify the exact number of virions that successfully reached the uninfected person. These simulations accurately capture airflow and aerosol transport during complex, asymmetric conversations. Understanding speech-driven aerosol dispersion is key to assessing infection risk in everyday interactions. This research can provide detailed insights to inform public health strategies for managing airborne disease transmission through speech.

3.1.6.2 SERC's resources:

Param Pravega was used for the simulations, utilizing a minimum of 256 cores and a maximum of 512 cores, depending on whether it was a test run or the final high-resolution simulation.

3.1.6.3 Parallelization strategies:

The MEGHA-5 code is used for this work, employing the pencil decomposition method to divide the computational domain among multiple processors along spatial directions. Processor communication is managed via the Message Passing Interface (MPI).

3.1.6.4 Research Outcome:

A journal publication is under preparation

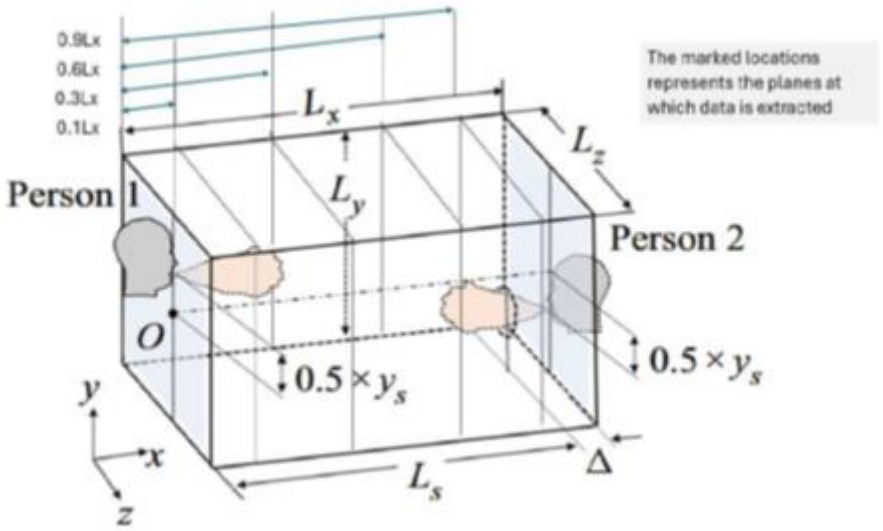


Figure 1: Schematic for computational domain for two-people conversations

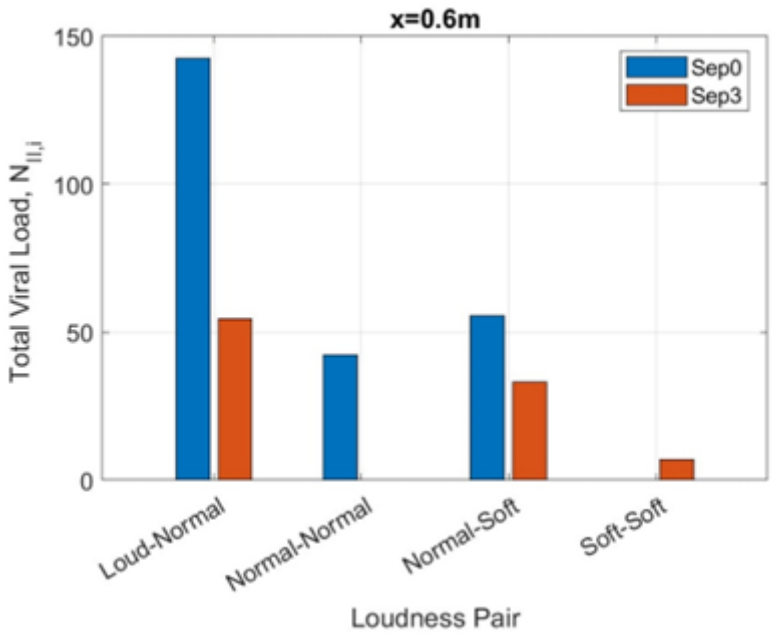


Figure 2 Total viral load on the susceptible speaker (right speaker) for different combinations of speech loudness in two-people conversations. Sep0, Sep3 indicate height differences of 0d and 3d respectively, where d is mouth diameter.

3.1.6.5 Problem areas:

Analysis of speech flows using Convolutional Neural Network

Computational fluid dynamics (CFD) simulations, while crucial for understanding complex physical phenomena like speech-driven aerosol transport during conversations, are computationally expensive. To address this, an efficient data-driven surrogate model was developed using Convolutional Neural Networks (CNNs). A robust, customized U-Net deep learning framework featuring residual dense blocks and attention mechanisms was designed for high-fidelity image-to-image regression on multi-channel CFD data. The model was trained on high-resolution DNS datasets of various speaker configurations (incorporating varying axial separations and vertical offsets) to predict the instantaneous state of complex, unsteady turbulent scalar fields. This AI surrogate allows for a rapid prediction of aerosol exposure and infection risk, offering significant speedups compared to traditional solvers while maintaining reasonable accuracy.

3.1.6.6 SERC's resources:

As detailed in the speech flow work above, the same SERC resources (Param Pravega) were utilized. However, in this specific study, these HPC runs were essential for generating the massive high-fidelity DNS datasets required for training the deep learning model, as well as for providing the ground truth data necessary for comparing and validating the AI predictions.

3.1.6.7 Parallelization strategies:

- **On SERC Resources (Data Generation):** For the foundational high-resolution DNS simulations run on Param Pravega, the MEGHA-5 code employed the pencil decomposition method to divide the computational domain among multiple processors along spatial directions. Processor communication was efficiently managed via the Message Passing Interface (MPI).

- **On External Resources (AI Model Training):** For the subsequent deep learning surrogate model training performed on external NVIDIA A100 GPUs (Google Colab), the pipeline was implemented using PyTorch, CUDA 11.8, and cuDNN 8.5.

a. PhD, Masters and UG students graduated during 2025:

Bhavesh Srivastava, Master of Technology in Aerospace Engineering. Thesis: *"Predicting Aerosol Exposure in Speech-Induced Flow Using Convolutional Neural Network"*.

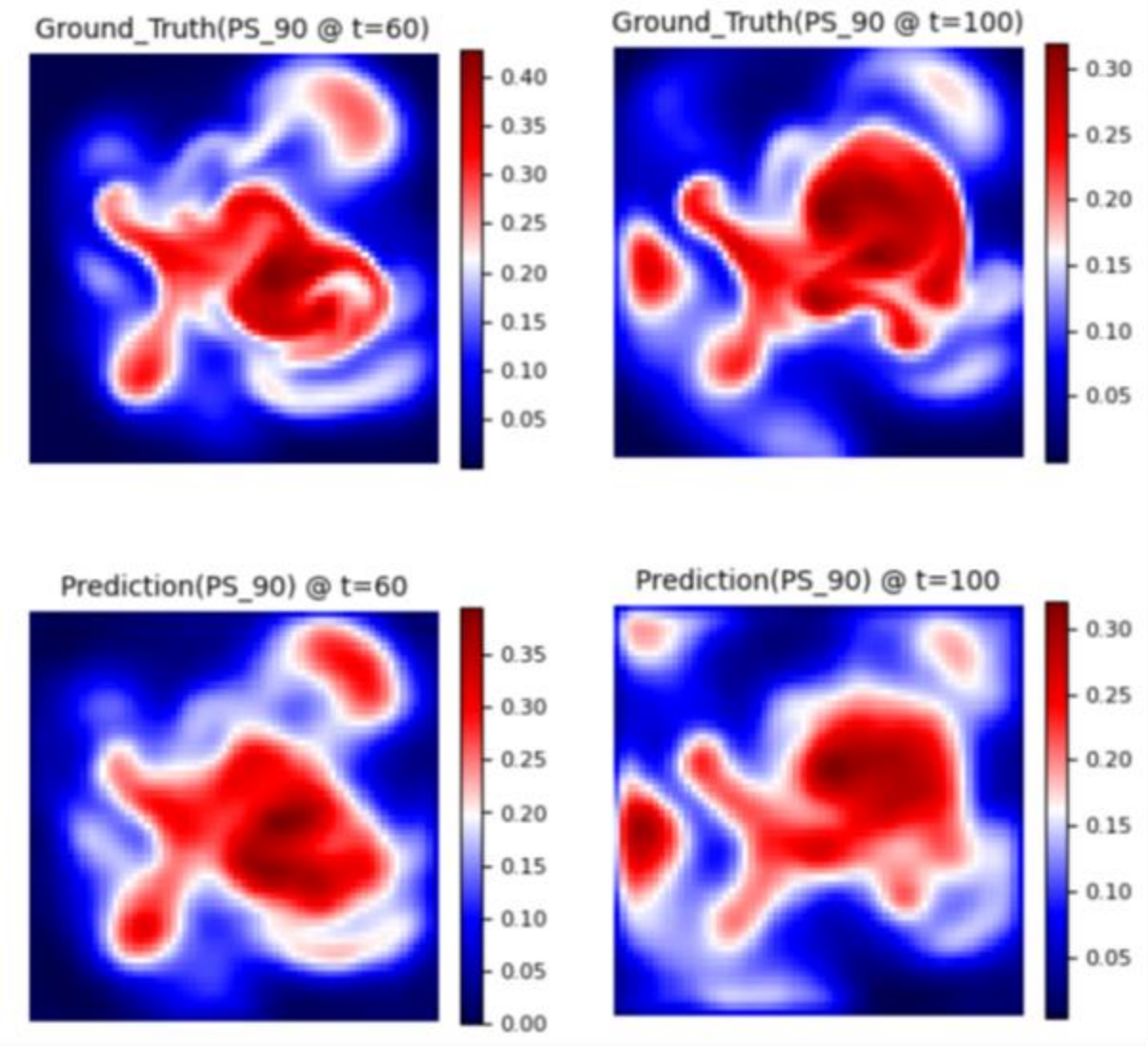


Figure 1 Comparison between ground truth and prediction of speech flow using CNN for two-time instants.

3.2 Centre for Atmospheric and Oceanic Sciences

3.2.1 Prof. Govindasamy Bala's Lab

3.2.1.1 Problem areas:

During 2025, SERC HPC resources were extensively used by Prof. Bala's research group for advanced Earth system modelling studies using the NCAR CESM framework. The primary research areas:

- Impacts of stratospheric aerosol geoengineering (SAG) on tropical hydrology and Indian Summer Monsoon (ISM).
- Quantification of the regional "safe aerosol boundary" for South Asia and its implications for drought risk.
- Paleoclimate simulations examining drivers of $\delta^{18}O$ changes in ISM precipitation between the Last Glacial Maximum and pre-industrial periods.
- Response of Indian monsoon low-pressure systems (LPS) under global warming and solar geoengineering scenarios.
- Forcing-dependent climate sensitivity for CH_4, CO_2, and Black Carbon (BC) forcing.

3.2.1.2 SERC's resources:

- Primary system used: **Param Pravega (SERC HPC facility)**.
- Simulations executed using 240–480 CPU cores for each of the several simulations.
- Large production runs used 480 continuously for ~7 days.
- Total core-hours utilized across projects: approximately 20–22 lakh core-hours during 2025.

3.2.1.3 Parallelization Strategies:

- MPI-based distributed memory parallelism.
- Horizontal domain decomposition for atmosphere (CAM) and ocean (POP) modelling components.
- Concurrent parallel execution of atmosphere, ocean, land, and sea-ice modules.
- Optimized component-wise load balancing across cores.

3.2.1.4 Performance and Scalability:

- Typical throughput: 12-24 model years per wall-clock day (depending on the climate model configuration).
- Some paleoclimate simulations achieved approximately 6–8 model years per wall-clock day.
- Compared to smaller local clusters (32 cores), SERC HPC reduced simulation time by approximately 3–4 times.

3.2.1.5 Research Outcome:

a. Journal Publications (2025)

1. Neethu, C., Tharammal, T., & Bala, G. (2025) A model-based assessment of the regional safe aerosol boundary for the South Asian monsoon region. Environmental Research Letters, 20(12), 124057. https://iopscience.iop.org/article/10.1088/1748-9326/ae2345
2. Kumar, S., A. K. Seshadri, and G. Bala, 2025: Contrast in Slow Climate Response to Methane and Carbon Dioxide Forcings Identified Using the Radiative Kernel Technique. J. Climate, 38, 6307–6328, https://doi.org/10.1175/JCLI-D-24-0728.1

3. Tharammal, T., Bala, G., & Nusbaumer, J. (2026), Drivers of the $\delta^{18}O$ Changes in Indian Summer Monsoon Precipitation between the Last Glacial Maximum and Pre-industrial Period. Climate of the Past, https://cp.copernicus.org/articles/22/427/2026/.

b. Conference Presentations

1. **Singh, M., Bala, G., & Seshadri, A. K. (2026)** *Response of the Characteristics of Monsoon Low-Pressure Systems to Stratospheric Aerosol Geoengineering during the Indian Summer Monsoon Season.* 106th Americal Meteorological Society Annual Meeting, Houston, Texas, US.
2. **Singh, M., Bala, G., & Seshadri, A. K. (2025)** Biases *in model simulations of Indian Summer Monsoon low-pressure systems.* European Geophysical Union meeting, Vienna, Austria

c. Contributions to National / Societal Impact

- Quantitatively established a regional safe aerosol limit for South Asia, directly relevant for air quality regulation and climate-risk policy.
- Demonstrated increased drought risk under elevated aerosol optical depth conditions.
- Improved quantitative understanding of differences in climate system response between methane (CH_4) and carbon dioxide (CO_2).
- Advanced modelling of monsoon low-pressure systems under solar geoengineering and extreme precipitation risk assessment.
- Hydrological impacts of solar geoengineering interventions.

d. Awards and Press Releases

Press release on safe regional Earth system boundary for aerosol loading over South Asia region:

- Earth Commission, Future Earth, Sweden: https://earthcommission.org/aerosol-boundary-confirmed-increased-air-pollution-could-tip-monsoon/
- IISc news magazine Kernel: https://kernel.iisc.ac.in/influence-of-aerosols-on-indian-summer-monsoon/

Images

Typical HPC-generated outputs include:

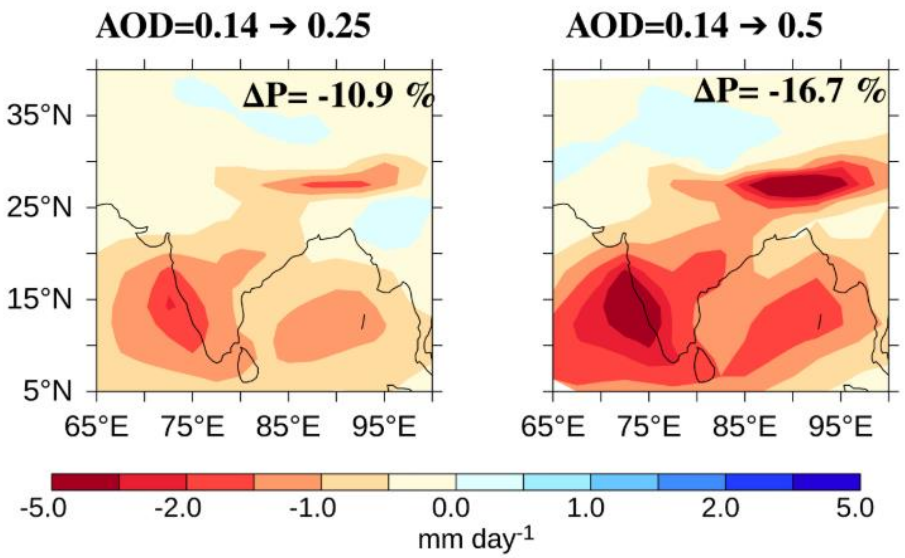


Figure 1: *Model-simulated spatial distribution of June–September (JJAS) mean precipitation change (ΔP; mm day $^{-1}$) over South Asia under enhanced aerosol forcing. Aerosol Optical Depth (AOD) over South Asia is increased from the present-day value (AOD = 0.14) to 0.25 (2.7× increase of aerosol burden) and 0.50 (~5.5× increase of aerosol burden). When regional mean aerosol loading increases to AOD = 0.25, the model simulates a ~10.9% reduction in Indian summer monsoon rainfall relative to the baseline state, indicating drought conditions. Further enhancement to AOD = 0.50 results in an additional reduction of approximately 16.7%. The domain-averaged percentage change in precipitation is indicated in the top-right corner of each panel.*

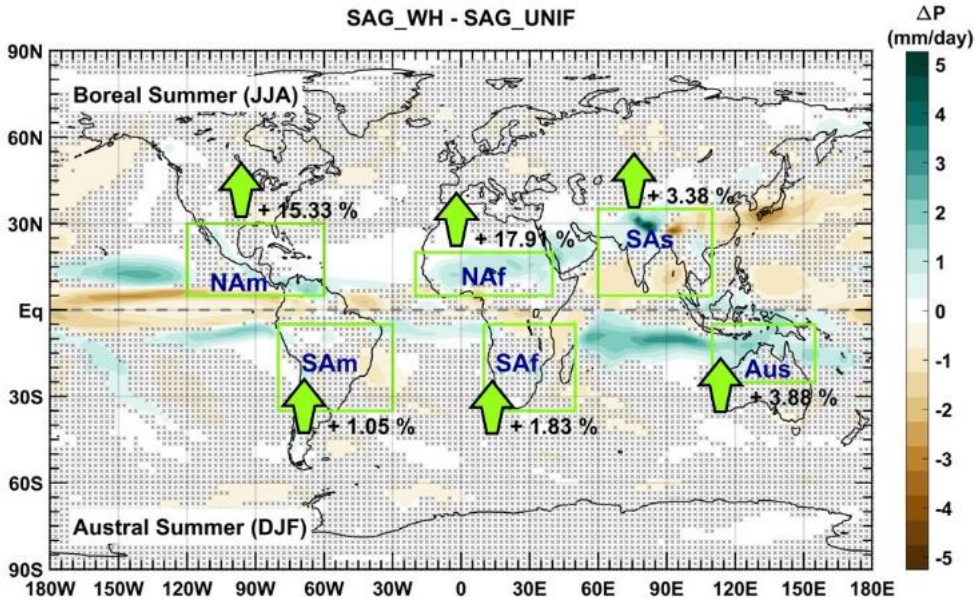


Figure 2: *The figure shows the summertime (June to August over Northern Hemisphere and December to February over Southern Hemisphere) rainfall difference between implementing stratospheric aerosol geoengineering (SAG) only in the winter hemisphere*

(SAG_WH) and implementing SAG uniformly around the globe (SAG_UNIF). Both SAG strategies are designed to cool the global mean warming by 1.9 C. The extent of six monsoon regions: South Asia (SAs), North Africa (NAf), North America (NAm), Australia (Aus), South Africa (SAf), and South America (SAm) are indicated by green boxes. We see that the summer rainfall is increased in the SAG_WH case compared to SAG_UNIF across all the six tropical monsoon domains

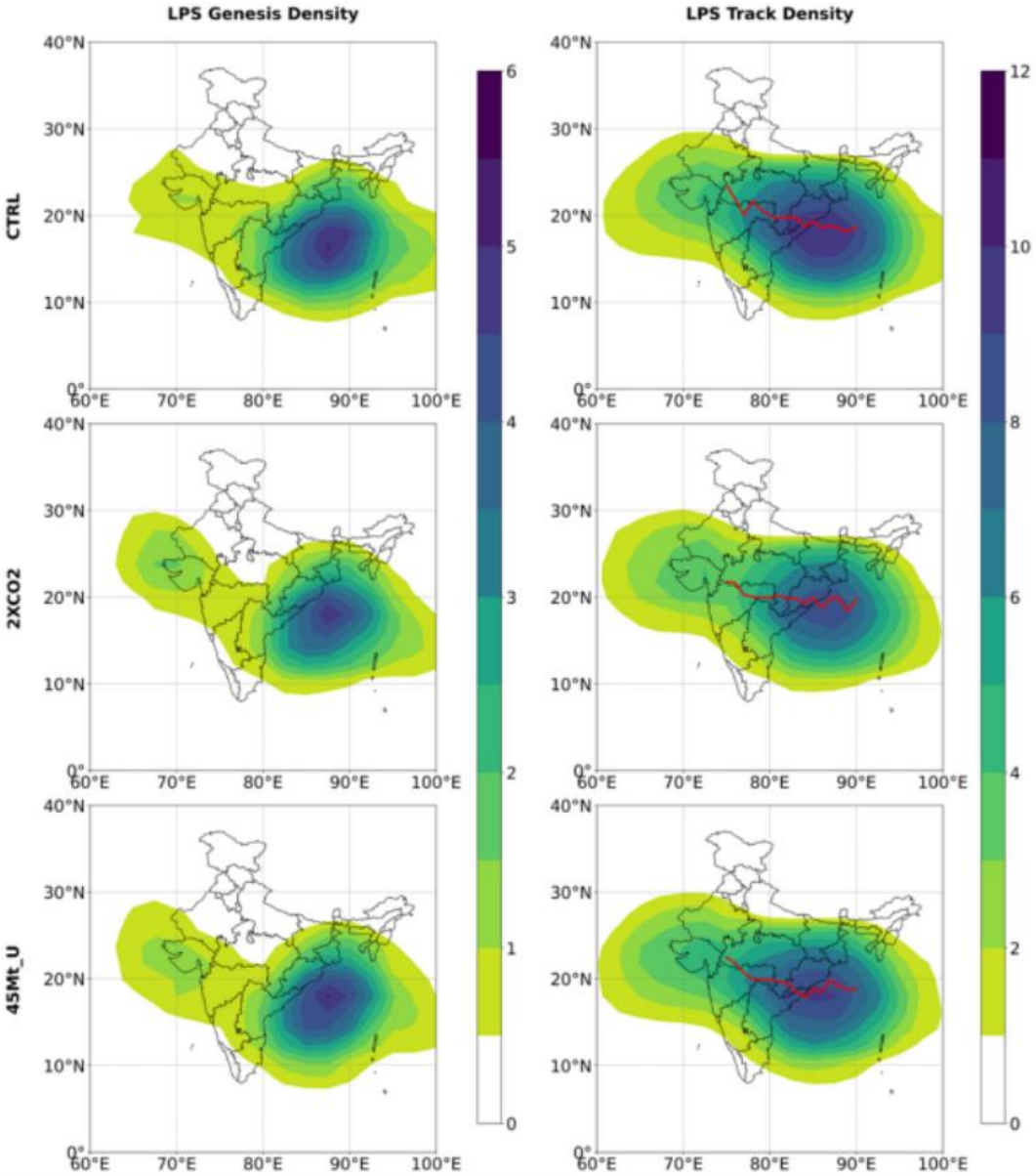


Figure 3: Low-pressure system (LPS) tracking diagnostics under global warming and stratospheric aerosol geoengineering (SAG). LPS (a–c) genesis density and (d–f) track density, defined as the number of genesis locations or the number of tracks passing within a 500-km radius of each grid point per year, for the baseline simulation, CTRL (top row; present day control climate with baseline greenhouse gas concentrations), 2XCO$_2$ (middle row; idealized warming experiment with doubled atmospheric CO$_2$), and 45Mt_U (bottom row; SAG experiment with prescribed uniform stratospheric sulphate aerosols of 45 megatons to offset greenhouse warming) experiments. The left column shows genesis density, and the right column shows track density. In the track density panels (d–f), the solid red line denotes the LPS median track.

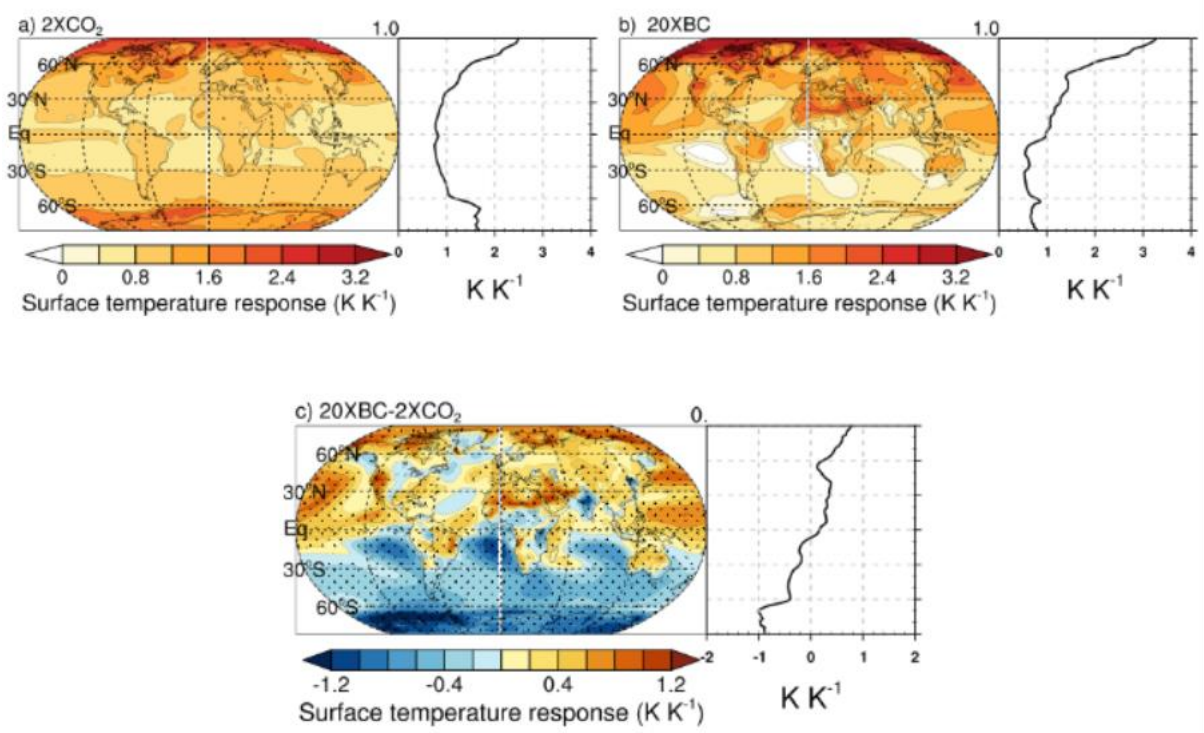


Figure 4*: Model-simulated spatial pattern of equilibrium surface temperature change (ΔTs) per unit global mean surface temperature change (in K K-1) in the (a) 20×BC, (b) 2×CO2 cases relative to baseline CTL (control) simulation and (c) the difference between two cases (20×BC - 2×CO2). In the simulation, 2xCO2, atmospheric CO2 concentration is doubled relative to CTL, and the black carbon concentration is increased by 20 times in the 20xBC simulation. The line plots show the corresponding zonal mean changes. Under* ***2×CO2****, warming is broadly hemispherically symmetric, with pronounced Arctic amplification and enhanced high-latitude warming in both hemispheres (Fig. a). In contrast, the* ***20×BC*** *simulations shows a strong asymmetric pattern: warming is concentrated in the Northern Hemisphere (NH), especially at high latitudes, while much of the Southern Hemisphere (NH) warms weakly (Fig. b). The difference map (Fig. c) highlights this structure, showing relative warming enhancement under BC in the NH and relative suppression in the SH, most clearly over the Southern Ocean.*

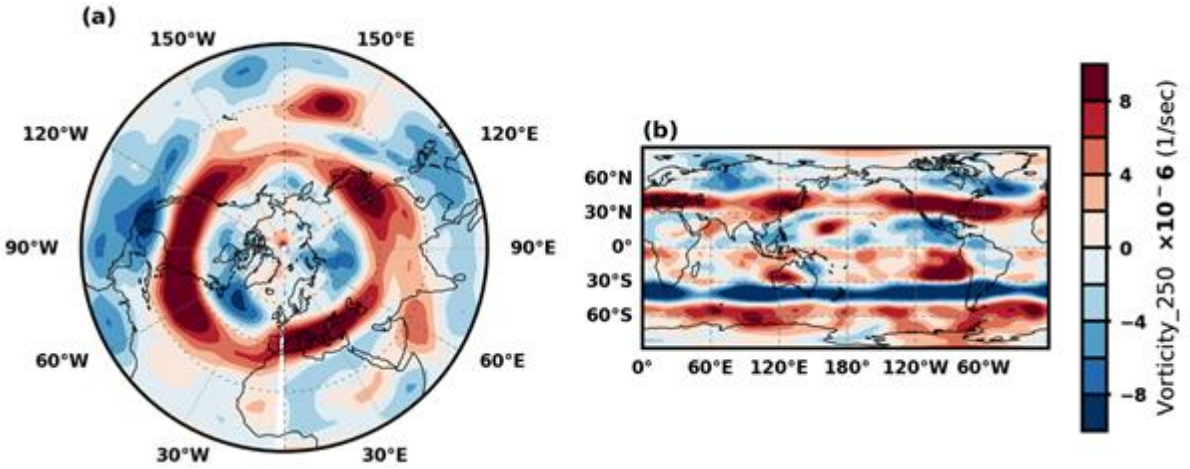
3.2.2 Prof. Jai Sukhatme's Lab

3.2.2.1 Problem areas:

Param Pravega was employed to run a set of global climate model experiments with CESM2.1.3 in an idealized "aquaplanet" configuration. The simulations were designed to study how tropical heating patterns influence large-scale atmospheric circulation. In this setup, the model planet is covered by oceans and is forced with simplified sea-surface temperatures. Specifically, our interest is in the El Nino Southern Oscillation (ENSO), and we therefore use sea surface conditions that occur during these events. Each experiment

was run at 2° spatial resolution using 384 MPI tasks for the atmosphere and 384 for the ocean and was integrated for roughly 4 model years.

From these runs, we produced a set of diagnostics that clearly illustrate the circulation response to the imposed heating patterns. These include global maps and vertical sections of zonal and meridional winds, temperature and vorticity at upper and lower levels of the troposphere. Further, latitude–pressure sections of differences between the control and perturbed experiments highlight changes in jet strength and vertical structure, the meridional overturning circulation, and upper-tropospheric vorticity anomaly fields that emphasize stationary wave patterns and extratropical teleconnections. An example of these distinct changes is provided in the figure below which shows the difference in the upper tropospheric vorticity between an El Nino year and the climatological mean control experiment. Indeed, changes in the midlatitude jet as well as in tropical stationary waves are clearly discernable.



3.2.3 Prof Arindam Chakraborty's Lab.

3.2.3.1 Problem areas:

El Niño–Southern Oscillation (ENSO) is the dominant mode of interannual climate variability in the tropical Pacific, oscillating between El Niño and La Niña on 2–7 year timescales and typically peaking in boreal winter before transitioning through spring. In recent decades, however, these winter-to-summer transitions have become more irregular, reflecting stronger tropical–extratropical interactions that modulate equatorial trade winds and, in turn, the ENSO lifecycle. In our study, we identify a distinct multidecadal climatic mode - characterized by a zonal sea-level pressure dipole over the extratropical South Pacific during boreal spring - that influences equatorial zonal winds and modulates the persistence of Niño3.4 SST anomalies from winter into summer; we refer to this mode as the ENSO Transition Mode (ETM). To isolate the atmospheric response to ETM-related low-frequency SST variability and assess its implications for multidecadal global monsoon variability- especially over the Indian and African monsoon regions - we designed a suite of Community Earth System Models version 2 (CESM2) - Community

Atmospheric Model version 6 experiments with prescribed sea-surface temperature patterns, enabling controlled attribution of regional monsoon circulation and rainfall responses to ETM-associated oceanic forcing.

3.2.3.2 SERC's resources:

All simulations were performed on SERC PARAM Pravega (CPU nodes) supercomputing facility. CESM2 was run at ~1° spatial resolution with daily output, using 6 nodes × 48 cores per node (288 CPU cores) per job. Runs were submitted through SLURM (sbatch) on the small partition with exclusive node allocation to ensure consistent performance. The workflow included a 30-year control integration executed as 15 chained 2-year segments using restart files to avoid long walltime constraints, followed by 30 branch runs of ~9 months each. The numerical modelling experiment required a total computational time of around **2,28,480 core-hours** excluding compilation and post-processing. The model build environment on Param Pravega used Intel compilers and parallel NetCDF/FORTRAN libraries.

3.2.3.3 Research Outcome:

These simulations provide a mechanistic basis for interpreting multidecadal shifts in monsoon rainfall distribution over vast monsoon-vulnerable regions like South Asia and Africa. The resulting model outputs and diagnostics directly support the Journal of Climate manuscript and create a reusable dataset for follow-on studies of multidecadal variability of climate and teleconnection pathways.

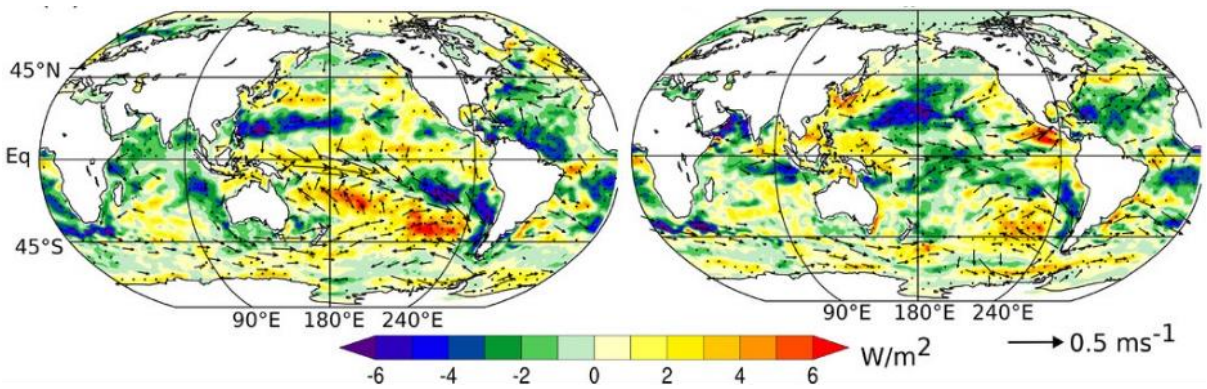


Figure: Spatial linear regressions of the ENSO transition mode with time scale exceeding 30 years against 10-m surface wind and surface latent heat flux anomalies in March-April-May (left) and June-July-August (right). Stippling indicates grid points where the signals are statistically significant at the 95% confidence level, based on Student's t test. Only vectors that are significant above the 95% confidence level and greater than 0.15 m/s are shown.

a. Publications:

1. Srivastava, Shikhar, Arindam Chakraborty, and Raghu Murtugudde, 2026: Unravelling the Teleconnections: Southern Hemisphere ENSO Transition Mode and the Global Boreal Summer Monsoons, Journal of Climate, 39, 861-874, doi: https://doi.org/10.1175/JCLI-D-25-0611.1

2. Samuel, J.B., and A. Chakraborty, 2023: Integration of a Groundwater Model to the Noah Land Surface Model for Aquifer-Soil Interaction, Journal of Advances in Modeling Earth Systems, doi: https://doi.org/10.1029/2022MS003153
3. Chakraborty, A., JB Samuel, and A. Paleri, 2023: Role of land-surface vegetation in the march of Indian monsoon onset isochrones in a coupled models, Quarterly Journal of the Royal Meteorological Society, 149, 115-132, doi: https://doi.org/10.1002/qj.4398

3.3 Centre for Earth Science

3.3.1 Prof. Attreyee Ghosh' Lab

3.3.1.1 Problem areas:

The Earth's mantle undergoes solid state convection over very long-time scales. Employing the fluid dynamical behavior of the mantle, we attempt to understand various observed phenomena on the Earth's surface. We solve the governing equations for mantle convection, which are based on the conservation of mass, momentum, and energy, along with the constitutive equation, using a finite element open-source code called CitcomS. Some of the problems my group has worked on using the SERC HPC system during Jan-Dec 2025 are: the sudden acceleration of the Indian plate 65 million years ago (Pal & Ghosh, in Review), comparing different plate reconstruction models using geodynamic constraints (Pal & Ghosh, in Revision), understanding the dynamics behind the observed anisotropy pattern in western United States (Aashruti et al., in Review), explaining the complex deformation in the India-Eurasia deformation zone, implementing visco-plastic rheology in global forward models of mantle convection. For the time-dependent convection models, we impose reconstructed plate motions as surface velocity boundary condition, which drive flow within the model mantle. Imposing these reconstructed velocities every 1 Myr starting from 140 Main forward models of mantle convection, we predict present-day temperature anomalies throughout the mantle, as well as surface observations, such as the geoid and dynamic topography. Another problem that my group is working on is building seismic tomography models that are constrained by geodynamics using neural network.

3.3.1.2 SERC's resources:

We used the CPU cores both in Param Pravega as well as in RNC. The runs in Param Pravega mostly used 384 cores while those in RNC used 96 cores. For the neural network problem, we used 2 GPU's in the NVIDIA DGXH100 cluster.

3.3.1.3 Research Outcome:

a. Publications

1. Aashruti, A. Ghosh, E. Humphreys, Western US Anisotropy: Role of Slabs, Lateral Viscosity Variations and Small- Scale Heterogeneity, Journal of Geophysical Research, (in Review).
2. D. Pal, A. Ghosh, What caused the sudden acceleration of the Indian plate during the late Cretaceous: Reunion Plume vs Double Subduction, Geology, (in Review).
3. D. Pal, A. Ghosh, On the consistency of plate reconstruction models using geodynamic constraints, Gcubed (in Revision).

b. PhD, Masters and UG students graduated during 2025

Debanjan Pal defended his PhD thesis in October 2025 and is now a postdoc at Columbia University, USA

3.4 Chemical Engineering

3.4.1 Prof. Ananth Govind Rajan's Lab

3.4.1.1 Problem areas:

During 2025, SERC's HPC resources supported extensive first-principles, atomistic, and multiscale simulations across two-dimensional materials, membranes, catalysis, and nanofluidics. Large-scale quantum-mechanical density functional theory (DFT) and kinetic Monte Carlo calculations enabled the prediction of size- and environment-dependent nanopore evolution in MoS_2, clarifying how irregular pores transition to triangular topologies for applications in separations and sensing. Hyper-realistic computational fluid dynamics (CFD) digital-twin simulations captured precursor-flux gradients and near-zero-velocity zones in chemical vapor deposition reactors, explaining nucleation-density control crucial for wafer-scale 2D-material growth. Molecular dynamics (MD) studies of interpenetrating-network-stabilized graphene-oxide membranes quantified water and ion transport in nanosieving applications, matching experimental performance metrics and guiding membrane design. DFT calculations for Ni-doped MoO_3 identified reduced oxygen-evolution overpotentials and provided mechanistic insights into overcoming activity–stability trade-offs in alkaline electrolysis. Ab initio MD-derived force fields for functionalized hBN nanopores enabled realistic modeling of water/ion transport, correcting overestimates arising from earlier bare-edge simulations and improving desalination predictions. In collaborative work, MD simulations of confined water in twisted MoS_2 and graphene revealed that identical structural motifs yield markedly different thermodynamic, dielectric, and frictional responses, informing nanoscale fluidic device engineering. Finally, atomistic modeling of surface and edge functionalization in graphene and graphene oxide clarified how chemical modifications tune mechanical response, supporting the rational design of robust 2D composites. Collectively, these HPC-driven studies provided predictive understanding across electronic-structure, molecular-dynamics, and continuum scales, advancing fundamental and applied research in catalysis, separations, and nanomaterials.

3.4.1.2 SERC's resources:

Our group made use of the Param Pravega supercomputer, the Roddam Narasimha cluster, and the DGX system. We relied on both CPU- and GPU-based computing, typically running jobs that required between 96 and 240 CPU cores along with multiple GPUs.

3.4.1.3 Parallelization strategies:

The workflows relied on parallel implementations within the open-source Large-scale Atomic/Molecular Massively Parallel Simulator (LAMMPS), GROningen MAchine for Chemical Simulations (GROMACS), and CP2K packages, as well as the commercial Vienna Ab initio Simulation Package (VASP) code.

3.4.1.4 Research Outcome:

a. Publications:

1. Bhowmik, S., **Govind Rajan, A.*** Size and Chemical Environment Control Nanopore Geometry in 2D MoS_2: From Irregular to Triangular Defects. *Small* **2025**, 21, 33, pp 2504611.
2. Sinha, A., Verma, M., Kumar, N., Kumar, K. S., **Govind Rajan, A.***, Singh, A.* Critical Role of Precursor Flux in Modulating Nucleation Density in 2D Material Synthesis Revealed by Digital Twin. *Nanoscale Adv.* **2025**, 7, pp 3568–3578.
3. Sen Gupta, R., Islam, S. S., Dhondi, P., Jose, T., **Govind Rajan, A.***, Bose, S.* Sequential Interpenetrating Polymer Network Confines Shear-Aligned Graphene Oxide Liquid Crystals Enabling Precise Molecular Sieving. *Small* **2025**, pp 2503746.
4. Verma, A. K., Atif, S., Padhy, A., Choksi, T. S., Barpanda, P., **Govind Rajan, A.*** Robust Oxygen Evolution on Ni-Doped MoO_3: Overcoming Activity-Stability Tradeoff in Alkaline Water Splitting. *Chem Bio Engg*. **2025**, 2, 4, pp 241–252. (*Invited article for the special issue "Electrochemical Engineering for Sustainability"*.)
5. Ghorai, S., Pradeep, D., **Govind Rajan, A.*** Molecular Dynamics Simulations of Functionalized hBN Nanopores in Water: Ab Initio Force Field and Implications for Water Desalination. *J. Chem. Phys*. **2025**, 162, 044705. (*Invited article for the special issue "Molecular Dynamics, Methods and Applications 60 Years after Rahman"*.)
6. Majumdar, J., Mandal, S., **Govind Rajan, A.**, Maiti, P. K.* Similar Structure but Different Thermodynamic, Dielectric, and Frictional Properties of Confined Water in Twisted 2D Materials: MoS_2 vs. Graphene. *Nanoscale* **2025**,17, pp 2354–2364.
7. Sharma, B. B., Kedare, A., Muralidharan, G., **Govind Rajan, A.*** Understanding the Effects of Surface and Edge Functionalization on the Mechanical Properties of Graphene and Graphene Oxide. *ChemPhysChem* **2025**, 26, 5, e202400919. (*Invited article, included in the special topics "Hot Topic: Carbon, Graphite, and Graphene" and "Hot Topic: Surfaces and Interfaces"*.)

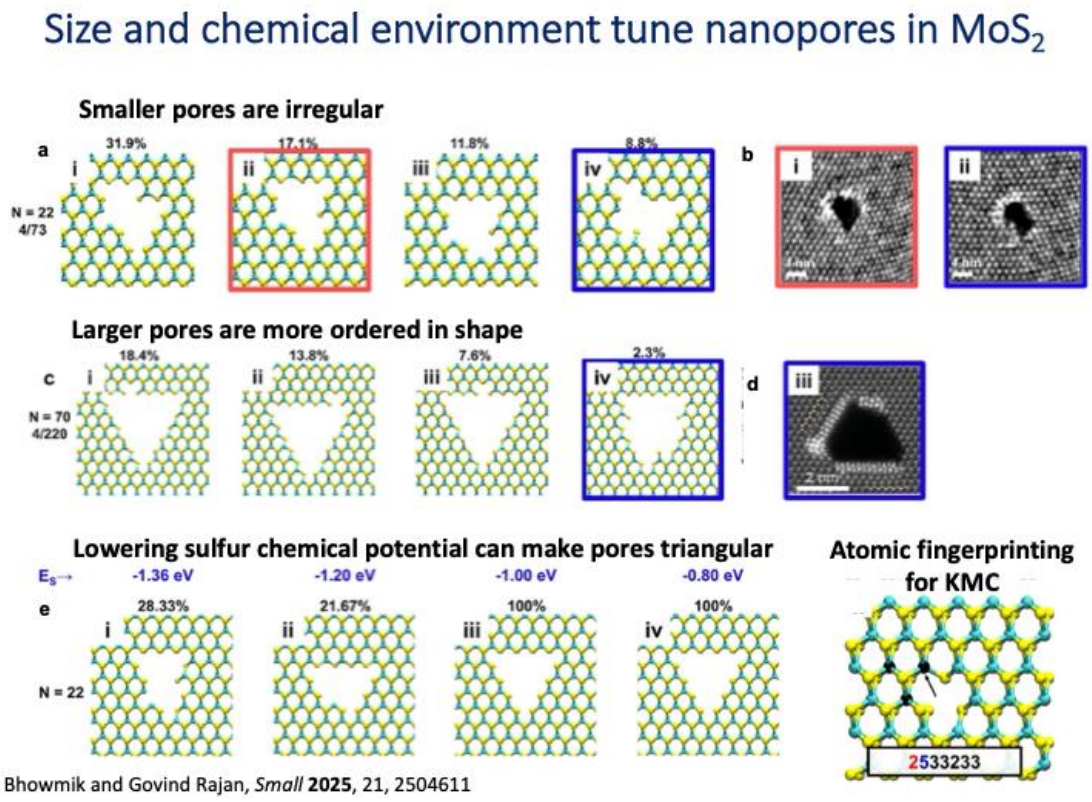
b. Contributions to the national/Industry/societal projects due to the executions, and the resulting impact and benefits.

The HPC-driven research efforts contributed directly to national, industrial, and societal priorities by advancing capabilities in clean energy, water purification, and advanced materials. First-principles and multiscale simulations supported catalyst discovery for sustainable water-splitting technologies, building on Ni-doped MoO_3 studies that identified low-overpotential oxygen-evolution pathways essential for green-hydrogen initiatives [supported by the **National Supercomputing Mission (NSM)**]. High-fidelity molecular-dynamics frameworks for functionalized hBN and graphene-oxide membranes provided insights into nanoscale water transport and ionic rejection, strengthening efforts toward affordable desalination and clean-water programs [supported by the **Anusandhan National Research Foundation**]. Digital-twin CFD models of CVD reactors accelerated the controlled synthesis of large-area 2D materials, informing scale-up strategies that are valuable to semiconductor and materials-manufacturing companies [supported by the **NSM**]. Atomistic simulations of nanopore formation in MoS_2 further enabled predictive membrane design relevant to separations and sensing applications [also supported by the **NSM**]. Collectively, these HPC-enabled advances bolster national missions in renewable energy and water security, provide industry with scientifically grounded pathways for catalyst optimization and 2D-materials fabrication, and

ultimately support societal goals in sustainability, resource efficiency, and environmental resilience.

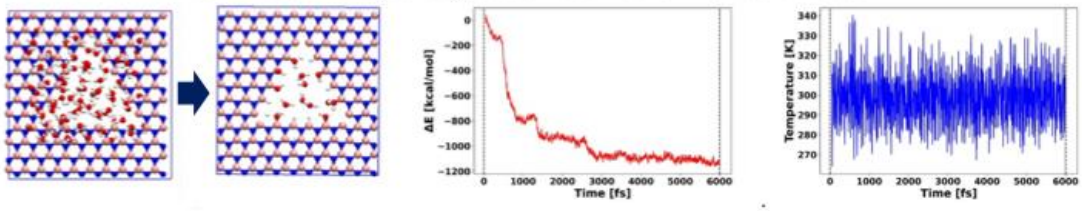
c. PhD, Masters and UG students graduated during 2025, whose work was based on the use of SERC HPC resources.

Name	Position	Onward Position
Raghavendra Rajagopalan	MTech Student (2023-25)	Project Associate, Indian Institute of Science
Virajkumar Pranavkumar Bhatt	MTech Student (2023-25)	Physical Science Researcher, Tata Research, Development and Design Centre
Kushagra	MTech Student (2023-25)	Officer, R&D, Hindustan Petroleum Corporation Limited

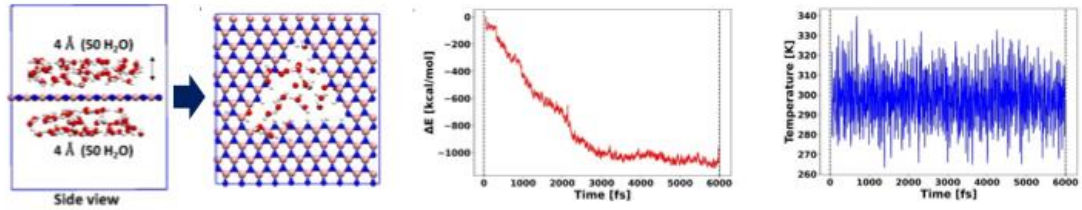


Ab initio molecular dynamics (AIMD) simulations reveal edge-dependent functionalization in hBN

B-terminated nanopores get alternate H & OH functionalization



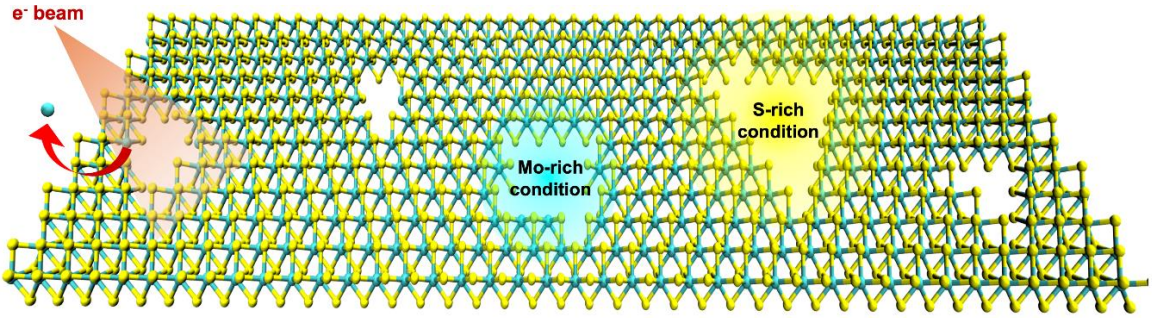
N-terminated nanopores get H & occasional O functionalization



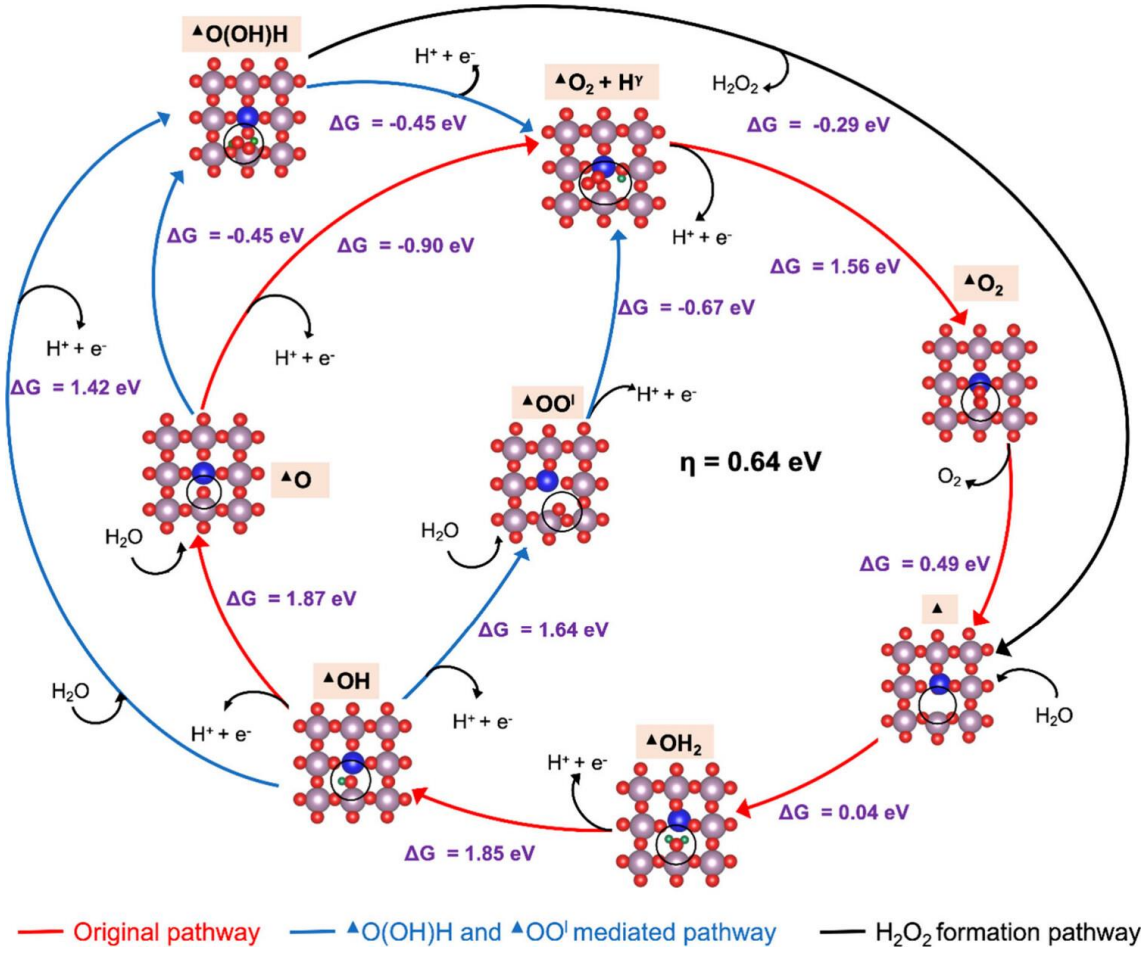
Can we use DFT calculations to design classical force fields for functionalized hBN?

Ghorai, Pradeep, and Govind Rajan, *J. Chem. Phys.* **2025**, 162, 044705

A schematic description of nanopores formed in 2D MoS_2, using multi-scale simulations



Pathway for the oxygen evolution reaction involved in electrochemical water splitting for green hydrogen production on Ni-doped MoO_3



3.4.2 Prof. Ganapathy Ayappa's Lab

3.4.2.1 Problem areas:

Membrane-Protein Biophysics: We have studied the influence of oxidized sterols and cholesterol on G-protein coupled receptors (GPCR) and pore forming proteins binding in phospholipid membranes using all-atom simulations. The membrane inserted critical signalling residues of CXCR4 helices which function in the presence of cholesterol remain strongly bound to oxysterols. The presence of oxysterols in aged and senescent cells has been shown to down regulate CXCR in the laboratory of Prof Deepak Saini and our computation study has shed light on the molecular reasons for this phenomenon. In other studies bipartite toxin assembly pathways has been investigated using molecular dynamics simulations

2D Nanoporous Materials: In an earlier study we have shown that 2D graphene nanopores enhance evaporation rates of water. We have extend these simulations to study evaporative separations of liquid mixtures like methanol-water and gas mixtures containing CO_2, N_2 and O_2. Flexibility of edge functional groups has shown to modulate gas transport and selectivity. These materials can potentially be used for low energy evaporative separations.

3.4.2.2 Research Outcome:

a. Publications

1. YaxA Pre-Pore Formation Underlies Bipartite YaxAB Toxin Assembly on Living Membranes, Harsh Kumar, Ganapathy Ayappa, Sandhya S. Visweswariah, and Vaishnavi Ananthanarayanan, Biophysical Journal (2025) https://doi.org/10.1016/j.bpj.2025.12.027
2. Perturbing Angstrom-Scale Interfacial Clusters in Functionalized Nanoporous Graphene for Selective Evaporative Methanol-Water Separations, Bharath Desikan and K. Ganapathy Ayappa, ***Langmuir,*** 41, 32, 21368–21379 (2025) DOI: 10.1021/acs.langmuir.5c01833
3. Oxysterols Outcompete Cholesterol Binding to the Membrane Inserted Cytolysin A Pore Complex, Samlesh Choudhury, K. Ganapathy Ayappa, ***Journal of Membrane Biology*** (2025) https://doi.org/10.1007/s00232-025-00349-0
4. Gated CO_2 Permeation across Dynamic Graphene Pores, Luc Bondaz, Anshaj Ronghe, K. Ganapathy Ayappa, Kumar Varoon Agarwal, ***Nature Communications*** 16, 6252 (2025). https://doi.org/10.1038/s41467-025-61518-2
5. Oxysterols Modulated Protein-Sterol Interactions to Impair CXCR4 Signalling in Aging Cells, Suramya Asthana, Anant Verma, Baivabi Bhattacharya, K. Ganapathy Ayappa, Deepak Kumar Saini, ACS-Biochemistry, 64 1606–1623 (2025) https://doi.org/10.1021/acs.biochem.4c00617

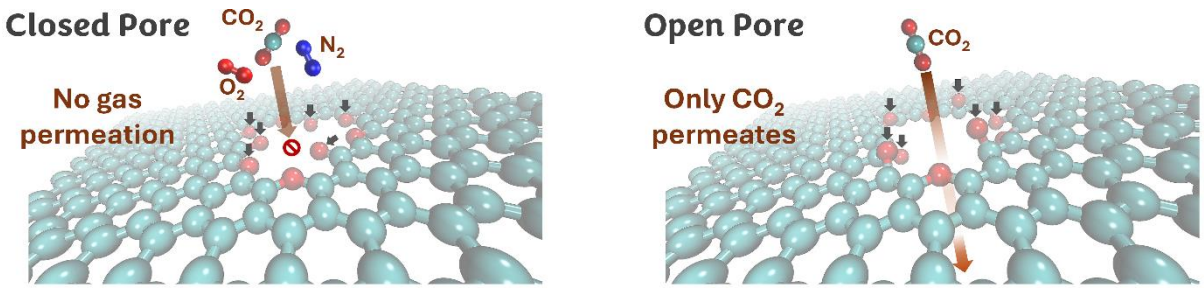


Figure 1 Illustration of edge functional group on gas transport in 2D graphene nanopores which enhances selectivity toward CO2. Nature Communications 16, 6252 (2025). https://doi.org/10.1038/s41467-025-61518-2

F

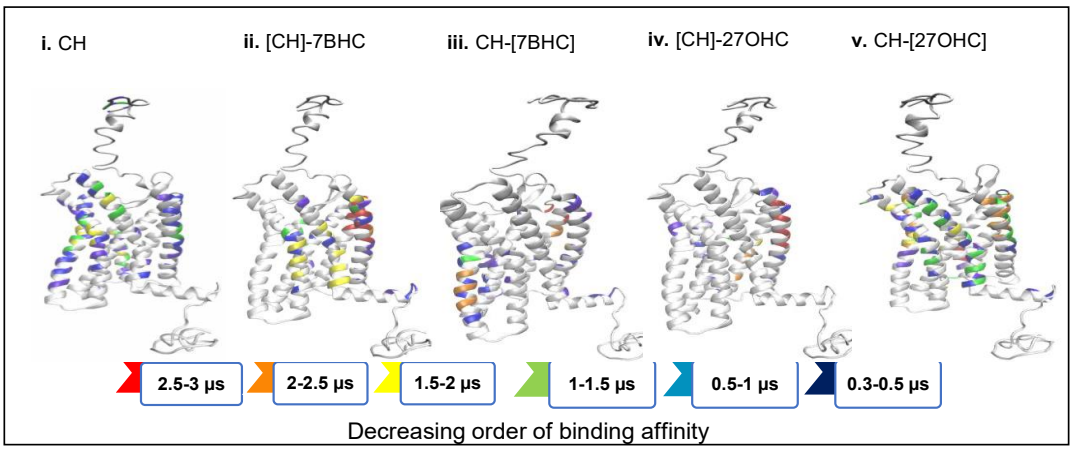


Figure 2: Binding lifetimes for oxysterols (7BHC and 27OHC) in the membrane inserted CXCR4 receptor. [ ] indicates the data for the given sterol. 27OHC (v) a tail oxidized sterol is found to completely replace cholesterol. (i) In contrast 7BHC (iii) a head oxidized sterol only binds moderately.

ACS-Biochemistry, 64 1606–1623 (2025) https://doi.org/10.1021/acs.biochem.4c00617

3.4.3 Prof. Sudeep N. Punnathanam's Lab

3.4.3.1 Problem areas:

Studying the mechanism of NaCl crystal nucleation from aqueous solutions:
We are trying to unravel the mechanism of crystal nucleation of sodium chloride using theoretical approach. In this approach we need the values of free energy changes for each step in the formation of a nuclei of sodium chloride to calculate the nucleation rate. However, such free energy calculations are required across a vast 3-dimensional phase space for the given system. In other words, there is a need to run many simulations corresponding to umbrella sampling method with different input parameters to obtain the free energy surfaces, which needs huge computational resources. Another factor that contributes to computational requirements is the nature of the system. The NaCl-water system is a simple looking system but has many complexities due to which it takes very long time to equilibrate the system. Hence, to study this system and obtain the free energy values, we need significant computational resources at our disposal.

3.4.3.2 SERC's resources:

Param-Pravega supercomputer:

- CPU queues – 15744 cores x 24 hours x 4 jobs (approximate)
- GPU queues – (1gpu + 4 cores) x 96 hours x 80 jobs (approximate)

Roddam-Narasimha supercomputer:

- CPU queues – 48 cores x 24 hours x 250 jobs (approximate)

3.4.3.3 Parallelization strategy:

The codes and software used in these simulations use MPI based parallelization.

3.4.3.4 Performance and Scalability:

The Param-Pravega supercomputer is very fast and offers comparable speed to the group-owned cluster machines, even when running jobs across multiple nodes, which is not the case elsewhere.

3.4.3.5 Result Outcome:

Param Pravega has been immensely helpful in free energy calculations. We are in process of writing a paper to publish these results. Apart from that, these results will form a significant chunk of Ph.D. of Mr. Chaitanya J. Shah.

3.5 Computation and Data Sciences (CDS)

3.5.1 Prof. Phani Motamarri's Lab

3.5.1.1 Problem areas:

a. Efficient hybrid CPU-GPU implementation strategies have been developed to incorporate non collinear magnetism and spin-orbit coupling (SOC) effects within the framework of norm-conserving pseudopotentials using finite-element discretization.
b. Efficient computational strategies have been developed for implementing meta-GGA functionals in the finite-element DFT-FE framework using norm-conserving pseudopotentials.
c. Efficient scalable matrix-free algorithms have been developed for finite-element discretization of DFT that substantially accelerates Hamiltonian application on large multivectors leveraging modern distributed CPU architectures.
d. A novel subspace iteration based eigensolver tolerant to approximations in matrix-vector multiplications has been developed which can leverage low precision arithmetic and CPU and GPU architectures.
e. Efficient hybrid CPU-GPU accelerated algorithms based on mixed precision have been developed to conduct finite-element DFT calculations using projector-augmented wave (PAW) method.
f. Leveraging the ability of real-space density functional theory (DFT) codes to accommodate generic boundary conditions, we introduce two methods for applying an external potential bias that can be suitable for modelling surfaces and interfaces.

3.5.1.2 SERC's resources:

a. We used around 3000 CPU cores on Param Pravega for conducting large-scale DFT calculations on monolayer van-der-Waals ferromagnet Fe-Ge-Te (FGT) system involving non collinear magnetism and spin-orbit coupling effects (item 1a)
b. Peformance studies involving proposed eigensolver (item 1d) and matrix-free algorithms (item 1c) used around 8000 cores
c. We performed accuracy and performance benchmark studies of the proposed finite-element based methodologies for large-scale electronic structure calculations up to 6500 Pravega CPU cores involving calculations up to 15000 electrons (item 1b and item 1e)

3.5.1.3 Parallelization strategies:

a. Finite-element discretization of the given simulation domain is carried out by decomposing it into non-overlapping finite-element cells. Further for efficient distributed parallelism, the simulation domain is further partitioned into subdomains with each subdomain assigned to a corresponding MPI task t.
b. The finite-element discretised Hermitian sparse generalised eigenproblem arising in the above proposed methods benefit from fully iterative eigensolvers that rely on Chebyshev filtered subspace iteration strategy (ChFSI) in a distributed setting.
c. We rely on ChFSI strategy since it is naturally amenable to the efficient use of high-performance computing architectures, as the construction of the filtered subspace does not involve any coupling among the vectors, allowing for matrix-multivector multiplications to be performed blockwise or in parallel over few blocks, reducing the peak memory requirement.

d. The global finite-element discretized sparse matrix is not assembled but instead the action of the matrix on trial multi-vectors is carried out at the finite-element cell level leveraging low level threaded Blas Kernels or using matrix-free methods and then the cell-level matrix vector products are assembled in a local processor. Contributions from shared processor boundary nodes are then accounted by using MPI point-to-point communication routines.
e. To reduce time to solution, we optimize the data movement costs both intra and inter node, by leveraging algorithms that can exploit overlapping compute and communication. Furthermore, we reduce communication costs by leveraging lower precision domain decomposition communication without sacrificing robustness by employing ChFSI solver that are tolerant to inexact matrix-vector multiplications.

3.5.1.4 Performance and scalability:

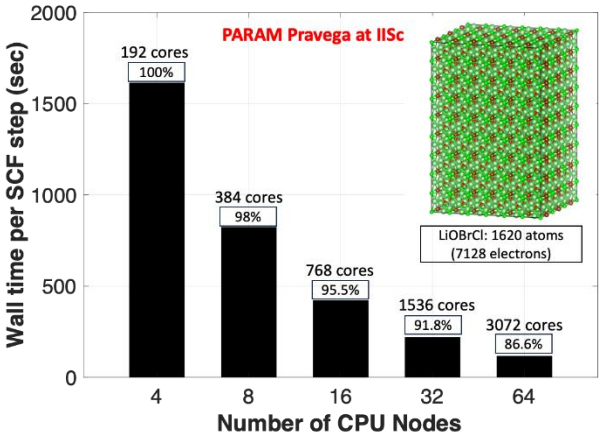


Figure 1 Scaling study of our in-house DFT-FE code on Param Pravega using norm-conserving pseudopotentials

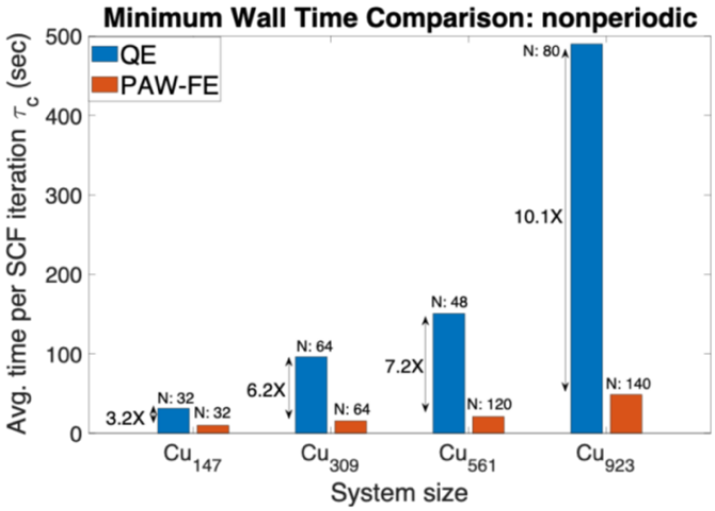


Figure 2 Minimum wall time comparison of our newly proposed PAW-DFT-FE formulation with state-of-the-art plane-wave basis code Quantum Espresso (QE). Case study: Cu nanoparticles of increasing size

3.5.1.5 Result Outcome:

a. List of Publications:

	Author(s)	*Title*	*Journal*	*Volume*	*Page*	*Year*
1	N. Kodali, K. Ramakrishnan, P.Motamarri	Residual-based Chebyshev filtered subspace iteration for sparse Hermitian eigenvalue problems tolerant to inexact matrix-vector products	Computer Physics Communication (accepted)	arXiv:2503.22652		2025
2	K. Ramakrishnan, S.G.Gopalakrishnan, P. Motamarri	Real-space methods for ab initio modelling of surfaces and interfaces under external potential bias	Journal of Chemical Theory and Computation	21	7087	2025
3	N. Kodali, P. Motamarri	Finite-element based methods for non-collinear magnetism and spin-orbit coupling in real-space pseudopotential density functional theory calculations,	Physical Review B	111	195129	2025
4	K. Ramakrishnan, S.Das, P.Motamarri	Fast and scalable finite-element-based approach for density functional theory calculations using projector-augmented wave method	Physical Review B	111	035101	2025
5	A. Rout, R.Pawar, S. Bhattacharjee, P. Motamarri	Robust light-weight graph neural network frameworks for accelerating crystal structure prediction	Journal of Chemical Information and Modelling	65	6470	2025

b. Contributions to national/Industry/societal projects due to the executions, and the resulting impact and benefits:

Contributed to open-source code development -via- the development of novel real-space computational methodologies for material modelling using massively parallel density functional theory calculations. These were built under the umbrella of DFT-FE code, an open source code and is now currently being installed on NSM machines all over India to increase the user base thereby providing an efficient and a scalable alternative to existing widely used plane-wave DFT codes like VASP or quantum espresso. These efforts are timely given that India is in the race to build exa-scale computer in the next 5 years.

c. PhD, Masters, and UG students graduated during 2025 whose work was based on SERC HPC resources:

2 MTech students graduated. 1 PhD student submitted thesis in Dec 2025. 2 more PhD students will graduate in 2026.

d. Awards and recognition in 2025:

S.No.	Name of Award	Awarding Agency	Year
1	Dr A P J Abdul Kalam HPC Award 2025	HP and Abdul Kalam Foundation	2025
2	Director's Discretionary Award for Compute Allocation on Frontier, world's first exascale supercomputer	Oak Ridge National Lab (ORNL)	2025
3	Kawazoe Poster Award for PhD student Srinibas Nandi	Asian Consortium on Computational Materials Science (ACCMS) - Japan	2025
4	Best Presentation Award for PhD student Kartick Ramakrishnan	EECS Symposium	2025
5	Institute Motorola Medal for MTech student Sundaresan	IISc	2025

e. Images

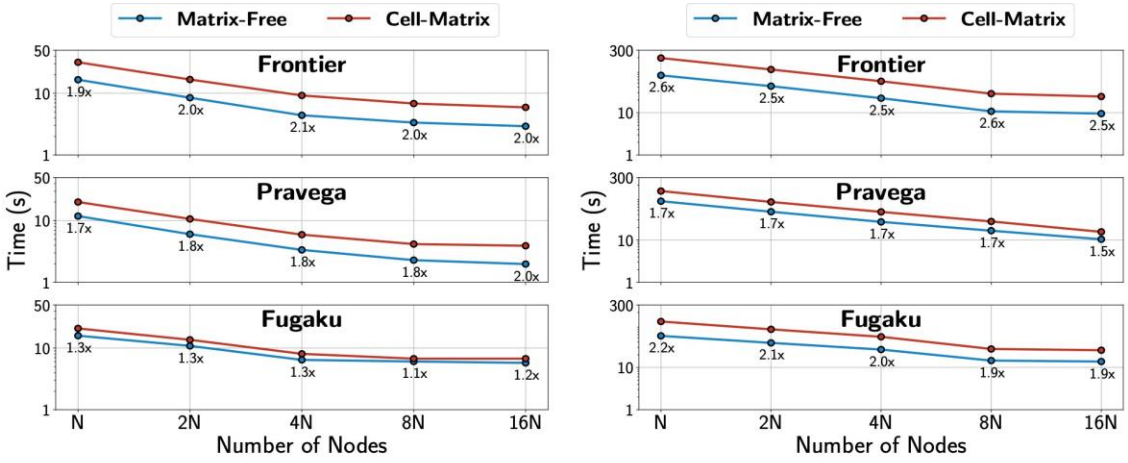
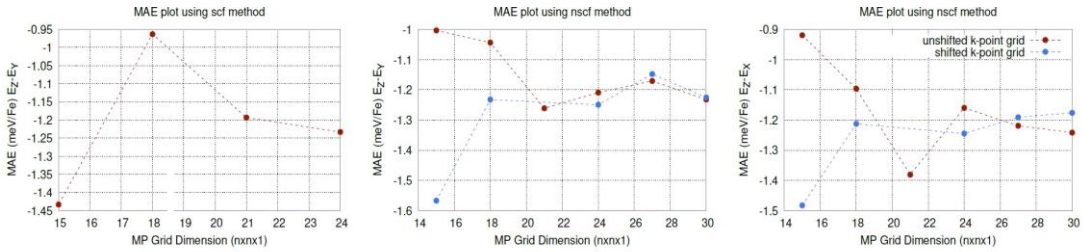


Figure 8: Scaling study comparisons of the proposed matrix-free implementation with cell-matrix baseline for subspace construction step of Al nanoparticle 561 atoms (left) and BCC molybdenum 1023 atoms (right) with `FEOrder` = 8, FP32 precision on Frontier (Left: N = 4, Right: N = 12), Param Pravega (Left: N = 4, Right: N = 10) and Fugaku (Left: N = 70, Right: N = 200) supercomputers.



(i) Convergence MAE between in the in-plane y direction and out of plane z-direction with Brillouin zone sampling computed using full ground state calculations

(ii) Convergence MAE between in the in-plane y direction and out of plane z-direction with Brillouin zone sampling computed using magnetic force theorem

(iii) Convergence MAE between in the in-plane x direction and out of plane z-direction with Brillouin zone sampling computed using magnetic force theorem

Figure 1: MAE of monolayer Fe_3GeTe_2 (FGT)

Te atom adsorption on WS_2 surface with DFT calculations involving 2004 atoms

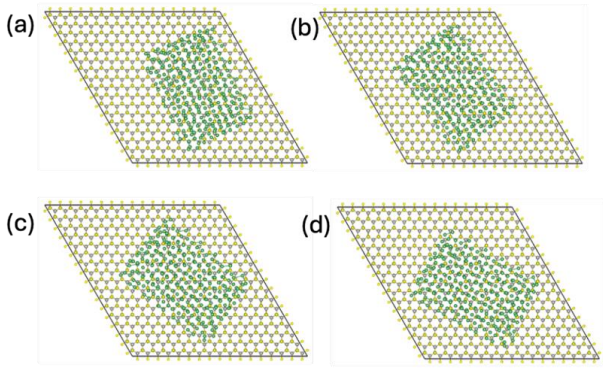


Figure: Top view of adsorption of Te on WS_2 surface for orientation angles (a) 0°, (b) 10°, (c) 20°, (d) 30°. Total number of S (Yellow) atoms = 1156, total number of W (Grey) atoms = 578, total number of Te(Green) atoms = 270.

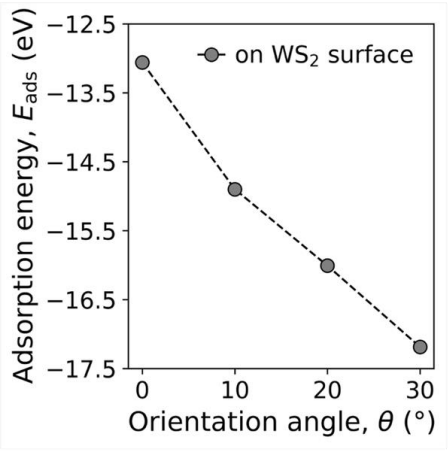


Figure: Total adsorption energy(eV) Vs. Orientation angle (°)

3.5.2 Prof. Sathish Vadhiyar's Lab

3.5.2.1 Problem areas:

A Fault-tolerant Framework for MPI Applications based on Adaptive Partial Replication:

In the previous years, we had implemented **FTHP-MPI** (Fault Tolerance and High-Performance MPI), a novel fault-tolerant MPI library that augments checkpoint/restart with replication to provide resilience from failures. In 2025, we proposed an adaptive replication mechanism that uses failure predictions. We utilized a simulated failure injection environment and a simulated failure predictor for the same environment to identify processes at high risk of failure and dynamically reassign replicas if needed. Our adaptive replication mechanism is implemented in FTHP-MPI.

A Hybrid CPU-GPU Framework for Accelerating LLM Training:

Heterogeneous CPU-GPU systems present opportunities for hybrid CPU-GPU executions to accommodate and run Large Language Models on limited GPU memory clusters by jointly exploiting the CPU's large memory and the GPU's computing capacity. Existing works that employ such hybrid executions schedule compute-intensive operations of forward and backward passes on the GPU and memory intensive operations of parameter updates on the CPU. However, these works fail to utilize the CPU's compute cycles and characteristics of the deep learning algorithm efficiently, resulting in idling of resources, primarily the GPUs. We introduce SkipPar, a highly optimized heterogeneous training framework that aims to minimize the parameter update overhead on the CPU that causes GPU idleness.

3.5.2.2 SERC's resources:

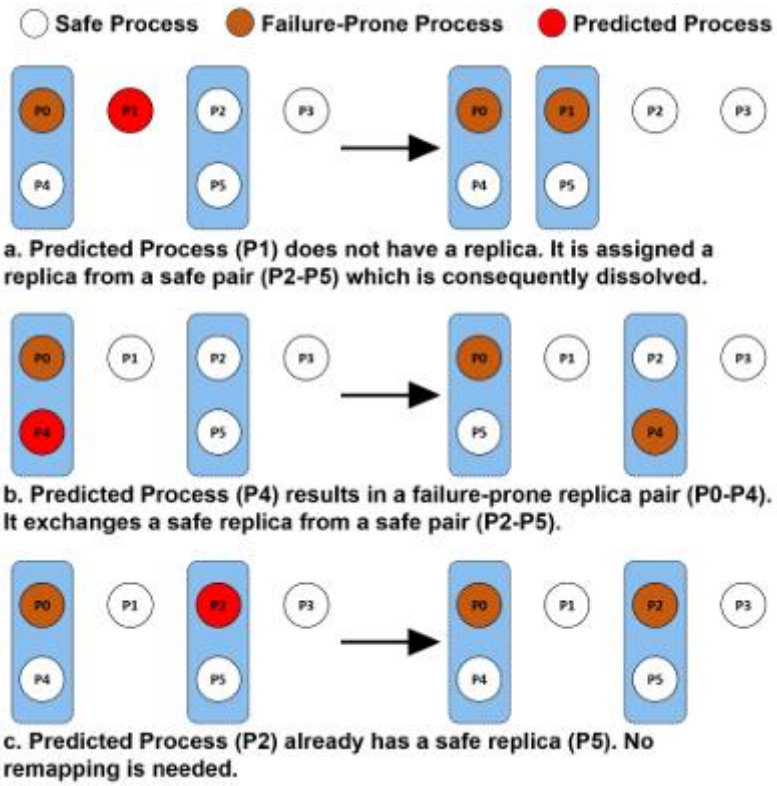
Studies related to fault tolerance were done by job executions up to 8192 CPU cores of Param Pravega.

The LLM training runs for hybrid CPU-GPU executions research was conducted with one GPU on DGX-H100 system.

3.5.2.3 Parallelization strategies:

A Fault-tolerant Framework for MPI Applications based on Adaptive Partial Replication:

We have devised an efficient replica remapping mechanism to handle the prediction of a failure. In a first such work, we have derived an optimal checkpointing interval for application execution, considering the degree of replication and recall of failure predictions for optimizing MTTI.



a. Predicted Process (P1) does not have a replica. It is assigned a replica from a safe pair (P2-P5) which is consequently dissolved.

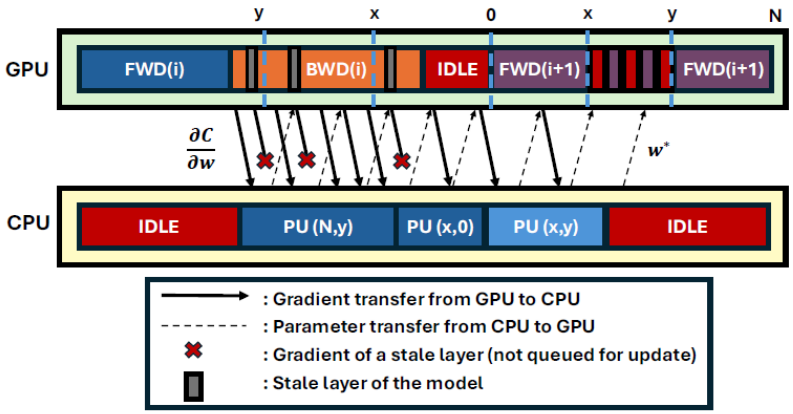
b. Predicted Process (P4) results in a failure-prone replica pair (P0-P4). It exchanges a safe replica from a safe pair (P2-P5).

c. Predicted Process (P2) already has a safe replica (P5). No remapping is needed.



A Hybrid CPU-GPU Framework for Accelerating LLM Training:

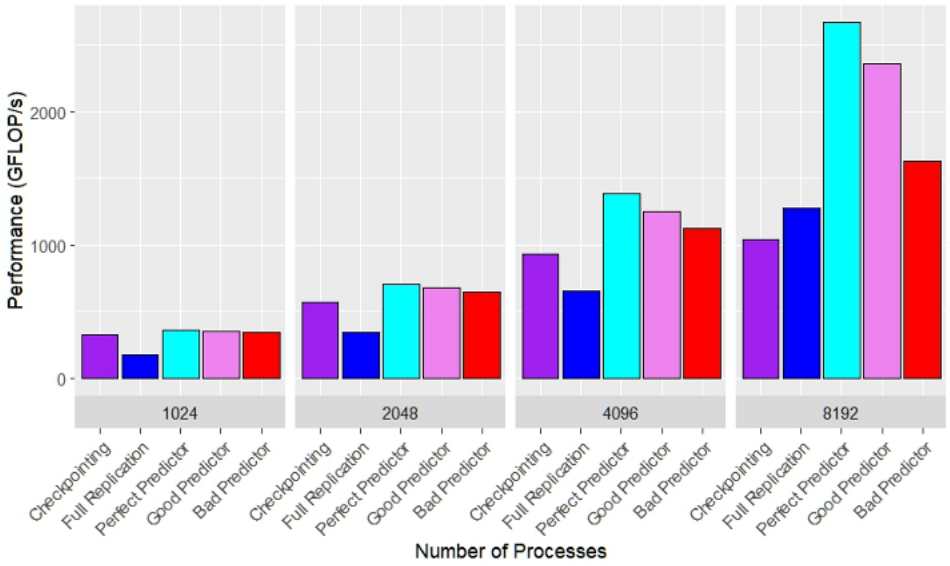
SkipPar employs dynamic and adaptive strategies for minimizing the GPU stalls. We propose a dual-stage scheduler for efficient CPU-side parameter updates. The first stage leverages the data-independent nature of inter-layer updates by skipping certain updates during the backward pass of iteration i and rescheduling them with the forward pass in iteration i+1, to minimize GPU stalls. The second stage further reduces the CPU bottleneck by identifying and filtering out converged layers from the update process. We formulate the dual-stage scheduling problem as a linear programming model to select the precise region of layers for skipping to maximize the parallelism between CPU and GPU computations, given the times taken for the various operations and the converged layers selected for filtering.



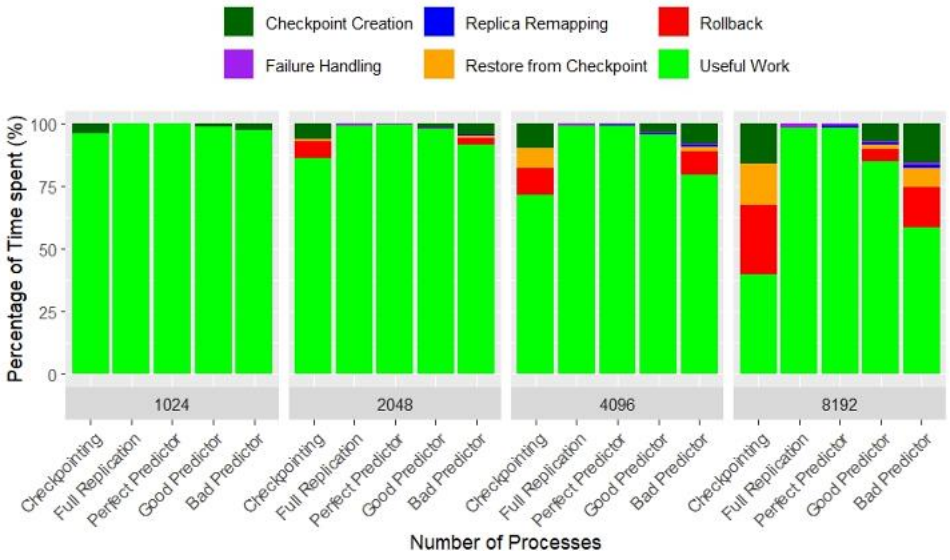
3.5.2.4 Performance and scalability:

A Fault-tolerant Framework for MPI Applications based on Adaptive Partial Replication:

We have tested our mechanism with various precision and recall metrics for failure predictions to emulate real large-scale systems where failure predictions can be challenging due to various system complexities. Based on experiments with the HPCG benchmark, PIC simulation codes, and the CloverLeaf mini-applications, we show that our adaptive replication mechanism with a replication degree of only 1% performs better than full-replication or only-checkpointing approaches, even with relatively low precision and recall values.



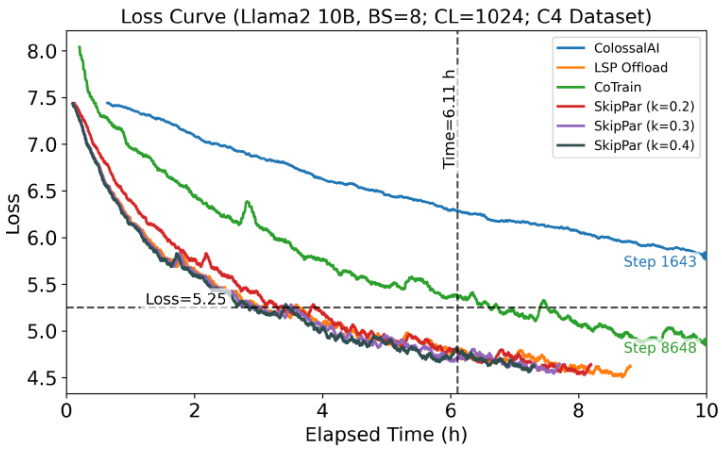
Performance Benefits of Adaptive Replication



Times Spent in Different Fault Tolerant Methods

A Hybrid CPU-GPU Framework for Accelerating LLM Training:

We showed results with two large LLMs, namely, LLama2 and GPT2, with two large-scale datasets, namely, C4 and SlimPajama, on A100, H100 and H200 GPU systems, and compared with three existing frameworks, namely, ColossalAI, CoTrain and LSP Offload. When trained for 10,000 time steps, SkipPar gives more than a day of saving in training when compared to ColossalAI, up to 7 hours of saving when compared to CoTrain, and up to 17% reduction in training time when compared to LSP Offload. SkipPar also shows very good linear scaling for up to eight GPUs.



Performance Benefits of SkipPar

3.5.2.5 Result Outcome:

a. Contributions to national/Industry/societal projects due to the executions, and the resulting impact and benefits:

The research on hybrid CPU-GPU executions is for a funded project by and for Shell India Marketing Pvt Ltd.

3.6 Department of Inorganic Physical Chemistry

3.6.1 Prof. Eluvathingal D. Jemmis' Lab

3.6.1.1 Problem areas:

Catalysis: Alkanes have extensive applications in diverse fields and their natural abundance is dwindling. Ethers are present in biomolecules, organic wastes, and synthetic compounds. Hence, catalytic synthesis of alkanes from bio-ample ethers is highly desirable. Along with the experimental group of Professor Gunanathan of National Institute of Science Education and Research, Bhubaneswar, we have studied computationally (Density Functional Theory) the possible ways in which such transformation can take place. These helped in the experiments.

Structure and bonding of unusual molecules especially involving boron and phosphorus: We have studied the electronic structure of complexes derived by replacing C-H by isoelectronic boron and phosphorus based ligands, explaining puzzling experimental observations and predicting novel chemistry.

3.6.1.2 SERC's resources:

We use electronic structure calculation software which is not massively parallelisable. Typically these use 32 cores only. The number of users who are in this category is very large. There is always a long queue.

3.6.1.3 Result Outcome:

a. Publications:

1. Cobalt-Catalyzed Deoxygenative Coupling of Ethers to Alkanes M. K. Sahu, S. Pattanaik, G. Joshi, E. D. Jemmis, and C. Gunanathan Angew. Chem. Int. Ed. 2026,65,e20176. (https://onlinelibrary.wiley.com/doi/10.1002/anie.202520176)
2. All-Boron Analogue of Planar Benzene on an Osmium Template K. Kar, G. Joshi, E. D. Jemmis, and S. Ghosh Chemical Science 2026, 17,196-204. (https://pubs.rsc.org/en/content/articlelanding/2026/sc/d5sc06992k)
3. Valence Electron Dependent Contraction Of P6 Ring In[(CpM)2(μ,η6:η6-P6)] (M=V, Mo): A DFT Study. G. Joshi, S. N. Moorkkannur, E. D. Jemmis Chem. A Eur. J, 2025, 30, e202501411. (https://chemistry-europe.onlinelibrary.wiley.com/doi/10.1002/chem.202501411)
4. Stabilization of Ethane-like Dianionic Diborane(6) in Monometallic Titanium Complexes and its Subsequent B(sp3)-B(sp3) Bond Cleavage. S. Bairagi, S. Giri, G. Joshi, E. D. Jemmis, S. Ghosh Angew. Chem. Int. Ed. 2025, 64, e202417170. (**https://doi.org/10.1002/anie.202417170**)

b. PhD, Masters and UG students graduated during 2025, whose work was based on the use of SERC HPC resources.

MSc and UG students who spent summer benefited from facilities associated with SERC. Nine students spent summer months.

1. Nayantara MSc IISc 2025
2. Mahadik Roshan-IISc-MSc
3. Mitali Tewari-IIT-Jodhpur
4. SK Suguna-Madurai Kamaraj University
5. Swadhin Sai Shankar-Bombay University
6. Manish Kumar-MSc-IITM
7. Anne Maria-2025 3rd year Int MSc UoHyd
8. Malavika Devi BS-MS, IISERTVM
9. Devika A- 3rd Year Int MSc NISER

3.7 Department of Material Research Centre

3.7.1 Prof. Abhishek Singh's Lab

3.7.1.1 Problem areas:

Our research leverages large-scale density functional theory (DFT) and molecular dynamics simulations on HPC platforms to address diverse problems in materials science. In catalysis, we developed a density functional theory (DFT) coupled recommendation system based approach to predict the d-band centre of the core-shell nanoparticles. For structural materials, ab initio and machine learning methods were combined to study phase stability and high-temperature strength in Ni-based superalloys and Ti alloys, enabling alloy optimization. Investigations of defects in semiconductors, we demonstrate that the substitution of carbon at the nitrogen site along with the Stone-Wales defect in hexagonal boron nitride (h–BN) acts as a source of a single-photon emitter. Studies on topological materials led to the development of a first-principles screening approach to identify Quantum anomalous Hall and valley-polarised QAH effects in

functionalized Ti-Cr-C MXenes due to their intrinsic magnetism and strong spin–orbit coupling. In thermoelectrics, machine learning interatomic potentials (MLIP) are eveloped to investigate thermal transport. Finally, studies on 2D materials presents a fast, low-cost, and scalable technique using 2D h-BN coatings to enhance heat dissipation in commercial electronics.

3.7.1.2 SERC's Resource:

The work extensively used Param Pravega and Narashima (RNC) clusters. Over the year 2025, our group utilized approximately 300,000 CPU cores. The simulations relied on VASP for DFT calculations and ab-initio molecular dynamics, supported by high-performance storage and interconnects.

3.7.1.3 Parallelization Strategies:

VASP simulations were parallelized using:

- **k-point parallelization** (distribution of k-points),
- **band parallelization** (distribution of electronic states).

3.7.1.4 Performance and Scalability:

Medium-sized catalytic systems (~200 atoms) scaled efficiently up to 512 cores, while larger models (>400 atoms) maintained good parallel efficiency up to 1024 cores. Compared to smaller departmental clusters, HPC wall-times were reduced by 3–4 times, enabling high-throughput screening and large descriptor datasets.

3.7.1.5 Result Outcome:

a. Publications (2025):

1. Probing Lattice Anharmonicity and Thermal Transport in Ultralow-κ Materials Using Machine Learning Interatomic Potentials, Small 2025, e13476 S. Mandal, A. Srivastava, T. Das, A. K. Singh, and P. K. Maiti
2. Conventional and Valley-Polarized Quantum Anomalous Hall Phases in Ti-Cr-C MXenes, Nano Lett. 2025, 25, 51, 17954–17961 S. Mishra, R. K. Barik, and A. K. Singh
3. Descriptors of Electrocatalysis for CO2 Reduction to C2+ Products Formation, ACS Appl. Energy Mater. 2025, 8, 23, 17085–17105 S. Midya, A. Chakraborty, S. Mishra, and A. K. Singh
4. Electronic Structure Modulation of AlN4 Single-Atom Catalyst for Oxygen Reduction Reaction, Small 2025, 21, e01869 S. Atif, O. Y. Bisen, S. Midya, A. K. Yadav, G. Ciatto, A. K. Singh, K. K. Nanda
5. Plasmonic Nanocomposite for Visible Light-Modulated BimorphActuator, Adv. Mater. Technol. 2025, 10, 2401037 P. Kumbhakar,* S. Narendhiran, S. Midya, M. Islam, M. Balachandran, and A. K. Singh*
6. High-throughput computational search for group-IV-related quantum defects as spin-photon interfaces in 4H-SiC, Phys. Rev. B 112, 184112 S. Meher, M.Dey, A. K. Singh
7. Enhanced Heat Dissipation and Reduced Power Consumption in Electronics Using 2D Hexagonal Boron Nitride, Small 2025, 2502007Karthik R, A. Srivastava, S. Midya, A. Shanu, S. Slathia, S. Vandana, S. Kar, N. R. Glavin, A. K. Roy, P. R. Sreeram, A. K. Singh*, C. S. Tiwary*
8. 2D MnTe/rGO Hybrid Structure for Moisture Energy Harvesting, ACS Appl. Mater. Interfaces 2025, 17, 22, 32973–32983 P. Kumbhakar, S. Mishra, C. C. Gowda, P. M. Nishma, A. Venugopal, A. K. Singh* and C. S. Tiwary*
9. Magnetocaloric effect in Mn-rich Heusler-derived alloys for room temperature-based applications, J. Mater. Chem. C, 2025,13, 10789-10803 N. Tiwari, S. Mishra, S. Sarkar, S. Talapatra, M. Palit, M. Paliwal, A. K. Singh and C. S. Tiwary

10. Strain and Charge Doping Modulated Optical Emission Signatures of Polycrystalline WSe2, Small, 2411297 (2025) S. Paul, S. Mishra, Abhijith M B, P. Ghosh, P. Barman, M. Altvater, V. Pandey, P. P. Chanda, S. Das, A. Roy, N. R Glavin, A. K. Singh, and V. Kochat
11. Defect Engineered Few Layered MoS2 for Human–Machine Interface, Small Methods, 2500068 (2025) R. D. Salian, S. Mishra, C. C. Gowda, R. K. Barik, A. K. Singh, C. S. Tiwary, P. Kumbhakar
12. 2D Materials Coated Flexible Origami for Low-Frequency Energy Harvesting, ACS Appl. Electron. Mater. 7, 3, 1111–1119 (2025) P. Kumbhakar, S. Mishra, P. V. Nayak, A. Sunny and A. K. Singh
13. Recommendation System to Predict the d-band Center of Core-Shell Bimetallic Nanoparticles Catalysts, Adv. Theory Simul. 2401460 (2025) S. Agarwal and A. K. Singh
14. Carbon with Stone-Wales Defect as Quantum Emitter in h−BN, Phys. Rev. B 111, 104109 (2025) M. Dey, S. Meher and A. K. Singh
15. Comprehensive insights into hydrolysis-mediated hydrogen production using high-entropy quintuple alloy-grafted carbon black, J. Mater. Chem. A,13, 5765-5776 (2025) G. Raj, R. Nandan, S. Midya, K. Kumar, A. K. Singh and K. K. Nanda

b. Contributions to National / Societal Goals:

Our work contributed to national research initiatives through a **SERB project** on data driven search for highly efficient CO2 electroreduction catalysts, a **DST project** providing theoretical insights on emergent phases in 2D quantum materials and heterostructures and a **DST, INAE project.**

c. Graduated Students (2025):

- One PhD students graduated (Dr. Arko Parui).

d. Awards and Recognitions:

- Shibu Meher – Poster Commendation Award in Materials for Information and Communication, Psik Conference, 2025
- Aditya Gollapalli – Best Oral Presentation, MRC Day, Jan 2025
- Subhendu Mishra – Best Oral Presentation, MRC Day, May 202

3.8 Mechanical Engineering

3.8.1 Prof. Ratnesh Shukla's Lab

3.8.1.1 Problem area:

Our research focuses on development and implementation of novel predictive simulation capabilities that make use of advanced discretization techniques on modern high performance computing platforms to resolve spatiotemporally complex flows with and without shocks to an unprecedented detail. The high fidelity computational tools developed in our group are being utilized to establish the operability limits of high-speed propulsion systems, to investigate cavitating flows (cavitation bubble dynamics, high-speed liquid jets, submerged supersonic gas jets, prediction of sound produced from collapsing bubbles) and for understanding thrust generation mechanics of undulatory propulsion.

3.8.1.2 SERC's resources:

Our typical runs utilize 1000 to 14400 CPU cores of parampravega. The queues we employ span from small and medium queues to large queues.

3.8.1.3 Parallelization strategies:

Our parallelization strategy centres around MPI, OpenMP and their combination.

3.8.1.4 Performance and scalability:

Our codes have been found to scale well from 100 to 10000 cores (typical parallel efficiency we achieve is about 95% for billion cell calculations using 14400 cores).

3.8.1.5 Result Outcome:

a. Publications:

1. P. Das, R. K. Shukla & J.B. Freund, "Acoustically excited bubble tunnelling through soft material" *Journal of Fluid Mechanics*, 1020, A45, 2025.
2. S. Dasika & R.K. Shukla, "Multilayer-Perceptron based Optimal Stencil Selection and Order Detection for High-Order Shock Capturing", The 18th Asian Congress on Fluid Mechanics, Seoul Korea, 2025.

b. Contributions to the national/Industry/societal projects due to the executions, and the resulting impact and benefits.

Computational prediction of acoustic emissions from collapsing bubbles using interface capturing multiphase flow simulations. Naval Research Board Project

High-resolution unstructured mesh simulations of shock-boundary layer interaction and flow separation for accurate prediction of start/unstart characteristics of hypersonic intakes, Project under the hypersonic vertical of DIA-COE IIT Bombay

Hydrodynamic tuning and vibration control of the wet end of a twin towed array system. Contract for Acquisition of Research Services, NPOL Kochi.

c. PhD, Masters and UG students graduated during 2024-25, whose work was based on the use of SERC HPC resources.

Pankaj Hooda, MTech student.

d. Awards and recognitions.

Invited Talks:

Thrust Generation Mechanics and Energetics of Undulatory Locomotion, Department Research Seminar Series, Department of Mechanical Engineering, University of Canterbury, May 27, 2025.

Detailed simulations of collective bubble growth and collapse dynamics, Australasian Fluid Mechanics Seminar Series, May 14, 2025.

Detailed simulations of cavitating bubble clouds, Department Seminar Series, Department of Mechanical and Mechatronics Engineering, University of Auckland, April 11, 2025.

e. Images and videos:

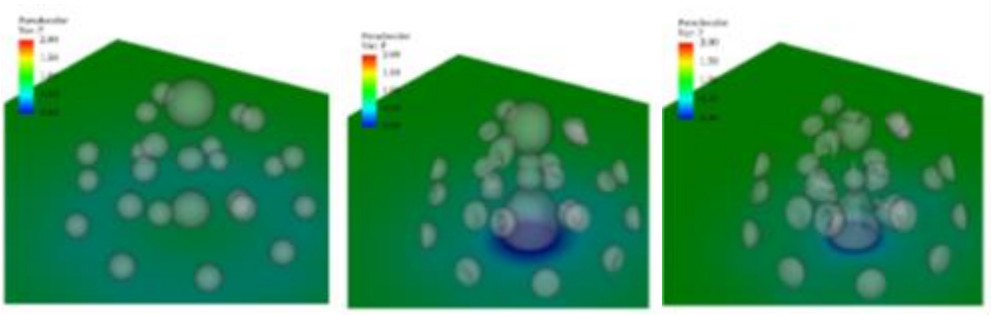


Figure: Growth and jetting collapse of a bubble cluster near a wall (bubbles are shown as grey/white isosurfaces). Coloured contour indicates the pressure exerted on the wall

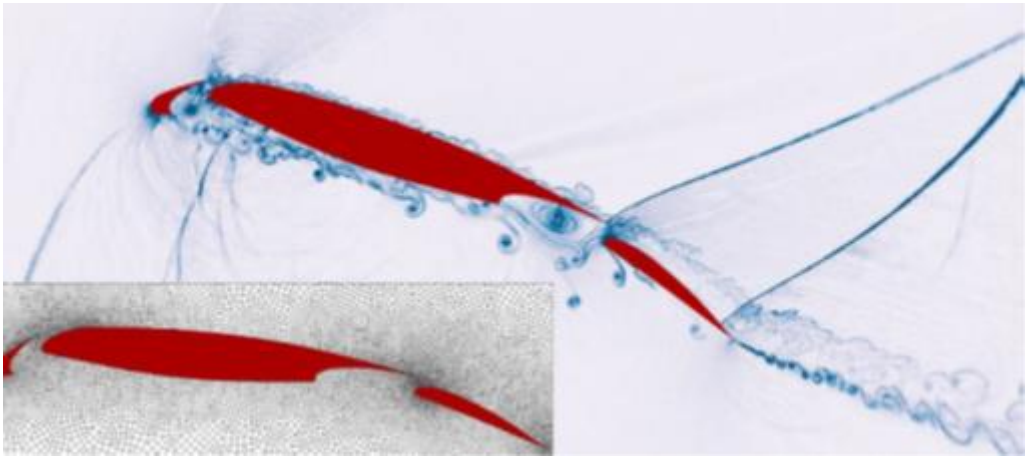


Figure: Simulation of Mach 0.8 past a three-element airfoil consisting of a slat, a main element and a flap using high-resolution unstructured mesh methods. Blue coloured contours depict normalized density gradient. Inset depicts the unstructured mesh used for discretization.

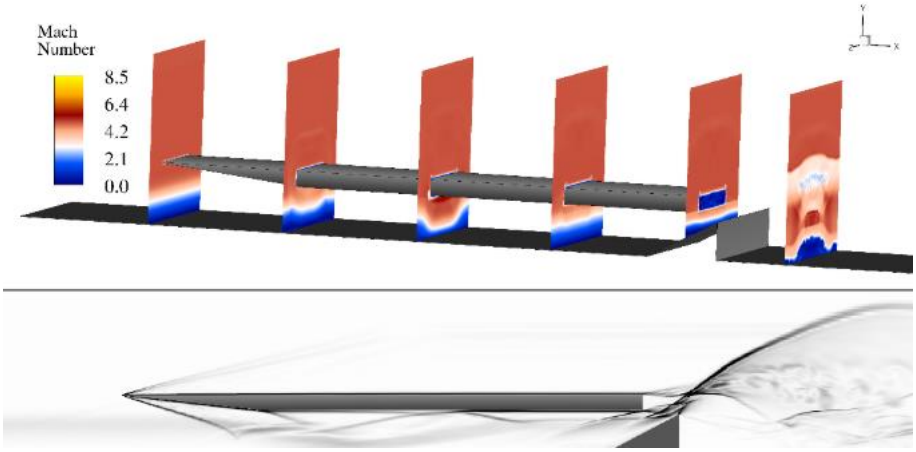


Figure: Shock boundary layer interactions in a hypersonic intake. Gray coloured regions depict the solid boundaries. The top frame illustrates Mach number contours along slices taken at select locations along the intake. The bottom frame depicts exponentially spaced normalized density gradients.

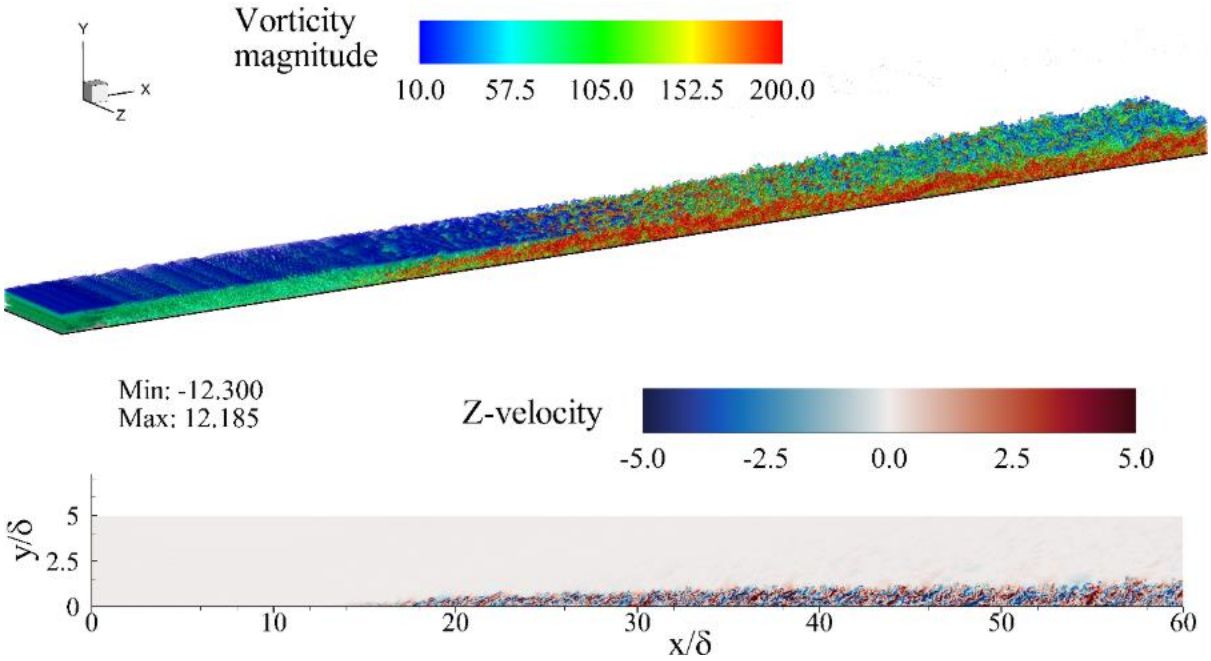


Figure: Compressible boundary layer at Mach number of 4.9: Top frame shows Q criterion isosurfaces coloured with vorticity magnitude. Bottom frame depicts spanwise velocity component contours over a two-dimensional slice taken along the midplane.

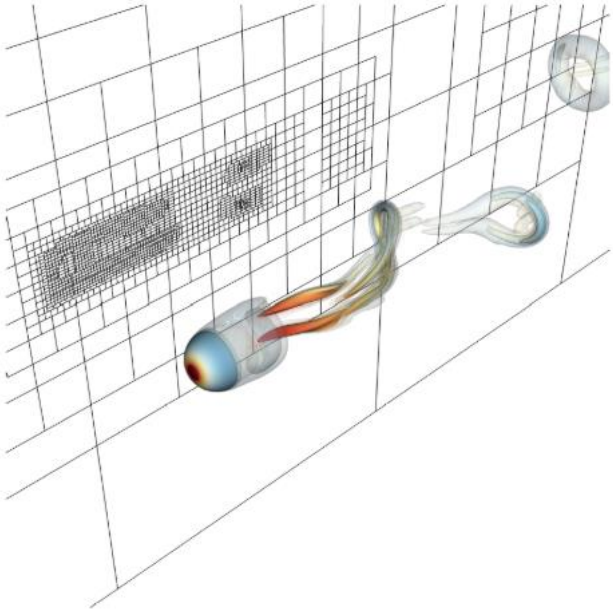


Figure: Vortical structures (coloured isosurfaces) in the wake of a translating sphere computed using a high-order immersed boundary method implemented in AMReX.

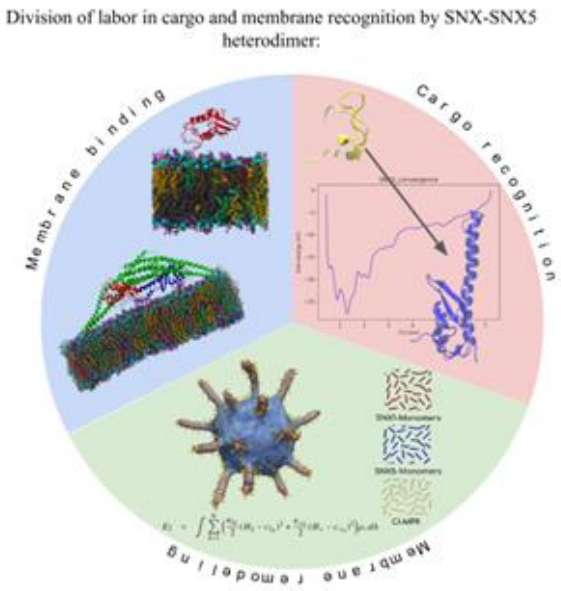
3.9 Molecular Biophysics Unit

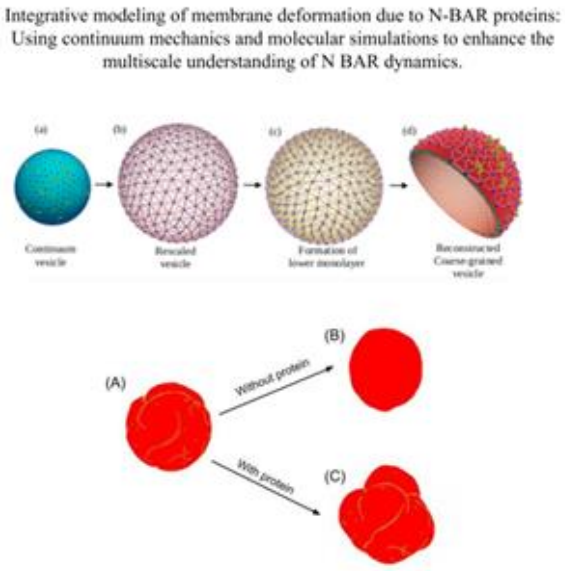
3.9.1 Prof. Anand Srivastava' group

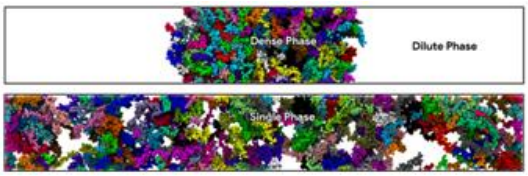
3.9.1.1 Problem areas:

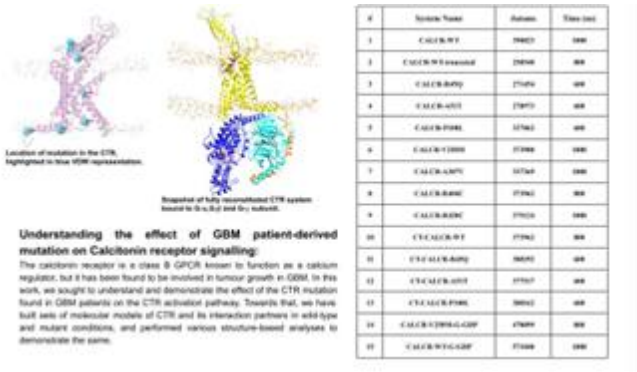
NSM resource allowed us to work on several large-scale molecular and mesoscopic simulations of biological systems that would not have been possible otherwise. For example, we worked on a large 5 lakh all-atom biological protein membrane complexes and showed how protein membrane interaction happens and gave a more molecular picture of it. This helps to understand the molecular picture of the protein binding to the membrane (Biophysics 2025). Also, we are able to simulate large coarse grained systems of 1.2 million atom systems which is constructed from a continuum model and studied in the higher resolution.

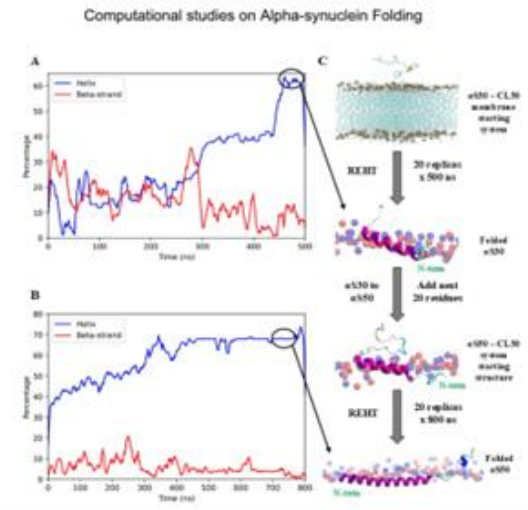
Similarly, we have carried out large scale simulations that have shed critical insights into the problems such as (i) Computational studies on Alpha-synuclein conformations, (ii) Understanding the effect of GBM patient-derived mutation on Calcitonin receptor signalling, (iii) Evolutionary differences among EHD paralogs affecting membrane remodelling in the endocytic recycling pathway and (iv) Physical characteristics of Biomolecular condensates. All of the above projects are described with images and movie files in the companion PPTX file (also see the collage below).

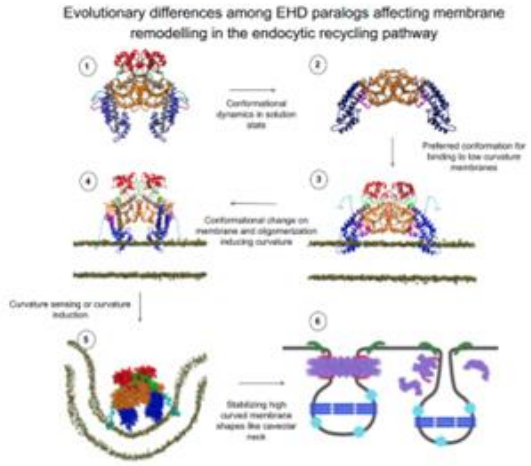












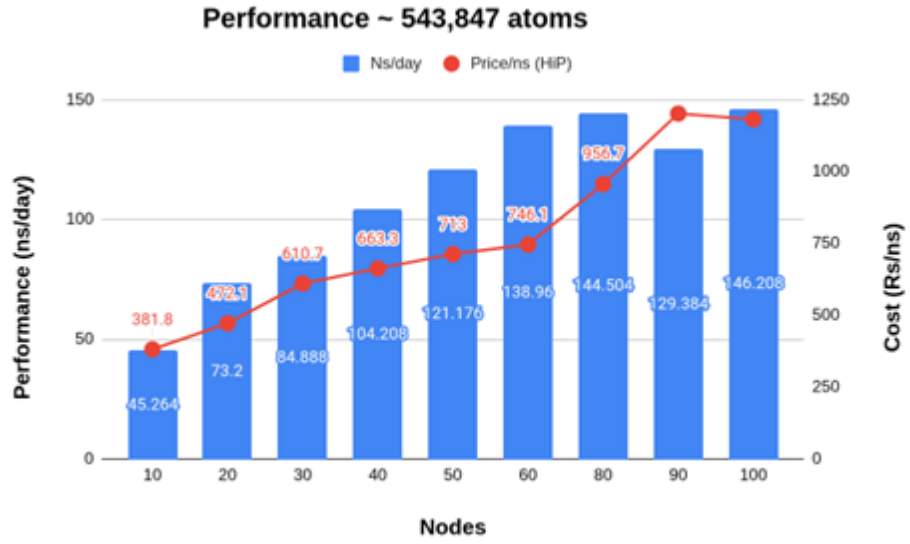
3.9.1.2 SERC's resources:

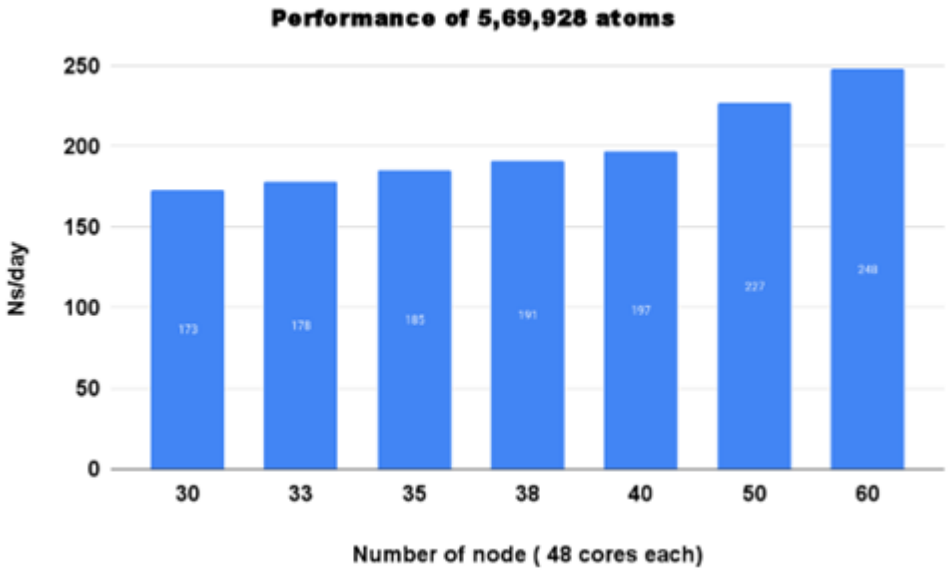
HPC resource	**CPU/GPU**	**Total No of Cores**	**Systems**
Param Pravega	CPU	1920	Solution state and membrane bound systems of EHD paralogs
Param Pravega	GPU	1 GPU node, 40 CPU cores	Advanced sampling metadynamics simulation setups for EHD.
Param Pravega	CPU	1200	SNX1-SNX5 hetrodimer interaction with Endosomal membrane.

3.9.1.3 Parallelization strategies:

We use the available strategy in the software, which is mostly domain decomposition and multithreading. We do not code our own parallelization software.

3.9.1.4 Performance and scalability:





3.9.1.5 Research Outcome:

a. Published

1. Balasubramanian, S., Roy, I., Appadurai, R., & Srivastava, A. (2025). The ribonucleoprotein hnRNPA1 mediates binding to RNA and DNA telomeric G-quadruplexes through an RGG-rich region. Journal of Biological Chemistry, 301(5).

2. Duggisetty, S. C., Kumar, G., Baratam, K., & Srivastava, A. (2026). Division of labor in cargo and membrane recognition by SNX1-SNX5: Insights from multiscale modeling. Biophysical Journal, 125(2), 652–667.
3. Joy, A., Srivastava, A., & Biswas, R. (2026). Azurin-based peptide p28 disrupts p53–HDM2 interactions: Insights from in silico studies. Physical Chemistry Chemical Physics, 28(1), 234–246.
4. Mallick, A. M., Chatterjee, A., Gurung, A. B., Uttarasili, P., Tripathi, A., Hembram, M., et al. (2025). Designed gramicidin-inspired stabilized peptide-based therapeutics to potentiate immunotherapy against aggressive kidney cancer. Biomaterials Science, 13(17), 4681–4705. Pandey, P., & Srivastava, A. (2025). sAMP-VGG16: Force-field assisted image-based deep neural network prediction model for short antimicrobial peptides. Proteins: Structure, Function, and Bioinformatics, 93(1), 372–383.
5. Roy, I., Appadurai, R., & Srivastava, A. (2025). Unambiguous assignment of kinked-β sheets leads to insights into molecular grammar of reversibility in biomolecular condensates. Protein Science, 34(9), e70266.
6. Srivastava, A. (2025). Emerging paradigms in the lateral and transverse organization in biological membrane and their functional implications: Connecting the dots with biomolecular simulations. Current Opinion in Structural Biology, 94, 103128.
7. Srivastava, A. (2025). It takes two to tango: The second membrane-binding site in peripheral proteins. Structure, 33(1), 10–12.
8. Subramanian, V., Appadurai, R., Venkatesh, H., Sekhar, A., & Srivastava, A. (2025). Morpheus: A fragment-based algorithm to predict fold-switching behaviour in proteins across proteomes. Bioinformatics, 41(12), btaf635.
9. SureshKumar, H., Iyer, S. S., Banerjee, A., Poduval, P., Lyman, E., & Srivastava, A. (2025). Signatures of glassy dynamics in highly ordered lipid bilayers with emergence of soft dynamic channels. The Journal of Chemical Physics, 162(14).

b. Manuscripts under Revision:

1. Das, P., Nair, D., & Srivastava, A. (2025). Palmitoylation of PSD95 flips the bilayer juxtaposed domain and drives cluster formation on membrane. bioRxiv. https://doi.org/10.1101/2025.10.09.679381
2. Shrama, A., Zi, Y., Pandit, A. S., Jha, K., Sinha, V. K., Ravi, V., et al. (2025). Sirtuin 2 controls global protein synthesis by regulating Rheb-GTPase. bioRxiv. https://doi.org/10.1101/2025.03.31.646364
3. Parui, S., & Srivastava, A. (2025). Statistical thermodynamics-based design principles in temperature-induced fold switching of a metamorphic protein. bioRxiv. https://doi.org/10.1101/2025.10.10.679401
4. Goswami, J., Uttarasili, P., Garg, L., Prasasvi, K. R., Chowdhury, A., Saha, S., et al. (2025). Calcitonin-driven reactivation of the Hippo tumor-suppressor cascade attenuates YAP/TAZ oncogenic signaling in glioblastoma. bioRxiv. https://doi.org/10.1101/2025.11.20.689524
5. Ekambaram, S., Prajapati, S., & Srivastava, A. (2025). Rational design of peptide inhibitors for α-synuclein liquid condensates and fibrillar aggregates using a multiscale modelling approach. bioRxiv. https://doi.org/10.1101/2025.01.12.632580

c. Contributions to the national/Industry/societal projects due to the executions, and the resulting impact and benefits:

Patent for kidney cancer treatment. Sinha Roy R., Srivastava A., Mallick A. M., Chatterjee A., Gurung A. B., Uttarasili P., Tripathi A., Hembram M. Indian Institute of Science Education and

Research Kolkata. Pharmaceutical Composition for Treatment of Kidney Cancer. Indian patent application no. 202533004009 (patent of addition to granted Indian patent number – 444719). 2025 Jan 17.

PhD, Masters and UG students graduated during 2025: 3 PhD students, 2 Masters

d. Conferences:

- Vinodhini: Flash talk and poster presentation in BPS thematic meeting "Understanding Peripheral Membrane Protein Interactions", November 9-13 2025, Thessaloniki, Greece.
- Vinodhini: Best poster presentation in SMCB'25, December 17-19, TIFR Hyderabad.
- Harini: Best Poster presentation in FracMeet'25, November 20-22 2025, SRM Guntur.
- Harini: Poster presentation in SBDD (structure-based drug design), October 1-3, 2025, Sestri Levante, Italy.
- Chandramouli: Poster presentation in BPS thematic meeting "Understanding Peripheral Membrane Protein Interactions", November 9-13 2025, Thessaloniki, Greece.
- Namrata: Best Poster in SPHERE'25, October 16-18, 2025, IISc Bangalore.
- Satya Chaithayna, Harini, Chandramouli, Vinodhini, Sangeetha, Prithvi, Vijay, Santhosh: Poster presentation in IBS 2025, March 6-9,2025, IIT Madras.

3.10 Department of Physics

3.10.1 Prof. Animesh Kuley's Lab

3.10.1.1 Problem areas:

Plasma Physics and Fusion Energy:
Nuclear fusion—the process that powers the Sun and stars—offers a promising pathway toward clean, safe, and virtually limitless energy. Achieving controlled fusion on Earth, however, requires a deep understanding of the behaviour of high-temperature plasmas confined by magnetic fields in devices such as tokamaks and stellarators. A major scientific challenge in these systems is plasma turbulence, which drives enhanced transport of particles and energy, degrades confinement, and can lead to disruptive instabilities that terminate plasma discharges.

To address these challenges, the Plasma Theory Group at Indian Institute of Science (IISc), Bangalore has developed advanced gyrokinetic simulation tools, including the G2C3 global toroidal code, to investigate turbulence and transport in magnetically confined plasmas. These simulations provide predictive insights into plasma behaviour and help interpret experimental observations from major fusion experiments such as DIII-D tokamak, ADITYA-U tokamak, Large Helical Device (LHD), and Wendelstein 7-X. This work contributes to improving the physics understanding necessary for optimising plasma confinement and guiding the design of next-generation fusion energy systems.

3.10.1.2 SERC's resources:

Large-scale simulations of plasma turbulence and transport in fusion devices such as tokamaks and stellarators require substantial high-performance computing resources. These studies are carried out on PARAM Pravega under the National Supercomputing Mission, where our gyrokinetic codes demonstrate excellent parallel scalability across thousands of CPU cores. Due to constraints related to node availability and queue times, the Plasma Theory Group typically

performs production runs using more than 2,000 CPU cores per simulation. Capturing the long nonlinear time scales required for turbulence studies often necessitates multiple sequential restarts of the simulations. Sustained access to large-scale HPC facilities is therefore essential for predictive modelling of plasma behaviour in magnetically confined fusion systems.

3.10.1.3 Parallelization strategies:

The G2C3 simulation framework utilises a hybrid parallel computing model to efficiently exploit modern high-performance computing systems. It incorporates three levels of parallelism: distributed-memory domain decomposition using MPI, particle-level decomposition across nodes using MPI, and shared-memory parallelism within nodes implemented through OpenMP. The development team is currently working closely with application scientists to optimise key software components for emerging HPC architectures, thereby improving performance and scalability. The code has been successfully deployed on major national supercomputing platforms, including PARAM Pravega and PARAM Rudra under the National Supercomputing Mission (NSM 1.0), as well as the ANTYA supercomputer operated by the Department of Atomic Energy.

3.10.1.4 Result Outcome:

a. Publications:

1. Stabilization of sawteeth instability by short gas pulse injection in ADITYA-U tokamak Suman Dolui, Kaushlender Singh, Bharat Hegde, T. Macwan, SK Injamul Hoque, Umesh Nagora, Jaya Kumar A., S. Purohit, A. N. Adhiya, K. A. Jadeja, Harshita Raj, Ankit Kumar, Ashok K. Kumawat, Suman Aich, Rohit Kumar, K. M. Patel, P. Gautam, Sharvil Patel, N. Yadava, N. Ramaiya, M. K. Gupta, S. K. Pathak, M. B. Chowdhuri, S. Sharma, A. Kuley, R. L. Tanna, P. K. Chattopadhyay, A. Sen, Y. C. Saxena, R. Pal and Joydeep Ghosh, Physical Review Research 7, 033161 (2025).
2. Zonal flow suppression of turbulent transport in the optimized stellarators W7-X and QSTK Abhishek Tiwari, Joydeep Das, Jaya Kumar Alageshan, Gareth Roberg-Clark, Gabriel Plunk, Pavlos Xanthopoulos, Sarveshwar Sharma, Zhihong Lin, Animesh Kuley, Plasma Physics and Controlled Fusion 67, 085025 (2025).
3. Global gyrokinetic simulations of kinetic ballooning mode in NSTX-U plasmas Tajinder Singh,Tariq Rafiq, Eugenio Schuster, Zhihong Lin, Animesh Kuley, Nuclear Fusion 65, 106039 (2025).

b. Contributions to the national/Industry/societal projects due to the executions, and the resulting impact and benefits.

This work actively supports India's domestic fusion energy programme through close collaboration with the Institute for Plasma Research (IPR), Gandhinagar, the national nodal agency for fusion research. The activities are further strengthened through collaborative initiatives and funding support from Centre for Development of Advanced Computing (C-DAC), Pune under major national programs such as Department of Atomic Energy–Board of Research in Nuclear Sciences (DAE-BRNS), National Supercomputing Mission (NSM 1.0), and Science and Engineering Research Board (SERB).

The overarching objective of these efforts is to advance fusion plasma science and technology toward the realization of clean and sustainable energy systems, thereby strengthening India's long-term energy security and supporting the country's sustainable socio-economic development. In addition to national program contributions, this work also extends to

interactions with emerging private fusion start-ups, providing scientific inputs for the development of magnetically confined plasma devices and assisting in long-term strategic research and technology planning.

c. Images and videos:

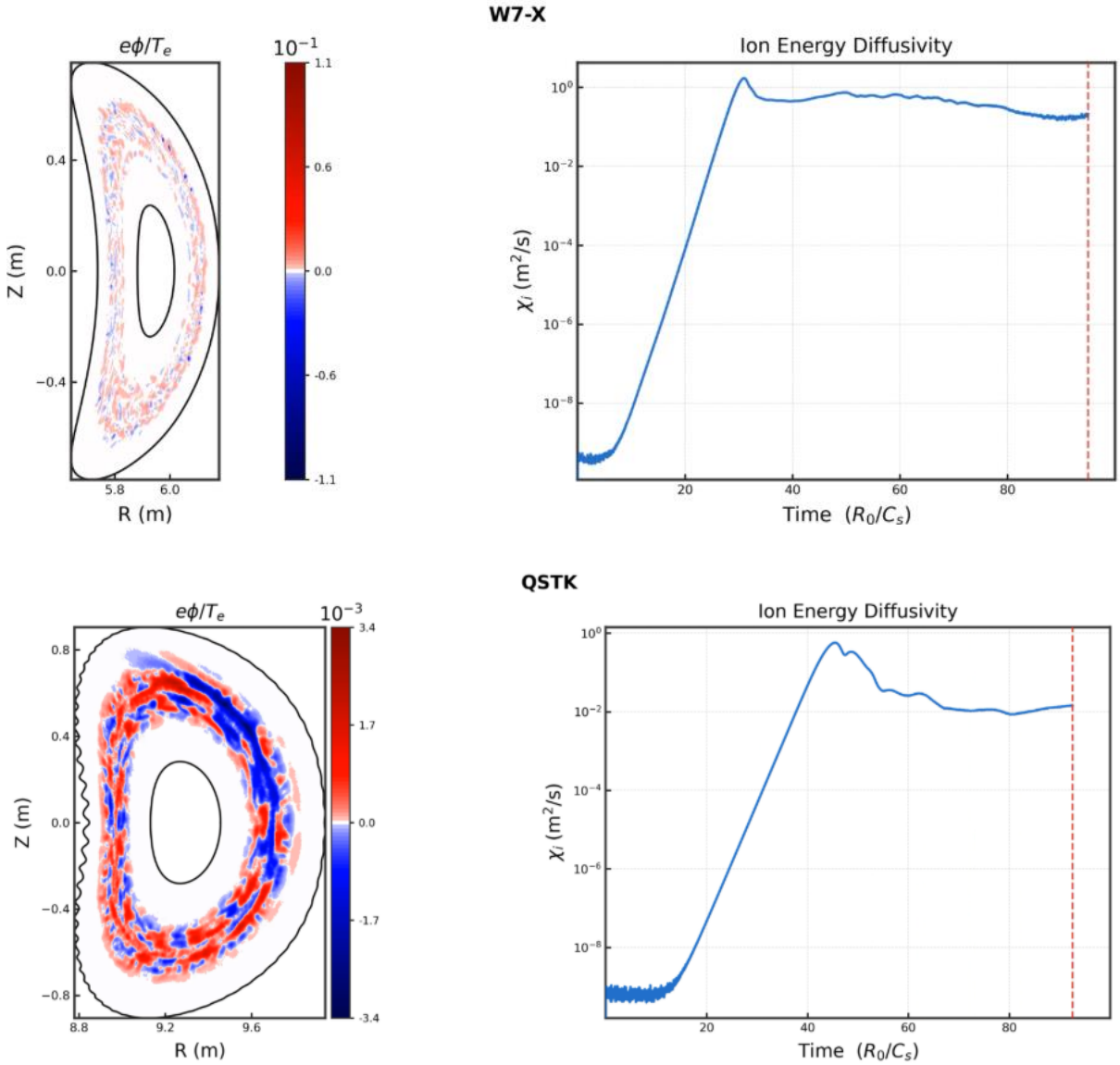


Figure: Evolution of mode structures for Ion temperature gradient mode for optimized Stellarator W7-X and QSTK and the ion heat diffusivities.

Paper link https://doi.org/10.1088/1361-6587/adf91b

4 Awards and Recognitions based on Research with SERC HPC Resources

1. Prof. N. Balakrishnan's Lab

The following paper was awarded the best paper award in AeSI CFD symposium, 2025:

- Argha Saha, O N Ramesh, N Balakrishnan, Effect of Mach Number on Cavity Acoustics, 26th Annual AeSI CFD Symposium 2025, 11th-13th August 2025, Bangalore.

2. Prof. Govindasamy Bala's Lab

Press release on safe regional Earth system boundary for aerosol loading over South Asia region:

- Earth Commission, Future Earth, Sweden: https://earthcommission.org/aerosol-boundary-confirmed-increased-air-pollution-could-tip-monsoon/
- IISc news magazine Kernel: https://kernel.iisc.ac.in/influence-of-aerosols-on-indian-summer-monsoon/

3. Prof. Phani Motamarri's Lab

S.No.	Name of Award	Awarding Agency	Year
1	Dr A P J Abdul Kalam HPC Award 2025	HP and Abdul Kalam Foundation	2025
2	Director's Discretionary Award for Compute Allocation on Frontier, world's first exascale supercomputer	Oak Ridge National Lab (ORNL)	2025
3	Kawazoe Poster Award for PhD student Srinibas Nandi	Asian Consortium on Computational Materials Science (ACCMS) - Japan	2025
4	Best Presentation Award for PhD student Kartick Ramakrishnan	EECS Symposium	2025
5	Institute Motorola Medal for MTech student Sundaresan	IISc	2025

4. Prof. Abhishek Singh's Lab

1. Shibu Meher – Poster Commendation Award in Materials for Information and Communication, Psik Conference, 2025
2. Aditya Gollapalli – Best Oral Presentation, MRC Day, Jan 2025
3. Subhendu Mishra – Best Oral Presentation, MRC Day, May 202

5. Prof. Ratnesh Shukla's Lab

Invited Talks:

1. Thrust Generation Mechanics and Energetics of Undulatory Locomotion, Department Research Seminar Series, Department of Mechanical Engineering, University of Canterbury, May 27, 2025.

2. Detailed simulations of collective bubble growth and collapse dynamics, Australasian Fluid Mechanics Seminar Series, May 14, 2025.
3. Detailed simulations of cavitating bubble clouds, Department Seminar Series, Department of Mechanical and Mechatronics Engineering, University of Auckland, April 11, 2025.

5 Access to External Users

SERC also provides access to its high-end resources to researchers of Academic organizations and Government-funded R&D laboratories for cutting-edge research. Users of the following Institutes have utilized more than 1.5 million CPU core hours in 2025.

1. IIT Madras
2. C-DAC, Pune

6 Publications in 2025 Using SERC HPC Resources

Journal Papers

1. Raghuram, S., & Ramesh, O. N. (2025). Bursting phenomenon in turbulent wall-bounded flows. Physics of Fluids, 37(2).
2. "Large Scale Motion in a Turbulent Channel Flow" to be submitted to Physical Review Letters shortly.
3. Neethu, C., Tharammal, T., & Bala, G. (2025) A model-based assessment of the regional safe aerosol boundary for the South Asian monsoon region. Environmental Research Letters, 20(12), 124057. https://iopscience.iop.org/article/10.1088/1748-9326/ae2345
4. Kumar, S., A. K. Seshadri, and G. Bala, 2025: Contrast in Slow Climate Response to Methane and Carbon Dioxide Forcings Identified Using the Radiative Kernel Technique. J. Climate, 38, 6307–6328, https://doi.org/10.1175/JCLI-D-24-0728.1
5. Tharammal, T., Bala, G., & Nusbaumer, J. (2026), Drivers of the $\delta^{18}O$ Changes in Indian Summer Monsoon Precipitation between the Last Glacial Maximum and Pre-industrial Period. Climate of the Past, https://cp.copernicus.org/articles/22/427/2026/.
6. Srivastava, Shikhar, Arindam Chakraborty, and Raghu Murtugudde, 2026: Unravelling the Teleconnections: Southern Hemisphere ENSO Transition Mode and the Global Boreal Summer Monsoons, Journal of Climate, 39, 861-874, doi: https://doi.org/10.1175/JCLI-D-25-0611.1
7. Samuel, J.B., and A. Chakraborty, 2023: Integration of a Groundwater Model to the Noah Land Surface Model for Aquifer-Soil Interaction, Journal of Advances in Modeling Earth Systems, doi: https://doi.org/10.1029/2022MS003153
8. Chakraborty, A., JB Samuel, and A. Paleri, 2023: Role of land-surface vegetation in the march of Indian monsoon onset isochrones in a coupled models, Quarterly Journal of the Royal Meteorological Society, 149, 115-132, doi: https://doi.org/10.1002/qj.4398

9. Aashruti, A. Ghosh, E. Humphreys, Western US Anisotropy: Role of Slabs, Lateral Viscosity Variations and Small- Scale Heterogeneity, Journal of Geophysical Research, (in Review).
10. D. Pal, A. Ghosh, What caused the sudden acceleration of the Indian plate during the late Cretaceous: Reunion Plume vs Double Subduction, Geology, (in Review).
11. D. Pal, A. Ghosh, On the consistency of plate reconstruction models using geodynamic constraints, Gcubed (in Revision).
12. Bhowmik, S., **Govind Rajan, A.*** Size and Chemical Environment Control Nanopore Geometry in 2D MoS_2: From Irregular to Triangular Defects. *Small* **2025**, 21, 33, pp 2504611.
13. Sinha, A., Verma, M., Kumar, N., Kumar, K. S., **Govind Rajan, A.***, Singh, A.* Critical Role of Precursor Flux in Modulating Nucleation Density in 2D Material Synthesis Revealed by Digital Twin. *Nanoscale Adv.* **2025**, 7, pp 3568–3578.
14. Sen Gupta, R., Islam, S. S., Dhondi, P., Jose, T., **Govind Rajan, A.***, Bose, S.* Sequential Interpenetrating Polymer Network Confines Shear-Aligned Graphene Oxide Liquid Crystals Enabling Precise Molecular Sieving. *Small* **2025**, pp 2503746.
15. Verma, A. K., Atif, S., Padhy, A., Choksi, T. S., Barpanda, P., **Govind Rajan, A.*** Robust Oxygen Evolution on Ni-Doped MoO_3: Overcoming Activity-Stability Tradeoff in Alkaline Water Splitting. *Chem Bio Engg.* **2025**, 2, 4, pp 241–252. (*Invited article for the special issue "Electrochemical Engineering for Sustainability"*.)
16. Ghorai, S., Pradeep, D., **Govind Rajan, A.*** Molecular Dynamics Simulations of Functionalized hBN Nanopores in Water: Ab Initio Force Field and Implications for Water Desalination. *J. Chem. Phys.* **2025**, 162, 044705. (*Invited article for the special issue "Molecular Dynamics, Methods and Applications 60 Years after Rahman"*.)
17. Majumdar, J., Mandal, S., **Govind Rajan, A.**, Maiti, P. K.* Similar Structure but Different Thermodynamic, Dielectric, and Frictional Properties of Confined Water in Twisted 2D Materials: MoS_2 vs. Graphene. *Nanoscale* **2025**,17, pp 2354–2364.
18. Sharma, B. B., Kedare, A., Muralidharan, G., **Govind Rajan, A.*** Understanding the Effects of Surface and Edge Functionalization on the Mechanical Properties of Graphene and Graphene Oxide. *ChemPhysChem* **2025**, 26, 5, e202400919. (*Invited article, included in the special topics "Hot Topic: Carbon, Graphite, and Graphene" and "Hot Topic: Surfaces and Interfaces"*.)
19. YaxA Pre-Pore Formation Underlies Bipartite YaxAB Toxin Assembly on Living Membranes, Harsh Kumar, Ganapathy Ayappa, Sandhya S. Visweswariah, and Vaishnavi Ananthanarayanan, Biophysical Journal (2025) https://doi.org/10.1016/j.bpj.2025.12.027
20. Perturbing Angstrom-Scale Interfacial Clusters in Functionalized Nanoporous Graphene for Selective Evaporative Methanol-Water Separations, Bharath Desikan and K. Ganapathy Ayappa, ***Langmuir,*** 41, 32, 21368–21379 (2025) DOI: 10.1021/acs.langmuir.5c01833
21. Oxysterols Outcompete Cholesterol Binding to the Membrane Inserted Cytolysin A Pore Complex, Samlesh Choudhury, K. Ganapathy Ayappa, ***Journal of Membrane Biology*** (2025) https://doi.org/10.1007/s00232-025-00349-0
22. Gated CO_2 Permeation across Dynamic Graphene Pores, Luc Bondaz, Anshaj Ronghe, K. Ganapathy Ayappa, Kumar Varoon Agarwal, ***Nature Communications*** 16, 6252 (2025). https://doi.org/10.1038/s41467-025-61518-2
23. Oxysterols Modulated Protein-Sterol Interactions to Impair CXCR4 Signalling in Aging Cells, Suramya Asthana, Anant Verma, Baivabi Bhattacharya, K. Ganapathy Ayappa, Deepak Kumar Saini, ACS-Biochemistry, 64 1606–1623 (2025) https://doi.org/10.1021/acs.biochem.4c00617

24. N. Kodali, K. Ramakrishnan, P.Motamarri, Residual-based Chebyshev filtered subspace iteration for sparse Hermitian eigenvalue problems tolerant to inexact matrix vector products, Computer Physics Communication (accepted) Volume: arXiv:2 503.22 652, 2025.
25. K. Ramakrishnan, S.G.Gopalakrishnan, P. Motamarri, Real-space methods for ab initio modelling of surfaces and interfaces under external potential bias, Journal of Chemical Theory and Computation Volume, 21 page 7087, 2025.
26. N. Kodali, P. Motamarri Finite-element based methods for non-collinear magnetism and spin-orbit coupling in real-space pseudopotential density functional theory calculations, Physical Review B Volume 111 page 195129, 2025.
27. K. Ramakrishnan, S.Das, P.Motamarri Fast and scalable finite-element based approach for density functional theory calculations using projector augmented wave method Physical Review B Volume 111 page 035101, 2025.
28. A. Rout, R.Pawar, S. Bhattacharjee, P. Motamarri Robust light-weight graph neural network frameworks for accelerating crystal structure prediction Journal of Chemical Information and Modelling volume 65 page 6470, 2025.
29. Cobalt-Catalyzed Deoxygenative Coupling of Ethers to Alkanes M. K. Sahu, S. Pattanaik, G. Joshi, E. D. Jemmis, and C. Gunanathan Angew. Chem. Int. Ed. 2026,65,e20176. (https://onlinelibrary.wiley.com/doi/10.1002/anie.202520176)
30. All-Boron Analogue of Planar Benzene on an Osmium Template K. Kar, G. Joshi, E.D. Jemmis, and S. Ghosh Chemical Science 2026, 17, 196-204. https://pubs.rsc.org/en/content/articlelanding/2026/sc/d5sc06992k)
31. Valence Electron Dependent Contraction Of P6 Ring In[(CpM)2(μ,η6:η6-P6)] (M=V, Mo): A DFT Study. G. Joshi, S. N. Moorkkannur, E. D. Jemmis Chem. A Eur. J, 2025, 30, e202501411. (https://chemistry-europe.onlinelibrary.wiley.com/doi/10.1002/chem.202501411)
32. Stabilization of Ethane-like Dianionic Diborane(6) in Monometallic Titanium Complexes and its Subsequent B(sp3)-B(sp3) Bond Cleavage. S. Bairagi, S. Giri, G. Joshi, E. D. Jemmis, S. Ghosh Angew. Chem. Int. Ed. 2025, 64, e202417170. (**https://doi.org/10.1002/anie.202417170**)
33. Probing Lattice Anharmonicity and Thermal Transport in Ultralow-κ Materials Using Machine Learning Interatomic Potentials, Small 2025, e13476 S. Mandal, A. Srivastava, T. Das, A. K. Singh, and P. K. Maiti
34. Conventional and Valley-Polarized Quantum Anomalous Hall Phases in Ti-Cr-C MXenes, Nano Lett. 2025, 25, 51, 17954–17961 S. Mishra, R. K. Barik, and A. K. Singh.
35. Descriptors of Electrocatalysis for CO2 Reduction to C2+ Products Formation, ACS Appl. Energy Mater. 2025, 8, 23, 17085–17105 S. Midya, A. Chakraborty, S. Mishra, and A. K. Singh
36. Electronic Structure Modulation of AlN4 Single-Atom Catalyst for Oxygen Reduction Reaction, Small 2025, 21, e01869 S. Atif, O. Y. Bisen, S. Midya, A. K. Yadav, G. Ciatto, A. K. Singh, K. K. Nanda.
37. Plasmonic Nanocomposite for Visible Light-Modulated BimorphActuator, Adv. Mater. Technol. 2025, 10, 2401037 P. Kumbhakar,* S. Narendhiran, S. Midya, M. Islam, M. Balachandran, and A. K. Singh*
38. High-throughput computational search for group-IV-related quantum defects as spin-photon interfaces in 4H-SiC, Phys. Rev. B 112, 184112 S. Meher, M.Dey, A. K. Singh.
39. Enhanced Heat Dissipation and Reduced Power Consumption in Electronics Using 2D Hexagonal Boron Nitride, Small 2025, 2502007Karthik R, A. Srivastava, S. Midya, A. Shanu, S. Slathia, S. Vandana, S. Kar, N. R. Glavin, A. K. Roy, P. R. Sreeram, A. K. Singh*, C. S. Tiwary*.

40. 2D MnTe/rGO Hybrid Structure for Moisture Energy Harvesting, ACS Appl. Mater. Interfaces 2025, 17, 22, 32973–32983 P. Kumbhakar, S. Mishra, C. C. Gowda, P. M. Nishma, A. Venugopal, A. K. Singh* and C. S. Tiwary*.
41. Magnetocaloric effect in Mn-rich Heusler-derived alloys for room temperature-based applications, J. Mater. Chem. C, 2025,13, 10789-10803 N. Tiwari, S. Mishra, S. Sarkar, S. Talapatra, M. Palit, M. Paliwal, A. K. Singh and C. S. Tiwary.
42. Strain and Charge Doping Modulated Optical Emission Signatures of Polycrystalline WSe2, Small, 2411297 (2025) S. Paul, S. Mishra, Abhijith M B, P. Ghosh, P. Barman, M. Altvater, V. Pandey, P. P. Chanda, S. Das, A. Roy, N. R Glavin, A. K. Singh, and V. Kochat
43. Defect Engineered Few Layered MoS2 for Human–Machine Interface, Small Methods, 2500068 (2025) R. D. Salian, S. Mishra, C. C. Gowda, R. K. Barik, A. K. Singh, C. S. Tiwary, P. Kumbhakar
44. 2D Materials Coated Flexible Origami for Low-Frequency Energy Harvesting, ACS Appl. Electron. Mater. 7, 3, 1111–1119 (2025) P. Kumbhakar, S. Mishra, P. V. Nayak, A. Sunny and A. K. Singh
45. Recommendation System to Predict the d-band Center of Core-Shell Bimetallic Nanoparticles Catalysts, Adv. Theory Simul. 2401460 (2025) S. Agarwal and A. K. Singh
46. Carbon with Stone-Wales Defect as Quantum Emitter in h−BN, Phys. Rev. B 111, 104109 (2025) M. Dey, S. Meher and A. K. Singh
47. Comprehensive insights into hydrolysis-mediated hydrogen production using high-entropy quintuple alloy-grafted carbon black, J. Mater. Chem. A,13, 5765-5776 (2025) G. Raj, R. Nandan, S. Midya, K. Kumar, A. K. Singh and K. K. Nanda
48. P. Das, R. K. Shukla & J.B. Freund, "Acoustically excited bubble tunnelling through soft material" *Journal of Fluid Mechanics*, 1020, A45, 2025.
49. Duggisetty, S. C., Kumar, G., Baratam, K., & Srivastava, A. (2026). Division of labor in cargo and membrane recognition by SNX1-SNX5: Insights from multiscale modeling. Biophysical Journal, 125(2), 652–667.
50. Joy, A., Srivastava, A., & Biswas, R. (2026). Azurin-based peptide p28 disrupts p53–HDM2 interactions: Insights from in silico studies. Physical Chemistry Chemical Physics, 28(1), 234–246.
51. Mallick, A. M., Chatterjee, A., Gurung, A. B., Uttarasili, P., Tripathi, A., Hembram, M., et al. (2025). Designed gramicidin-inspired stabilized peptide-based therapeutics to potentiate immunotherapy against aggressive kidney cancer. Biomaterials Science, 13(17), 4681–4705.
52. Pandey, P., & Srivastava, A. (2025). sAMP-VGG16: Force-field assisted image-based deep neural network prediction model for short antimicrobial peptides. Proteins: Structure, Function, and Bioinformatics, 93(1), 372–383.
53. Roy, I., Appadurai, R., & Srivastava, A. (2025). Unambiguous assignment of kinked-β sheets leads to insights into molecular grammar of reversibility in biomolecular condensates. Protein Science, 34(9), e70266.
54. Srivastava, A. (2025). Emerging paradigms in the lateral and transverse organization in biological membrane and their functional implications: Connecting the dots with biomolecular simulations. Current Opinion in Structural Biology, 94, 103128.
55. Srivastava, A. (2025). It takes two to tango: The second membrane-binding site in peripheral proteins. Structure, 33(1), 10–12.
56. Subramanian, V., Appadurai, R., Venkatesh, H., Sekhar, A., & Srivastava, A. (2025). Morpheus: A fragment-based algorithm to predict fold-switching behaviour in proteins across proteomes. Bioinformatics, 41(12), btaf635.

57. SureshKumar, H., Iyer, S. S., Banerjee, A., Poduval, P., Lyman, E., & Srivastava, A. (2025). Signatures of glassy dynamics in highly ordered lipid bilayers with emergence of soft dynamic channels. The Journal of Chemical Physics, 162(14).
58. Stabilization of sawteeth instability by short gas pulse injection in ADITYA-U tokamak Suman Dolui, Kaushlender Singh, Bharat Hegde, T. Macwan, SK Injamul Hoque, Umesh Nagora, Jaya Kumar A., S. Purohit, A. N. Adhiya, K. A. Jadeja, Harshita Raj, Ankit Kumar, Ashok K. Kumawat, Suman Aich, Rohit Kumar, K. M. Patel, P. Gautam, Sharvil Patel, N. Yadava, N. Ramaiya, M. K. Gupta, S. K. Pathak, M. B. Chowdhuri, S. Sharma, A. Kuley, R. L. Tanna, P. K. Chattopadhyay, A. Sen, Y. C. Saxena, R. Pal and Joydeep Ghosh, Physical Review Research 7, 033161 (2025).
59. Zonal flow suppression of turbulent transport in the optimized stellarators W7-X and QSTK Abhishek Tiwari, Joydeep Das, Jaya Kumar Alageshan, Gareth Roberg-Clark, Gabriel Plunk, Pavlos Xanthopoulos, Sarveshwar Sharma, Zhihong Lin, Animesh Kuley, Plasma Physics and Controlled Fusion 67, 085025 (2025).
60. Global gyrokinetic simulations of kinetic ballooning mode in NSTX-U plasmas Tajinder Singh,Tariq Rafiq, Eugenio Schuster, Zhihong Lin, Animesh Kuley, Nuclear Fusion 65, 106039 (2025).

Conference Papers

1. Abhiyan Paudel, Sharanjeet Kaur, Nikhil Vijay Shende and N Balakrishnan, Aerodynamic shape optimization of a rectangular wing for long endurance Unmanned Aerial Vehicle, ECCOMAS AeroBest 202, 22–24 April 2025, Lisboa, Portugal.
2. Saranraj A, Saha Argha, Akshay Nagdeve, Mohideen Ansar, Ramesh O N, Balakrishnan N, Uncertainty Quantification of Aerodynamic Loads on a Store Using Detached Eddy Simulation (DES), 26th Annual AeSI CFD Symposium 2025, 11th-13th August 2025, Bangalore.
3. Mohammed Shaheen Suhail, Munikrishna, Balakrishnan N, Residual Driven Adaptive Time Stepping for Unsteady Flows, 26th Annual AeSI CFD Symposium 2025, 11th-13th August 2025, Bangalore.
4. Mohideen Ansar A, Akshay Nagadeve, Manoj Kumar K, Rajni Kanth B and N Balakrishnan, CFD Analysis of SPICES 4 Hypersonic Intake Configuration using HiFUN, 26th Annual AeSI CFD Symposium 2025, 11th-13th August 2025, Bangalore.
5. M I Vellaisamy Dinu, Adithya Udupa, Sudha U P V, and Kartik Venkatraman. 2025. Horizontal and vertical tail buffeting of a trapezoidal planform in a transonic flow. Aeronautical Society of India 26th Annual CFD Symposium 2025. August 11th -13th.
6. Argha Saha, O. N. Ramesh, and N. Balakrishnan, “Effect of Mach Number on Cavity Acoustics,” 26th Annual AeSI CFD Symposium, Bangalore, India, August 2025. – This paper won 3rd prize in the conference.
7. Muruganandam, A.P., Hemchandra, S. and Das, R., 2026. Oblique Shock Wave/Turbulent Boundary Layer Interaction: Information-Theoretic Approach. In *AIAA SCITECH 2026 Forum* (p. 2341).
8. **Singh, M., Bala, G., & Seshadri, A. K. (2026)** *Response of the Characteristics of Monsoon Low-Pressure Systems to Stratospheric Aerosol Geoengineering during the Indian Summer Monsoon Season.*106th Americal Meteorological Society Annual Meeting, Houston, Texas, US.
9. **Singh, M., Bala, G., & Seshadri, A. K. (2025)** *Biases in model simulations of Indian Summer Monsoon low-pressure systems.* European Geophysical Union meeting, Vienna, Austria

10. S. Dasika & R.K. Shukla, “Multilayer-Perceptron based Optimal Stencil Selection and Order Detection for High-Order Shock Capturing”, The 18th Asian Congress on Fluid Mechanics, Seoul Korea, 2025.